

SPSD II

ADVANCED MODELING AND RESEARCH ON EUTROPHICATION (AMORE II)

C. LANCELOT, K. RUDDICK, M-H. DARO



PART 2
GLOBAL CHANGE, ECOSYSTEMS AND BIODIVERSITY



ATMOSPHERE AND CLIMATE



MARINE ECOSYSTEMS AND BIODIVERSITY



TERRESTRIAL ECOSYSTEMS AND BIODIVERSITY



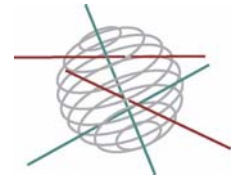
NORTH SEA



ANTARCTICA

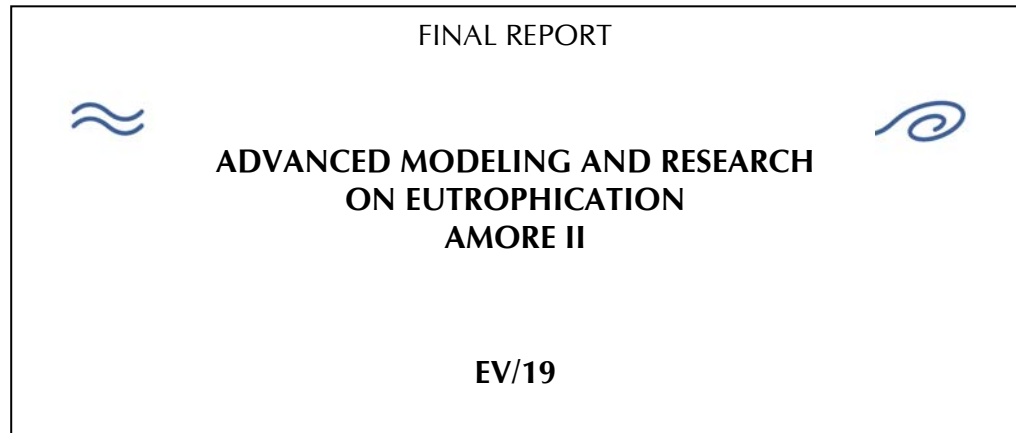


BIODIVERSITY



Part 2:

Global change, Ecosystems and Biodiversity



Christiane Lancelot¹, Véronique Rousseau¹, Nathalie Gypens¹,
Jean-Yves Parent¹, Aya Bissar¹, Juliette Lemaire¹
Elsa Breton², Marie-Hermande Daro²
Geneviève Lacroix³, Kevin Ruddick³, José Ozer³
Yvette Spitz⁴
Karline Soetaert⁵
Marie-Josèphe Chrétiennot-Dinet⁶, François Lantoiné⁶
Francisco Rodriguez⁷

¹**Université Libre de Bruxelles - Ecologie des Systèmes Aquatiques**
bd du Triomphe, CP-221 - B-1050 Bruxelles - Belgium

²**Vrije Universiteit Brussel - Laboratorium Voor Ekologie And Systematiek**
Pleinlaan, 2 B-1050 Bruxelles - Belgium

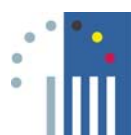
³**Belgian Royal Institut of Natural Science - Management Unit of North Sea
Mathematical Models**
Gulledelle, 100 - B-1200 Bruxelles - Belgium

⁴**Oregon State University - College of Oceanic and Atmospheric Sciences**
USA

⁵**Netherlands Institute for Ecology - Centre for Estuarine and Coastal Research
(NIOO-CEME)**
Korringaweg, 7 - 4401 NT Yerseke - The Netherlands

⁶**Laboratoire d'Océanographie Biologique de Banyuls**
UMR 7621, CNRS/INSU/Université Paris 6
BP 44 – 66651 - Banyuls sur Mer - France

⁷**Station Biologique**
UMR 7127 CNRS/INSU/UPMC, BP 74 - 29682 Roscoff - France.





D/2007/1191/5

Published in 2007 by the Belgian Science Policy

Rue de la Science 8

Wetenschapsstraat 8

B-1000 Brussels

Belgium

Tel: + 32 (0)2 238 34 11 – Fax: + 32 (0)2 230 59 12

<http://www.belspo.be>

Contact person:

Mr David Cox

Secretariat: + 32 (0)2 238 36 13

Neither the Belgian Science Policy nor any person acting on behalf of the Belgian Science Policy is responsible for the use which might be made of the following information. The authors are responsible for the content.

No part of this publication may be reproduced, stored in a retrieval system, or transmitted in any form or by any means, electronic, mechanical, photocopying, recording, or otherwise, without indicating the reference.

TABLE OF CONTENT

1	ABSTRACT	1
2	INTRODUCTION	9
3	MATERIAL AND METHODS	13
3.1	Field and laboratory eco-physiological studies	13
3.1.1	Field sampling	13
3.1.2	Phytoplankton cultures	14
3.1.3	Analytical methods	17
3.2	Long-term trend analysis of diatom and <i>Phaeocystis</i> blooms	18
3.2.1	Data sets	19
3.2.2	Statistical analysis	20
3.3	Mathematical modelling	20
3.3.1	Model description	20
3.3.2	Model implementation	23
3.3.3	Validation data	25
3.3.4	Model sensitivity analysis	25
4	RESULTS AND DISCUSSION	27
4.1	Eco-physiological studies	27
4.1.1	<i>Phaeocystis</i> species identification, morphotypes and life cycle	27
4.1.2	Seasonal dynamics of phosphorus and microbial dominance	34
4.1.3	Dynamics of gelatinous zooplankton: <i>Noctiluca</i> and <i>Oikopleura</i>	36
4.2	Long-term trend analysis of diatom and <i>Phaeocystis</i> blooms in BCZ	46
4.2.1	Diatom/ <i>Phaeocystis</i> blooms at St 330 between 1988 and 2001	46
4.2.2	Hydroclimatic modulation of diatom- <i>Phaeocystis</i> blooms	46
4.3	Mathematical modelling	50
4.3.1	Analyzing and testing the current 0D multi-box MIRO model	50
4.3.2	Upgrading the current 0D multi-box MIRO model	57
4.3.3	Testing the prediction capability of MIRO&CO-3D	61
4.3.4	0D multi-box MIRO application: river nutrient reductions	66
4.3.5	MIRO&CO-3D application: contribution of different rivers	68

5	CONCLUSION AND RECOMMENDATIONS	71
5.1	Improved knowledge on the ecology of <i>Phaeocystis</i> -dominated system	71
5.1.1	<i>Phaeocystis</i> species identification and life cycle	71
5.1.2	Mechanisms controlling diatom- <i>Phaeocystis</i> -diatom successions	71
5.1.3	Fate of <i>Phaeocystis</i> blooms	72
5.2	Advances in ecological modeling: 0D multi-box MIRO	72
5.2.1	New developments	72
5.2.2	Sensitivity analysis	72
5.2.3	Mitigation	73
5.3	Advances in ecological modeling: MIRO&CO-3D	73
6	ACKNOWLEDGMENTS	75
7	REFERENCES	77

1 ABSTRACT

AMORE (Advanced Modeling and Research on Eutrophication) is an interdisciplinary consortium composed of biologists and physical and ecological modellers focusing their research activities on coastal eutrophication in the eastern Channel and Southern Bight of the North Sea with special interest in harmful *Phaeocystis* colony blooms. The long-term objective of AMORE is to develop a a tri-dimensional ecological model - MIRO&CO - able to predict the magnitude and geographical extent of *Phaeocystis* colony blooms in the Eastern Channel and Southern Bight of the North Sea with focus on the Belgian Coastal Zone (BCZ) and in response to varying short-term climate conditions and riverine nutrient (N, P, Si) loads. To achieve this objective, AMORE has developed an integrated research methodology that involves and combines in an interactive way the collection of historical and new field data, process-level studies, statistical analysis, mathematical modelling and data assimilation. In this approach, the ecological model plays a central role as integrator of new knowledge gained from experimental studies and as tool for eutrophication assessment and prediction as well as decision support.

Between 2002 and 2006, AMORE research focused on mechanisms determining *Phaeocystis* colony bloom inception and development, their dominance over diatoms in spring and their trophic fate. Particular attention was paid to the role of gelatinous organisms, especially *Noctiluca* which blooms at *Phaeocystis* colony decline. The relevant knowledge gained was synthesized for integration in the existing ecological MIRO which in turn was coupled with the 3D COHSNS hydrodynamical model developed for describing water transport in the studied domain. Progress achieved in our understanding of eutrophication mechanisms in the BCZ as well as our present ability to predict *Phaeocystis* spreading and magnitude in response to riverine nutrient delivery are discussed in the present report.

For the first time in the region, molecular tools identified as *P. globosa* the *Phaeocystis* species blooming in the Southern Bight of the North Sea. Experimental studies on *Phaeocystis* life cycle evidenced a haploid-diploid cycle in which haploid flagellates persist in the water column between blooms of diploid colonial cells, suggesting that colony bloom initiation and termination involve sexual processes. The recurrent diatom-*Phaeocystis* succession observed in the area suggests that early spring diatoms could play a triggering role in syngamy.

Statistical analysis of diatom and *Phaeocystis* data collected between 1992 and 2000 in BCZ showed that their relative contribution to the spring community was regulated by both river nutrient loads (mankind) and hydro-climatic conditions themselves under the influence of the North Atlantic Oscillation (NAO). Years with elevated *Phaeocystis* blooms in central BCZ were identified as those characterized by a medium NAO index, *i.e.* when a maximum of NO₃ delivered by the Scheldt is spread

over BCZ. This observation, also supported by 0D multi-box MIRO runs, suggests that excess NO_3 (but low PO_4) sustain the growth of *Phaeocystis* colonies. For the first time, PO_4 limitation was demonstrated in the BCZ *via* the detection of alkaline phosphatase activity in spring. One major result is that this enzymatic activity is associated mainly to large particles including phytoplankton cells and their attached bacteria.

Specific grazing experiments on *Phaeocystis* ultimately concluded that healthy *Phaeocystis* colonies are not grazed by either copepods or gelatinous organisms but are mostly degraded in the water column rather than the sediment.

Numerical experiments included 0D and 3D modelling. The published version of 0D multi-box MIRO was further tested and upgraded. Results of the sensitivity analysis (variational adjoint method and sensitivity factor computation) identified processes associated to the microbial loop dynamics as main controls of the time evolution of all the MIRO state variables in BCZ. More specific sensitivity tests were showing in addition that the timing of the spring bloom of both diatom and *Phaeocystis* was determined by the light availability and their maximum photosynthetic specific rate. New developments and applications of 0D multi-box MIRO included (i) the addition and test of a CO_2 module pointing the role of riverine nutrient loads in stimulating the uptake of atmospheric CO_2 in BCZ, (ii) the upgrading of the sediment diagenetic module and its further simplified parameterization for integration in MIRO&CO-3D and, (iii) the exploration of causes of diatom-*Phaeocystis* bloom variability in the Belgian waters over the last decade. The latter study concluded that while the diatom variability was depending on both meteorological conditions (light and temperature) and nutrient loads, *Phaeocystis* blooms were mainly controlled by nutrients, especially NO_3 .

The MIRO&CO-3D was implemented by coupling the published version of MIRO to the COHSNS-3D hydrodynamical model. The geographical domain extended between 4° W (48.5° N) and 52.5° N (4.5° E) with a grid resolution of $5.6 \times 4.6 \text{ km}$ and included inputs from the main rivers within this domain (Rhine/Meuse, Scheldt/Leie/Ijzer, Thames, Seine). Model simulations were performed for the period 1993-2003 and validated based on a successful comparison of simulated salinity and *in situ* measurements and by comparing biogeochemical results [nutrient and phytoplankton (Chl *a*)] with field measurements (time series at fixed stations, surface seasonal mean, monthly mean MERIS-derived Chl *a*). MIRO&CO-3D sensitivity tests with decreasing (1%) river nitrogen and phosphorus inputs from different origins explored the relative impact of the different rivers (Scheldt/Rhine/Seine) and Channel waters on the nutrient availability in the Belgian waters. Results showed that Channel nutrient inflow had a direct effect on the surface nutrients over the whole domain. The comparison between the three rivers suggested that the effect of the Seine River is

the most important for the whole domain considered except in BCZ areas where eutrophication is severe due to Scheldt loads. Interestingly enough, the effect of nutrient reduction from all rivers was higher for DIN than that for PO₄, expressing a stronger sensitivity of DIN to riverine nutrient reduction because rivers supply relatively more DIN than PO₄ as compared to the Atlantic inflow. Finally, these results in agreement with mitigation scenarios conducted with 0D multi-box MIRO, concluded that an integrated management plan involving riparian countries of the eastern Channel and Southern Bight of the North Sea and targeting NO₃ delivery is needed to decrease eutrophication and *Phaeocystis* blooms in BCZ.

2 INTRODUCTION

AMORE (Advanced Modelling and Research on Eutrophication) is an interdisciplinary consortium composed of biologists, microbiologists and physical and ecological modellers joining their research effort on understanding causes and consequences of eutrophication in the Southern Bight of the North Sea with a focus on Belgian coastal waters. Man-made eutrophication is investigated in the general frame of large-scale atmospheric variability that has a substantial effect on phytoplankton bloom dynamics and species dominance in the northwest European shelf seas (Belgrano *et al.*, 1999; Irigoien *et al.*, 2000; Edwards *et al.*, 2001). The nutrient-driven potential of the Belgian Coastal Zone (BCZ) for absorbing increased atmospheric CO₂ is considered as well.

Eutrophication in the BCZ results from transboundary (SW- Atlantic waters enriched by the Seine, Somme, Authie and Canche, and Rhine) and local (Ijzer, Leie and Scheldt) inputs (Fig.1) of land-based nutrients (N, P, Si). The relative importance of these different nutrient sources in the BCZ is not accurately known and varies depending on human activity on the watershed and on large scale climatic phenomena such as the North Atlantic Oscillation (NAO; Hurrell, 1995) which determines the weather conditions over North-western Europe climatic conditions. Eutrophication along the continental coastline of the Southern Bight of the North Sea manifests as massive undesirable algal blooms in spring (mainly colony forms of the Haptophyceae *Phaeocystis*) that spread over the whole area along a SW-NE gradient (Lancelot *et al.*, 1987) impacting the ecosystem function (Lancelot, 1995). Additionally, mass developments of undesirable gelatinous organisms (mainly *Noctiluca scintillans*) are recurrently recorded in BCZ after the *Phaeocystis* colony bloom (*i.e.* in June; Hecq, 1982; Rousseau *et al.*, 2000) but their link with phytoplankton blooms and eutrophication in general needs still to be assessed.

Historical analysis of nutrient inputs to the BCZ shows a 77% reduction of phosphate (PO₄) between 1989 and 2000 with no discernible change in dissolved inorganic nitrogen and silicate (Rousseau *et al.*, 2004). Although these trends induce significant qualitative (N:P:Si) changes in the nutrient coastal environment, there is no observable effect on the magnitude of *Phaeocystis* colony spring blooms (Rousseau, 2000) bringing forward the unresolved debate on the contribution of climate (Owens *et al.*, 1989) and land-based nutrients (Cadée & Hegeman, 1991) changes to the magnitude of *Phaeocystis* colony blooms.

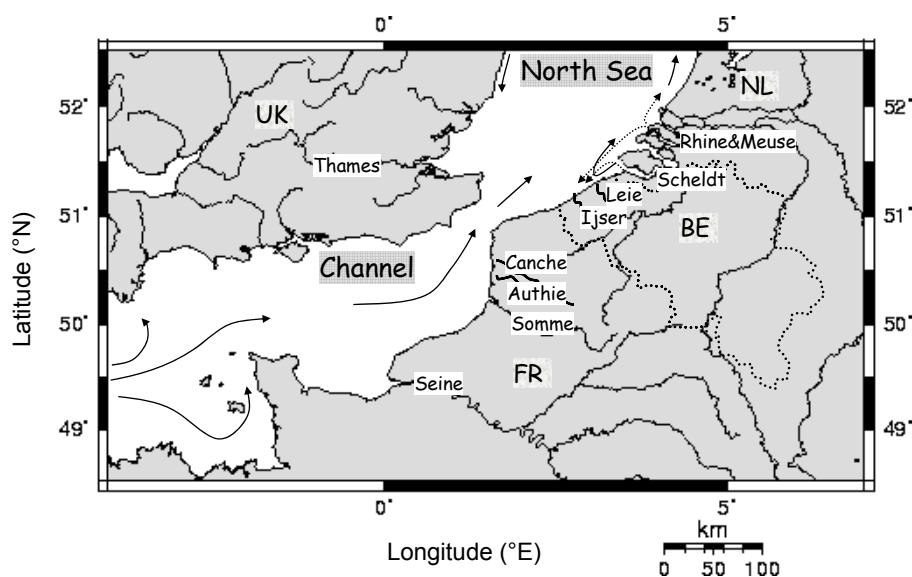


Figure 1: Map showing the Channel and the Southern Bight of the North Sea with river inputs and a schematic representation of the circulation (solid line) and dispersion (dotted line). Redrawn from Lacroix *et al.* (2004).

Current knowledge reports that the massive development of *Phaeocystis* colonies after the early spring bloom of diatoms is associated with excess nitrates (NO_3) but low phosphate (PO_4) suggesting that *Phaeocystis* P requirements are supplied by organic forms although not demonstrated. To what extent the *Phaeocystis* dominance affects the ecosystem structure and function and hence the overall yield of harvestable biological resources is not fully known yet. Observational evidence of complex changing planktonic food-webs does however exist (Hansen *et al.*, 1994; Rousseau *et al.*, 2000). Increased understanding of the links between nutrient changes, phytoplankton eco-physiology and ecosystem response is therefore needed to guide the implementation of European regulations for the reduction of land-based nutrient loads to the North Sea. Due to the complexity of bottom-up and top-down controls of marine planktonic food webs, the link between nutrient change and the coastal ecosystem function cannot be understood by simple correlation between events. Mechanistic models which are based on chemical and biological principles and describe ecosystem carbon and nutrient cycles as a function of environmental pressure are ideal tools to handle this complexity. These models are evolving conceptual tools integrating the current knowledge of ecosystem functioning. For this reason they are powerful tools for basic research identifying new research requirements by comparison between model results and observations and by model sensitivity studies. When validated these models can be used to better understand the dynamics of the ecosystem and assess the magnitude and extent of harmful algal blooms (and the related impact) in response to changes in land-based

nutrients and climate. As a first step in this direction the mechanistic biogeochemical MIRO model (Lancelot *et al.*, 2005) was successfully constructed in the scope of the AMORE I project (Lancelot *et al.*, 2004). This model simulates carbon and nutrient cycles, resolving the complex biology associated to *Phaeocystis* and the coupling between the benthic and pelagic realms that characterise this shallow coastal shelf sea ecosystem. The model was first tested and investigated in a multi-box frame (0D-MIRO; Lancelot *et al.*, 2005) and then implemented in a tri-dimensional frame (3D MIRO&CO) by integrating it in the 3D COHSNS model of Lacroix *et al.* (2004). Based on these applications, it is clear that the model is excellent in simulating *Phaeocystis* blooms in the BCZ (Lancelot *et al.*, 2004). However careful analysis of results obtained with the 0D-MIRO and the 3D-MIRO&CO models applied in the Eastern Channel and Southern Bight of the North Sea revealed some failure and weakness (Lancelot *et al.*, 2004) that have to be solved before transferring model results to decision makers and stake-holders. These are:

- The imperfect knowledge of *Phaeocystis* origin and of the mechanisms triggering colony formation which causes MIRO&CO simulation of *Phaeocystis* blooms in the Baie de Seine area where colonies have never been reported.
- The mechanisms of P acquisition by *Phaeocystis* colonies
- The poor description of zooplankton dynamics including the intriguing role of gelatinous organisms such as *Noctiluca*.

Resolving these unknowns for improving the prediction capability of the 0D-MIRO and 3D-MIRO&CO models was the objective of the AMORE II project. Recognizing the multiplicity of processes, changes and forces behind the dynamics of coastal ecosystems, the methodology involved and combined field observations, process-level studies, statistical analysis of long term trends and mathematical modeling in an iterative way. In this methodology the ecological model plays a central role as integrator of new knowledge and prediction tool. Basically new knowledge is first integrated in the ecological module MIRO and tested in a multi-box frame (Lancelot *et al.*, 2005) prior to being integrated in the fully coupled physical-ecological 3D-MIRO&CO model. The improved prediction capacity of the latter is evaluated based on a comparison of simulations with existing or newly collected field data.

Between 2002 and 2006, AMORE II research therefore focused on establishing quantitative and qualitative links between nutrient enrichment, spreading of high-biomass algal blooms (*Phaeocystis* but also the co-occurrent diatom *Guinardia delicatula*), presence of gelatinous zooplankton (mainly *Noctiluca* but also the appendicularian *Oikopleura dioica*) and impact on ecosystem function.

Progress achieved is discussed in the present report in terms of nutrient enrichment and *Phaeocystis* eco-physiology, food-web structure and trophic role of gelatinous organisms, long term trends of *Phaeocystis* blooms and development and prediction capability of mathematical models and ability of models to understand ecosystem dynamics and resolve environmental questions. In accordance and in support to government policy, the upgraded 3D-MIRO&CO is tested for its ability to:

- predict the magnitude and geographical extent of undesirable *Phaeocystis* blooms in the Southern Bight of the North Sea in response to changing nutrient loads and present-day meteorological conditions;
- trace the origin and fate of anthropogenic nutrients in the BCZ distinguishing between in-flowing Atlantic waters, Scheldt, IJzer and Rhine river inputs, local pelagic and benthic recycling and the export to adjacent areas.

3 MATERIAL AND METHODS

The AMORE II methodology involves and combines field observations, process-level studies under field and laboratory conditions and numerical tools (statistical analysis and mathematical models) that are specifically detailed in this section.

3.1 Field and laboratory eco-physiological studies

3.1.1 Field sampling

Field work was conducted aboard RV Belgica and Zeeleeuw. Due to the complex dynamic of the BCZ, the chosen sampling strategy included a high-time resolution survey of surface water core physico-chemical and biological parameters at a reference station for BCZ and seasonal measurements of targeted biological activities according to a geographical grid.

3.1.1.1 Reference station 330

In addition to the existing 1988-2001 time series monitoring of nutrients and diatom-*Phaeocystis* blooms at station 330 (St 330; N 51°26.05; E 002° 48.50; Fig.2), surface seawater was collected on 23 February, 6 April, 10 May, 15 July and 10 September 2004 for electron microscope identification of *Phaeocystis* morphotypes. In 1988, 1993, 1994 and 1998-2001, seawater was analysed for bacteria, protozooplankton and *Noctiluca* abundance and biomass.

3.1.1.2 Geographical surveys

Field work was performed during 10 campaigns from February to September between 2002 and 2005. The geographical grid (Fig. 2) was chosen along inshore-offshore gradients in order to sample different water masses, *i.e.* those influenced by Atlantic vs Scheldt waters. Ten stations in the Channel and the BCZ (Fig. 2) were sampled in February 2004. During these cruises different instruments (Niskin bottles of 5L to 30 L, plankton nets) were deployed for collecting the different biological organisms under study. Seawater was sampled for major nutrients and Chlorophyll *a* (Chl *a*) concentrations, phyto-, bacterio- and nanoproto-plankton enumeration and biomass, suspended particulate matter content (SPM), particulate organic carbon (POC) and detrital DAPI yellow particles (DYP) abundance. Specific samples for electron microscopy were collected for the identification of *Phaeocystis* cell types present along year. Surface seawater samples were taken for dissolved (DOP) and particulate organic phosphorus (POP) and alkaline phosphatase activity (APA) measurements. *Noctiluca* and *Oikopleura* samples were collected for determination of their abundance, biomass, diet and metabolic activities. These organisms were sampled from bottom to surface according to oblique hauls using a 200 µm plankton net but with 30L Niskin bottles at 2-3 depths during *Phaeocystis* blooms due to

clogging of plankton nets. Depth sub-samples were then mixed and concentrated using a 200 µm sieve.

3.1.2 Phytoplankton cultures

Strains BCZ99 and BCZ05 were isolated from St 330 during the *Phaeocystis* colony blooms in spring 1999 and 2005 respectively. Both isolates included spherical colonies and two types of flagellates, a large one produced when colonial cells released from colony after mechanical disruption transform into motile cells within few days (Rousseau *et al.*, 1994) and a small one. The latter was isolated from BCZ05 and maintained as pure culture.

Diatom (*Chaetoceros costatum*, *Rhizosolenia shrubsolei*, *Nitzschia closterium* and *Skeletonema costatum*) cultures set up for running *Noctiluca* feeding experiments were also isolated from BCZ samples.

All pure cultures were maintained in F20 medium as described in Rousseau *et al.* (1990) at 8-11°C and 100 µmol quanta m⁻² s⁻¹ under a 12h:12h light:dark cycle.

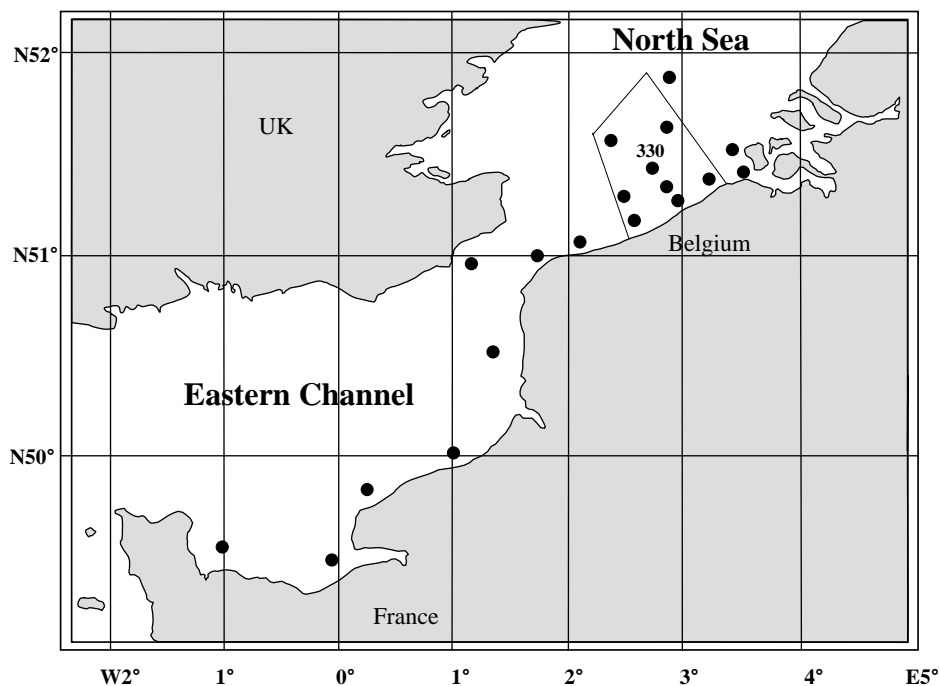


Figure 2: Map of the Eastern Channel and the Southern Bight of the North Sea indicating stations sampled from 1999 to 2004. Borders of the BCZ and St 330 are indicated.

3.1.2.1 Microbial ability of using dissolved organic phosphorus (DOP)

The potential rate of DOP hydrolysis was measured in relationship with biological variables such as Chl *a*, phytoplankton and bacteria biomass. DOP hydrolysis was estimated based on measurement of alkaline phosphatase activity (APA) using

fluorescent substrate analogous 4-methylumbelliferyl- Phosphate (MUF-P, Sigma, St. Louis, USA) which produces fluorescent 4-methylumbelliferone after hydrolysis. The procedure was adapted from the protocol of Ammernan (1991). Potential APA was determined at a saturating substrate concentration of 2000 nM MUF-phosphate during kinetics conducted at in situ temperature and in the dark. During spring, the contribution of phytoplankton and attached bacteria to APA was estimated from two fractionated sub-samples (Total, < 2 μm) obtained by reverse filtration using 2 μm Nuclepore membrane.

3.1.2.2 *Noctiluca* diet and metabolic activities

3.1.2.2.1 *Noctiluca* diet

The diet of *Noctiluca* was determined based on the analysis of food vacuole content. Phytoplankton and protists were identified at the lowest taxonomic level possible, enumerated and their carbon content was estimated. Carbon content of copepod moult was estimated using the dry weight-length relationships of Klein-Breteler *et al.*, (1982) and a contribution of chitin to the dry weight (DW) of 6% (Gervasi *et al.*, 1988). Chitin was converted into carbon using the factor 0.45 gC (gDW chitin)⁻¹. Carbon content of copepod eggs was assumed to be 0.14 pg C μm^{-3} (Kiørboe *et al.* 1985). Faecal pellet carbon content was estimated from biovolume measurements and using a carbon conversion factor of 5.6 10⁻⁷ $\mu\text{g C } \mu\text{m}^{-3}$ (Honjo & Roman, 1978). *Noctiluca* diet and feeding strategy was estimated based on the graphical method of Costello (1990). The analysis is based on a two-dimensional representation of prey-specific relative abundance (% A = $(S_i / S_t) \times 100$) and frequency of occurrence (% F = $(n_i / N) \times 100$) in the diet ; where n_i is the number of *Noctiluca* cells with prey i in vacuole, N the total number of *Noctiluca* cells observed, S_i the number of prey i and S_t the total number of prey. Equivalence between % A and % F indicates a generalist feeding behaviour with the most important preys closed to the top right corner. On the contrary, prey ingested at low occurrence but high abundance indicates a specialized feeding behaviour of the predator.

3.1.2.2.2 *Noctiluca* ingestion and growth

Ingestion experiments were conducted in the laboratory with a natural population of *Noctiluca* collected in April 2005 at St 330. Different prey such as *Phaeocystis* colonies in various growth phases (exponential, early and late stationary) and size, the diatoms *C. compressus*, *R. shrubsolei*, *N. closterium* and *S. costatum* and copepod eggs were offered to *Noctiluca*. Copepod (mainly *Temora longicornis*) eggs were produced by spawning before grazing experiments. Food item was supplied at various concentrations obtained from dilution of the culture with sterile filtered seawater. Three controls without *Noctiluca* were incubated under the same

conditions. Some 24 h prior the experiments, *Noctiluca* cells were acclimated with the selected food item and were then rinsed three times with filtered seawater. Ingestion and growth rates of each prey provided at various concentrations were measured after incubation in the dark for 24 h and 96 h, respectively. At the end of the incubation, phytoplankton, copepod eggs and *Noctiluca* cells were sampled for enumeration. Ingestion rates ($\mu\text{g C d}^{-1}\text{cell}^{-1}$) were calculated using the equations of Frost (1972). Growth rate (μ, d^{-1}) of *Noctiluca* was estimated by fitting the exponential growth curve.

In the natural environment, ingestion rates were estimated from vacuole content using the equation $I = G k$ where G is the mean vacuole content ($\mu\text{g C cell}^{-1}$) and k (min^{-1}) is the vacuole evacuation rate. The latter rate was determined from shipboard digestion experiments where the vacuole content of 40 *Noctiluca* cells was measured kinetically over 12 h. Evacuation rate was then calculated as the slope of the exponential decrease of vacuole content. As a result, k was in average $2.2 \pm 1.0 \cdot 10^{-3} \text{ min}^{-1}$. *Noctiluca* ingestion was then expressed as % of diatom, *Phaeocystis* and copepod eggs standing stock daily consumed by *Noctiluca* population. Copepod eggs standing stock was estimated by the total female copepod biomass recorded at each station and survey, and the average weight-specific egg production of $6.62 \cdot 10^{-2} \mu\text{gC } \mu\text{gC}^{-1} \text{ d}^{-1}$ estimated by Antajan (2004).

The effect of food composition on diet of *Noctiluca* populations was investigated using a redundancy analysis (RDA). In this latter the ordination of the dependant variables (% occurrence of prey items in the *Noctiluca* diet) is constrained by linear combinations of the food parameters. The significance of RDA was tested with Monte Carlo testing based on 1000 permutations. RDA was performed with ADE-4 software (Thioulouse *et al.*, 1997), of which the package can be freely downloaded from the website <http://pbil.univ-lyon1.fr/ADE-4.html>. Fitting of least squares linear as well as nonlinear regression was performed using Sigmaplot (V.7, SPSS). Accuracy was evaluated based on r^2 , p values, and pattern of residuals.

3.1.2.3 *Oikopleura* ingestion rates

Ingestion rate of *Oikopleura* on total particles was estimated based on the gut food-volume content (GVC) method (López-Urrutia *et al.*, 2003). Trunk length (TL) and the dimensions of food parcels (both unpacked and packed in faecal pellets) of 40 organisms were measured by inverted light microscopy at each sampling station. A total of 3023 individuals were examined. For each station, GVC was then classified into 50 μm TL size classes, and the average of GVC was calculated for each size class. Ingestion rate on autotrophic prey was estimated from gut chl *a* content according to the method of Mackas & Bohrer (1976) and using the equation of López-Urrutia & Acuna (1999).

3.1.3 Analytical methods

3.1.3.1 Physico-chemical and biological parameters

Salinity was measured at a depth of 3 m with a Seacat thermosalinograph (SBE21, Washington, USA). Major nutrient [NO_3 , NH_4 , $\text{Si}(\text{OH})_4$ and PO_4] concentrations were determined on 0.45 μm filtered seawater according to the colorimetric methods described in Grasshof *et al.* (1983). DOP and POP concentrations were measured after persulfate oxidation of organic matter in alkaline conditions and determined spectrophotometrically as PO_4 . Chl *a* concentrations were determined on 90 % (v:v) acetone extracted particulate material isolated on glass fiber filters (GF/C, Whatman) and measured by spectrophotometry using the method and equations recommended by Lorenzen (1967). SPM was determined by gravimetry. POC was measured with a CHN analyser (Interscience) after acidification of the particulate matter with HCl 1N.

3.1.3.2 Identification, enumeration and biomass of organisms

Phytoplankton. Some 10-50 mL of phytoplankton sub-sample, preserved with 1% lugol-glutaraldehyde solution and stored at 4°C in the dark, were analysed under inverted microscopy (Leitz Fluovert, Germany) according to the Utermöhl method. At least 400 cells were enumerated in each sample. Magnification was chosen according to cell or colony size: 40X or 100X for *Phaeocystis* colonies, and 100X or 200X for diatoms. *Phaeocystis* morphotypes from strains BCZ99 and BCZ05 and field samples were analysed at a magnification of 1000X. The size of 50 cells of each morphotype was measured on alive and fixed cells by comparison with a graduated reticule. Diatom carbon biomass was calculated on the basis of cell concentration and specific biometry using the size-dependant density relationship recommended by Menden-Deuer and Lessard (2000). The carbon biomass of *Phaeocystis* colonies was estimated by biovolume measurement (Rousseau *et al.*, 1990).

SEM analysis. *Phaeocystis* morphotypes were observed under SEM on material preserved with 1:1 (v:v) lugol-glutaraldehyde solution at a 10% final concentration. Preserved samples were centrifuged on a plastic coverslip coated with Poly-L-Lysine, dehydrated in a gradient of ethanol concentrations and processed according to the critical point drying procedure with a Balzer's equipment. Samples were then gold coated and observed with a field emission SEM (HITACHI 4500, Japan) at the Centre de Caractérisation de la Matière, Service de Microscopie électronique à balayage et Microanalyse (Université de Perpignan, France).

Bacterio- and nanoproto-plankton. Bacteria, auto- and hetero-trophic nanoflagellates were enumerated by epifluorescence microscopy after DAPI staining following the method of Porter & Feig (1980). The carbon biomass of protists was estimated from biovolume measurements using the equation $\log C (\mu\text{gC}) = 0.94 (\log V (\mu\text{m}^3)) - 0.6$ for

flagellates (Smayda, 1978), and the conversion factor $0.16 \text{ pgC } \mu\text{m}^{-3}$ for ciliates (Putt & Stoecker, 1989). Bacterial biovolumes were calculated by treating rods and cocci, respectively, as cylinders and spheres (Watson *et al.*, 1977) and converted to carbon biomass by using the biovolume dependant conversion factor of Simon & Azam (1989). DYP were enumerated after DAPI staining procedure.

Gelatinous zooplankton. *Noctiluca* and *Oikopleura* abundance was determined on 4% formalin fixed samples, using a stereomicroscope. *Noctiluca* cell diameter and *Oikopleura* trunk length were measured by light microscopy at a magnitude of 200 X. *Noctiluca* carbon biomass was calculated using a conversion factor of $2.41 \text{ fg C } \mu\text{m}^{-3}$ as measured from elemental analysis (Breton *et al.*, in preparation). Carbon biomass of *Oikopleura* was calculated based on the average trunk length (TL) of 40 organisms, using the equation $\log \text{DW } (\mu\text{g}) = 2.49 \log \text{TL } (\mu\text{m}) - 6.22$ (Paffenhöfer, 1976) and assuming a C:DW ratio of 0.45 (Uye, 1982).

3.1.3.3 Identification of the *Phaeocystis* species based on molecular analysis

DNA extraction, SSU rDNA amplification and sequencing. Some 50 mL of BCZ99 culture were centrifuged at 7500 rpm before DNA extraction using a modified CTAB protocol (Ishida *et al.*, 1999). The entire SSU rDNA gene was amplified using the eukaryotic primers Euk 328f (5'-ACCTGGTTGATCCGCCAG-3') and Euk 329r (5'-TGATCCTTCYGCAGGTTTAC-3') as previously described in Moon-van der Staay *et al.* (2001). PCR products were cloned using the TOPO TA cloning kit (Invitrogen) following the manufacturer's recommendations. Complete sequences of SSU rDNA were determined using the Plate-forme Séquençage Génotypage (GENOMER) at the Station Biologique of Roscoff, France.

Phylogenetic analyses. The SSU rDNA sequence of strain BCZ99 was deposited in GenBank under accession number (Acc No AY851301). The sequence was compared to existing *Phaeocystis* spp. SSU rDNA full-length sequences available in GenBank. The MP, NJ and ML methods were used for the phylogenetic analysis. *Emiliania huxleyi* (Prymnesiophyceae) was used to root the trees. Different nested models of DNA substitution and associated parameters were estimated using Modeltest 3.06 (Posada & Crandall, 1998). The Akaike Information Criterion (AIC) in Modeltest selected a TrN+I (Tamura-Nei including the proportion of invariable sites; Tamura & Nei, 1993) model of DNA substitution. NJ, MP and ML were done using the PAUP*4.0b10 version (Swofford, 2002). Bootstrap values for NJ and MP were estimated from 1000 replicates.

3.2 Long-term trend analysis of diatom and *Phaeocystis* blooms

The effect of climate variability (NAO index) and human activities (Scheldt nutrient loads) on the magnitude of diatom and *Phaeocystis* blooms in BCZ, was investigated

by conducting a serial statistical analysis based on a comprehensive suite of nutrient loads, hydro-meteorology, and phytoplankton collected at St 330 between 1988 and 2001.

3.2.1 Data sets

3.2.1.1 Physical and biological data at St 330

The time series data was collected at St 330 (N 51°26.05; E 002° 48.50; Fig. 2). From 1988 to 2001, subsurface seawater was sampled at weekly intervals except during winter and summer, when the interval was 2 weeks. From 1988 to 1991 and in 2001, the survey period only ran from February to mid-June. Surface seawater was analysed for major nutrients, suspended matter, temperature, salinity, Chl *a* and phytoplankton.

3.2.1.2 Hydrodynamics

Monthly English Channel Water Inflow (ECWI) in the BCZ was calculated between 1992 and 2000 using a conventional, vertically integrated, two-dimensional model with a resolution of 5' in longitude and 2.5' in latitude (de Vries *et al.* 1995; see Breton *et al.*, 2006 for details).

Freshwater influence of Scheldt at St 330 was estimated based on salinity difference between St 330 (S_{330}) and station S04 (S_{S04}) in the Scheldt estuary (51°21 N; 3° 49.8 E), normalized to S_{S04} . S_{S04} data (1992-1997) were downloaded from the ICES website (<http://www.ices.dk/ocean/>). Monthly Scheldt runoff ($m^3 s^{-1}$) was obtained from the Department of Environment and Infrastructure (Ministry of Flemish Community, Belgium).

3.2.1.3 NAO index and meteorological data

Monthly NAO and winter NAO_w index were downloaded from the National Center for Atmospheric Research website (<http://www.cgd.ucar.edu/cas/jhurrell/indices.html>).

Meteorological data from 1987 to 2001 was obtained from the Royal Institute of Meteorology of Belgium. Daily rainfall ($mm d^{-1}$) corresponded to the average of 20 stations distributed in the Scheldt watershed. Wind speed ($m s^{-1}$) and direction (0-360°) data were taken at the coastal meteorological station of Middelkerke every 6 hours. Southwesterly (SW) and northerly and easterly (N+E) winds were considered to be originating from sectors 180°-270° and 270°-180° respectively. The magnitude of SW and N+E winds was calculated as the product of wind speed ($m s^{-1}$) and persistence (number of days) in each direction.

3.2.2 Statistical analysis

Correlations between month-to-month variations of diatom biomass and climatic, meteorological and hydrological variables were computed for monthly averaged data using a cumulative sum (Cusum) function (e.g., Beamish *et al.*, 1999):

$$Cusum = \sum_{t_i}^{t_f} (x_t - \bar{x})$$

where x_t is the monthly averaged variable at time t (varying between initial t_i and final t_f), and \bar{x} is the variable averaged over the whole period of investigation. This function is such that it attributes less weight to single values. In Cusum plots, positive and negative slopes reflect increasing and decreasing trends respectively. Prior to Cusum processing, monthly data were $\log(x+1)$ -transformed to stabilize the variance and give less weight to outliers. They were then deseasonalized using the Census I method (Makridakis *et al.*, 1983). However deseasonalization was not performed on the monthly NAO index and wind magnitude data, which do not display seasonal variation. Regression analysis was then conducted on Cusum data with Pearson coefficient analysis (SYSTAT version 8, SPSS Inc), and cross-correlation was used to detect a possible delayed effect. Statistical significance was set at $p < 0.05$.

Because of the transient nature of *Phaeocystis* blooms as compared to those of diatoms, the use of Cusum was not relevant. The magnitude of *Phaeocystis* and diatom blooms was therefore estimated by integrating over time the phytoplankton data for the spring bloom period. Correlations were calculated between *Phaeocystis* and diatom spring blooms, NAO_w , wind magnitude, and the available nitrate stock. The latter was estimated by integrating concentrations between December and March-April, *i.e.*, up to the date of *Phaeocystis* onset. Fitting of least-squares nonlinear regression was performed using Sigmaplot (version 7, SPSS Inc). Accuracy was evaluated based on r^2 , p values, and the pattern of residuals.

3.3 Mathematical modelling

3.3.1 Model description

3.3.1.1 The biogeochemical model MIRO

Basically, MIRO is a mechanistic biogeochemical model describing C, N, P and Si cycling through aggregated components of the planktonic and benthic realms of *Phaeocystis* dominated ecosystem (Lancelot *et al.*, 2005). Its structure includes thirty-eight state variables assembled in four modules describing the dynamics of phytoplankton (diatoms, nanoflagellates and *Phaeocystis*), zooplankton (copepods and microzooplankton), dissolved and particulate organic matter (each with two classes of biodegradability) degradation and nutrients [NO_3 , NH_4 , PO_4 and $Si(OH)_4$]

regeneration by bacteria in the water column and the sediment. Equations and parameters were formulated based on current knowledge on the kinetics and the factors controlling the main auto- and heterotrophic processes involved in the functioning of the coastal marine ecosystem. These are fully documented in Lancelot *et al.* (2005) and www.int-res.com/journals/suppl/appendix_lancelot.pdf. Further numerical development of MIRO included an improvement of the diagenetic module as well as the addition of a chemical module describing the carbonate system and air-sea CO₂ exchanges.

3.3.1.1.1 The diagenetic model.

The diagenetic model (Gypens *et al.*, submitted) describes organic matter mineralization, the resulting C, O₂, N and P diagenetic processes and the sediment-water nutrient exchange fluxes as a function of bottom water nutrient concentration, total sediment organic matter mineralisation, temperature and the characteristics of the sediment (porosity, tortuosity, bioturbation). Basically the sediment depth is partitioned in two functional layers: an oxidized surface zone (oxic layer) extending from the sediment surface to the oxygen penetration depth (z_n) and below this depth, a reduced zone (anoxic layer) where biogeochemical processes are described with a different set of equations.

In the oxic zone ($z < z_n$), organic matter mineralization uses O₂ and releases NH₄, part of which is nitrified to NO₃. Below z_n, O₂ concentration is zero, whilst NH₄ is produced and NO₃ is consumed by denitrification (Billen, 1982). The NH₄ equation also includes its fast adsorption as an instantaneous equilibrium reaction. Compared to the current version (Billen *et al.*, 1989), the new diagenetic module now considers O₂ consumption due to the re-oxidation of reduced substances formed in the anoxic layer (Mn²⁺, Fe²⁺, NH₄,...) and diffusing into the oxic layer (Gypens *et al.*, submitted). The P diagenetic module (Slomp *et al.*, 1996) describes the changes with sediment depth of pore water phosphate (PO₄) and of Fe-bound P. Basically biodegradable organic P is mineralized and the resulting PO₄ is released in the pore water. PO₄ sorption is described as two simultaneous, reversible reactions: an instantaneous equilibrium reaction and a first order rate (Slomp *et al.*, 1998). In the oxidized layer, a substantial fraction of PO₄ can be adsorbed to sediment Fe oxides resulting in a Fe-bound P formation (e.g. Krom & Berner, 1980b; Slomp *et al.*, 1998). Reversible equilibrium sorption of PO₄ leads to the presence of sorbed P in the oxic and anoxic layers. In the anoxic layer, PO₄ is produced by either organic matter degradation or by P desorption due to the reduction of Fe oxides. Moreover, the PO₄ concentration in the anoxic pore water may become high enough for the precipitation of authigenic carbonate fluorapatite (CFA; Van Cappellen & Berner, 1988). Whereas we take into account the effect of the latter process on the PO₄ concentration, the formation of CFA does not need to be modelled explicitly, as the process is not reversible. Hence,

in contrast to the original paper (Slomp *et al.*, 1996), we only describe pore water PO₄ and Fe-bound P.

3.3.1.1.2 The carbonate system and air-sea CO₂ exchange.

A description of the carbonate system and air-sea CO₂ exchange (Hannon *et al.*, 2001) has been incorporated in the MIRO code of Lancelot *et al.* (2005) to investigate the contribution of diatom and *Phaeocystis* blooms to the seasonal dynamics of air-sea CO₂ exchanges in the Eastern Channel and Southern Bight of the North Sea, with focus on the eutrophied Belgian coastal waters (Gypens *et al.*, 2004). The physico-chemical module of Hannon *et al.* (2001) details the carbonate system in seawater and calculates CO₂ exchange between the surface water and the atmosphere. The speciation of the carbonate system, in particular pCO₂, is calculated based on the knowledge of DIC and total alkalinity (TA), using stoichiometric relationships and apparent equilibrium constants, which are function of temperature, pressure and salinity (Weiss, 1974; Millero *et al.*, 1993). DIC and TA are computed taking into account, respectively, the biological uptake or release of carbon and the phytoplankton assimilation of NO₃, all provided by the MIRO model. Air-sea CO₂ fluxes are calculated from the pCO₂ gradient across the air-sea interface and the gas transfer velocity estimated from wind speed and using the parameterisation of Nightingale *et al.* (2000). The latter was chosen among several existing empirical formulations since it was established from dual tracer experiments in the Southern Bight of the North Sea.

3.3.1.2 The coupled Hydrodynamical-Biogeochemical MIRO&CO model

The MIRO biogeochemical model described in Lancelot *et al.* (2005) has been coupled to the 3D hydrodynamical COHSNS model (Lacroix *et al.*, 2004) to simulate the transport and dynamics of inorganic and organic nutrients, phytoplankton, bacterioplankton and zooplankton biomass in the eastern Channel and Southern Bight of the North Sea.

The 3D hydrodynamic model solves the continuity, momentum, heat and salinity transport equations on a staggered Cartesian, sigma coordinate grid with an explicit mode-splitting treatment of the barotropic and baroclinic modes. Advection of scalar quantities is discretised by a direction-split Total Variation Diminishing (TVD) scheme. Vertical diffusion is modelled using an evolution equation for turbulent kinetic energy and a quasi-parabolic vertical profile for turbulence macrolength scale. Minimal vertical diffusion and viscosity coefficients of 10⁻⁶ m² s⁻¹ are used. Horizontal diffusion is not considered explicitly, but the process of horizontal diffusion arising from the combination of horizontal advection with vertical diffusion is resolved. Advection of momentum is treated with a first order upwind scheme. Full details and original references can be found in Ruddick (1995) and Luyten *et al.* (1999).

3.3.2 Model implementation

3.3.2.1 Multibox MIRO

In a first step, the upgraded MIRO model was implemented in a multi-box frame delineated on basis of the hydrological regime and river inputs. In order to take into account the cumulated nutrient enrichment of Atlantic waters by the Seine and Scheldt rivers, three successive boxes, assumed to be homogeneous (the ‘oceanic’ Western Channel WCH, the French Coastal Zone FCZ and the BCZ; Fig. 3), were chosen in the domain between the Baie de Seine and the northern limit of BCZ. Each box has its own morphological characteristics (Table 1 in Lancelot *et al.* 2005) and is treated as an open system, receiving waters from the SW adjacent box and exporting water to the NE. The seasonal variation of the state variables was calculated by solving the different equations expressing mass conservation according to the Euler procedure. A time step of 15 min was adopted for computation of the numerical integration.

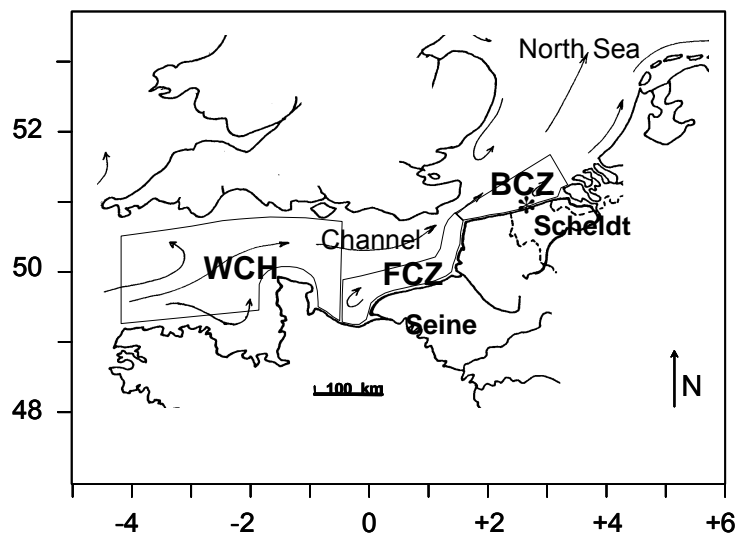


Figure 3: The OD multi-box frame of MIRO with position of St 330

3.3.2.2 MIRO&CO-3D

The coupled MIRO&CO-3D model has been set up for the region between 4° W (48.5°N) and 52.5°N (4.5°E) with the bathymetry shown in Fig. 4 using a 109 by 97 horizontal grid with resolution 5' longitude (approx. 5.6 km) by 2.5' latitude (approx. 4.6 km) and with 5 vertical sigma coordinate layers. The model is run with mode-splitting time steps of 60 s and 900 s respectively for 2D and 3D calculations. All details of its implementation and the description of forcing, boundary and initial conditions can be found in Lacroix *et al.* (2007a).

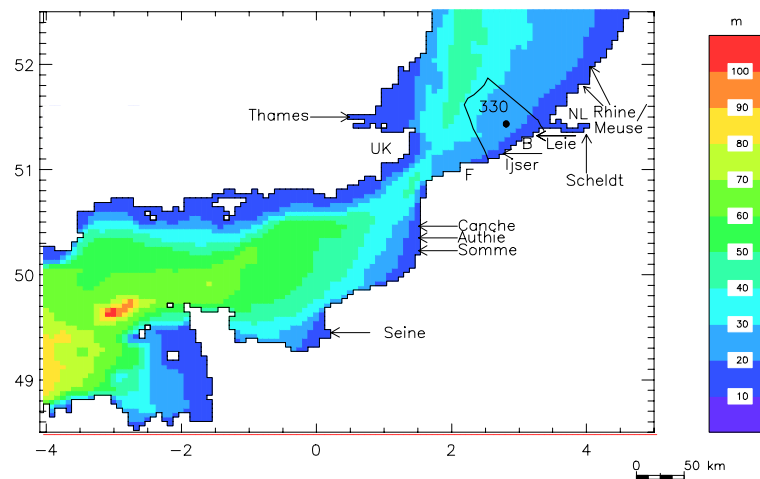


Figure 4: Bathymetry of the Southern North Sea and Channel model and geographical domain of MIRO&CO-3D

Compared to the 0D multi-box implementation, two key forcings (light penetration and river inputs) were modified in order to take into account the increased spatial resolution of MIRO&CO-3D.

The light penetration is described by a new algorithm (KPARv1) estimating for each grid the visible light (PAR) attenuation coefficient as function of: (i) non-algae particle concentration, (ii) Chl *a* (computed by MIRO&CO), (iii) coloured dissolved organic matter (CDOM) absorption at 443nm estimated from salinity (computed by MIRO&CO) and (iv) depth. The non-algae particle concentration is estimated from total suspended matter (TSM) minus a fraction (function of MIRO&CO Chl *a*) representing the algae contribution. A TSM seasonal climatology, spatially averaged to match the model grid cells, has been built from 1997-2002 SeaWiFS images using the algorithm of Nechad *et al.* (2003). Between seasons, TSM is temporally interpolated. The satellite-derived TSM images presently available are insufficient for increasing the temporal resolution and for accounting for the interannual variability. The KPARv1 model is based on a look up table which has been generated using typical specific inherent optical properties for North Sea water in a similar way to the model of Buiteveld (1995). This provides a much better representation of spatial variability of light attenuation for the whole range of conditions from the deep and relatively clear water of the central English Channel to the turbid coastal waters of the Belgian and Dutch coasts.

Nutrient inputs from rivers are advected from the estuaries by simulated MIRO&CO-3D currents.

3.3.3 Validation data

3.3.3.1 Time-series

Biogeochemical data sets for model validation were obtained from existing time series at 3 reference stations (see Fig. 2) in WCH (N 48° 43.30; W 03° 50.00), FCZ (N 50° 44.50; E 01° 30.80) and BCZ (St 330: N 51° 26.05; E 02° 48.50). The WCH and FCZ data sets are limited to the 1989–1993 period (Lancelot *et al.*, 1994) and include temperature, nutrients and phytoplankton data (Chl *a*, diatoms and *Phaeocystis*). For the BCZ a better time series and state variable resolution is available (see 3.2.1.1).

DIC was calculated from TA and pCO₂ measured between 1996 and 1999 in the BCZ and WCH (Borges & Frankignoulle, 1999; 2002; 2003).

3.3.3.2 MERIS-derived surface Chl *a* images

Validated MERIS products for Belgian waters in spring 2003 (Park *et al.*, 2003) were used to assess the MIRO&CO-3D capability of describing average regional trends. Basically, each MERIS image was spatially averaged to match the model grid cells. These daily images were then aggregated to give weekly binned images, which were also further processed to yield monthly images (see for details Lacroix *et al.*, 2007a).

3.3.4 Model sensitivity analysis

Two approaches were used to analyze the sensitivity of MIRO state variables to the parameter choice and address the question of eutrophication and formation of *Phaeocystis* blooms. These are the variational adjoint method (Lawson *et al.*, 1995; 1996; Spitz *et al.*, 1998; 2001) and a sensitivity factor (*e.g.* Fasham *et al.*, 1993) to perturbations of individual parameters. Additionally, we analyzed the impact of any parameter perturbation on the magnitude and timing of the spring and summer phytoplankton blooms.

The variational adjoint method determines an optimal solution by minimizing an objective function, the cost function, which measures the difference between the model solution and the available observations. Most minimization algorithms [*e.g.* the subroutine N1QN3 from Gilbert & Lemaréchal (1989)] require the computation of the gradient of the cost function with respect to the control variables, *e.g.* model parameters. This can be done using the adjoint model (see description of the technique in Lawson *et al.*, 1995; Spitz *et al.*, 1998; 2001).

The sensitivity of MIRO simulations to the parameters described in www.int-res.com/journals/suppl/appendix_lancelot.pdf was assessed based on a twin experiment. In this experiment, the data in the cost function and weights are the model state variable values obtained with the reference parameter set and the model

equivalents are obtained with a perturbed set of parameters. Under these conditions the parameters that require the lowest numbers of iterations to approach their reference value during the minimization procedure determine the set of parameters that impact the most on the model state variables.

The perturbation of individual parameters and their effect on all the model variables with a particular interest on the diatom and *Phaeocystis* maximum biomass were investigated using a Monte Carlo approach (Metropolis & Ulam, 1949) and calculating a normalized sensitivity factor $S_c(k)$:

$$S_c(k) = \frac{\frac{C(k) - C_s}{C_s}}{\frac{k - k_s}{k_s}}, \quad (1)$$

where C_s is the value of the state variable C obtained with the reference parameter value k_s and $C(k)$ that obtained with the perturbed value k (Fasham *et al.*, 1993). The higher the value of $S_c(k)$ is the higher the influence of the parameter k on the state variable C is. Since it is not guaranteed that a decrease or an increase of a given parameter with respect to its reference value will lead to the same result, we can choose to perturb the parameter reference value by an amount of $\pm \alpha$ and compute the following sensitivity factor:

$$S_c(k) = \frac{C_{(s+\alpha)} - C_{(s-\alpha)}}{k_{(s+\alpha)} - k_{(s-\alpha)}} \quad (2)$$

where $k_{(s+\alpha)}$ and $k_{(s-\alpha)}$ correspond to the reference value increased and decreased by α , respectively. $C_{(s+\alpha)}$ and $C_{(s-\alpha)}$ are the values of the state variable C (or its maximum) using $k_{(s+\alpha)}$ and $k_{(s-\alpha)}$ as parameters. Finally, the sensitivity of N model state variables was addressed by computing the global sensitivity factor S_g :

$$S_g = \frac{1}{N} \sum_{i=1}^N S_{ic}(k) = \frac{1}{N} \sum_{i=1}^N \frac{C_{i(s+\alpha)} - C_{i(s-\alpha)}}{k_{i(s+\alpha)} - k_{i(s-\alpha)}} \quad (3)$$

This global sensitivity factor can be used to rank the model parameters based on the effect that they have on the model state variable values. The software FEMME was used to run simultaneously the Monte Carlo simulations and compute the global sensitivity factor (Soetaert *et al.*, 2002).

4 RESULTS AND DISCUSSION

4.1 Eco-physiological studies

4.1.1 *Phaeocystis* species identification, morphotypes and life cycle

4.1.1.1 Species identification.

Despite numerous investigations devoted to *Phaeocystis* ecophysiology, confusion still exists on the identification of the *Phaeocystis* species blooming in the Eastern Channel and the Southern Bight of the North Sea. Based on colony morphology, *i.e.* a globular shape (Antajan *et al.* 2004), physiological and biochemical properties (Baumann *et al.*, 1994; Jahnke & Baumann, 1987; Vaultot *et al.*, 1994), it is currently admitted that the *Phaeocystis* species forming large blooms during spring in the Southern Bight of the North Sea is *P. globosa*. However, this was not confirmed by molecular methods such as SSU rDNA sequence analysis.

The full-length sequence of SSU rDNA was therefore determined for *Phaeocystis* strain BCZ99 (Rousseau *et al.*, submitted) and compared with the full-length SSU rDNA sequences available in GenBank for *Phaeocystis*. Similar SSU rDNA phylogeny was obtained using maximum parsimony (MP), neighbour-joining (NJ) and maximum likelihood (ML) methods. A ML tree with bootstrap values for NJ/MP is shown in Fig.5. The phylogenetic reconstruction identifies five described *Phaeocystis* species, *i.e.* *P. globosa*, *P. pouchetii*, *P. antarctica*, *P. cordata* and *P. jahnii* in agreement with previous analyses (Edwardsen *et al.*, 2000; Lange *et al.*, 2002; Zingone *et al.*, 1999). Among undescribed species, strain PCC559 (PLY559), an unicellular strain from North Atlantic, is closely related to *P. jahnii* as shown by Lange *et al.* (2002). The environmental sequence OLI51004, originating from the warm waters of the Equatorial Pacific, is closer to *P. globosa* but is separated as a sister group in all bootstrap analyses (Moon-van der Staay *et al.*, 2000). This phylogeny confirms that BCZ99 unambiguously belongs to the *P. globosa* clade, which regroups strains from cold-temperate and tropical waters (Lange *et al.*, 2002). This study suggests, however, that the *P. globosa* group is not homogenous, strains BCZ99 and SK35 constituting a small subgroup (Fig. 5). Interestingly, BCZ99 and SK35 are the only two isolates sequenced up to now that originate from the southern North Sea. Strain SK35 was isolated from the German Bight, close to Helgoland (Medlin *et al.*, 1994), the type locality given by Scherffel (1900) for *P. globosa*. These two strains can therefore be considered as representatives of the original *P. globosa*. The genotypic differentiation within the *P. globosa* clade suggests that sub-species or cryptic species may exist within this clade as suggested by Vaultot *et al.* (1994) who separated North European from tropical *P. globosa* strains based on their pigment composition and genome size differences.

4.1.1.2 *P. globosa* morphotypes in cultures and in the field.

Our current knowledge of *Phaeocystis* cell types relies on a composite of investigations combining light (LM), transmission (TEM) and scanning electron (SEM) microscopy as well as flow cytometry. The number and role of different cell types involved in *Phaeocystis* life cycle is however still debated (Lancelot & Rousseau, 2002). The cell morphology of only one type of motile cell, the haploid flagellate, was examined in details with electron microscopy (Parke *et al.*, 1971; Vaultot *et al.*, 1994). The precise morphological description of the other cell types using SEM is still missing. This precludes the complete understanding of *Phaeocystis* life cycle and its controlling mechanisms.

Light and scanning electron microscope observation of BCZ99 and BCZ05 subcultures, identifies 3 morphologically different cell types of *P. globosa*: the colonial cell (Fig. 6A,B), and two types of flagellates (Fig. 7E-F, 8). The analysis reveals some important morphological characters not described up to now. Colonial cells, which are embedded in a mucilaginous matrix, have a size of $7.92 \pm 0.96 \mu\text{m}$ when alive and $5.98 \pm 0.63 \mu\text{m}$ when preserved in agreement with previous observations (Kornmann, 1955; Peperzak *et al.*, 2000). These diploid cells (Cariou *et al.*, 1994; Vaultot *et al.*, 1994) have 2-4 parietal chloroplasts and are deprived of body scales, haptonema, and flagella (Fig. 6A-B). Never reported before from the few existing SEM micrographs of colonial cells, two appendages of very reduced length (Fig. 6 A-B) are located on their apical pole. These appendages were visible on a *P. jahnii* cell (Fig. 30 in Zingone *et al.*, 1999) although not described and have been recently observed on *P. antarctica* colonial cells (Rousseau *et al.*, 2007). This suggests that they might be specific to the colonial morphotype. Within 24 hours after release from the colony, colonial cells progressively transform and acquire two flagella and a haptonema (Fig. 6C-F). Flagella develop from the lengthening of the appendages existing in colonial cells. Flagellate formation from colonial cell has been previously reported (Kornmann, 1955; Rousseau *et al.*, 1990; Cariou *et al.*, 1994; Kayser, 1970; Rousseau *et al.*, 1994) but never observed using high resolution microscopy. The SEM observations provide also the first evidence that these flagellates lack scales, filaments and stars (Fig. 6E-F; Rousseau *et al.*, 2007). These flagellates have the same size range as colonial cells *i.e.*, $7.4 \pm 0.78 \mu\text{m}$ when alive and $5.95 \pm 0.5 \mu\text{m}$ when fixed. We also conclude that this flagellate is diploid as no ploidy change was found during the transformation of colonial cells into flagellates (Cariou *et al.*, 1994; Rousseau *et al.*, 1994). These flagellates are able to rapidly form new colonies within a day after adhesion to a surface (Kornmann, 1955; Kayser, 1970; Cariou *et al.*, 1994; Rousseau *et al.*, 1994). It is not clear however if it is able to mitotically divide. Its rapid transformation into a colony suggests rather a short-lived stage (Kornmann, 1955; Rousseau *et al.*, 1994).

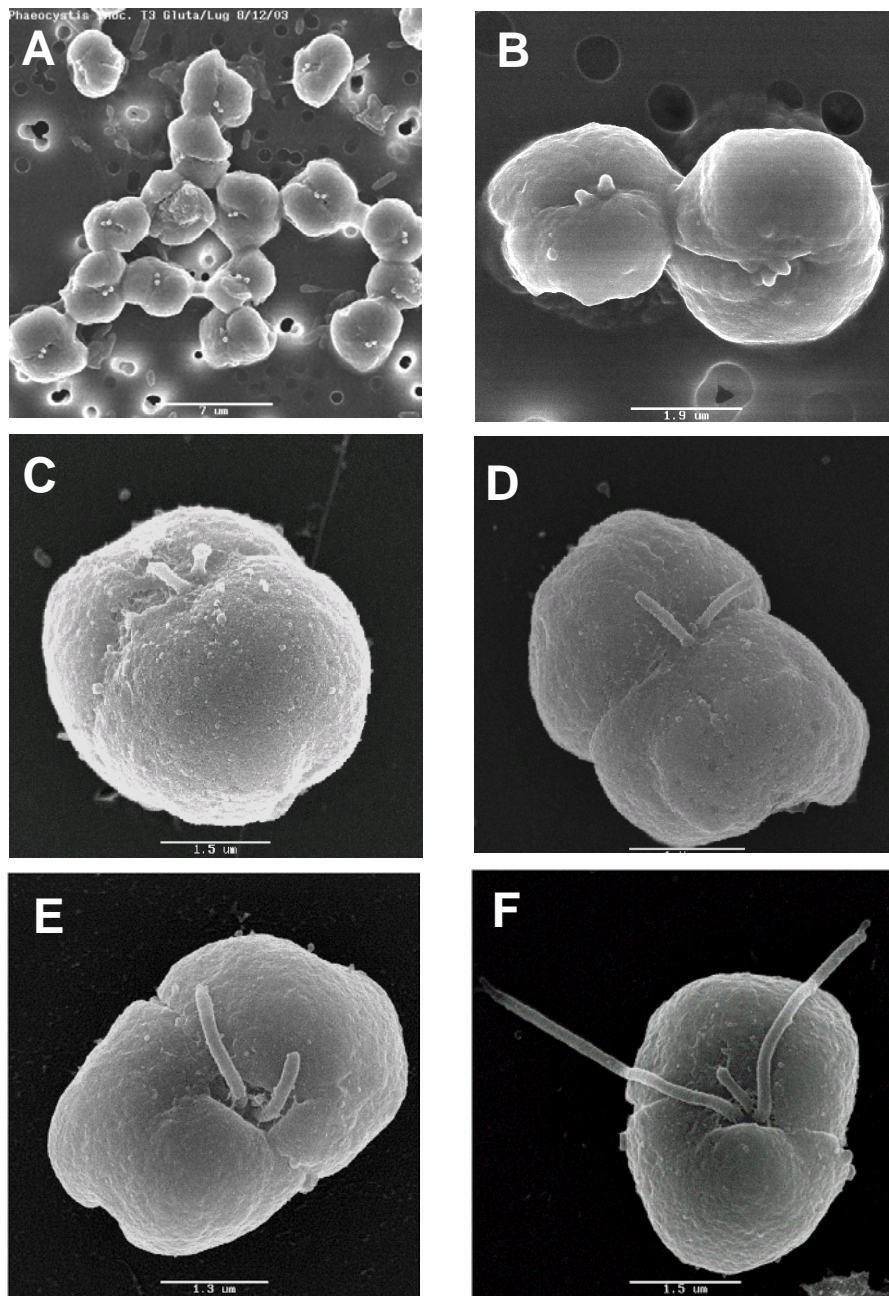


Figure 6: SEM micrographs of the diploid stage of *P. globosa*.
 A-B) Colonial cells of strain BCZ99 showing the two short appendages;
 C-F) transformation of colonial cell into diploid flagellate deprived of organic scales.

The third morphotype, a smaller flagellate, has two equal flagella and a short haptorium characterized by a distal swelling (Fig. 7D-E). They have a rounded shape, and are smaller than colonial cells, with a diameter of $4.65 \pm 0.56 \mu\text{m}$ alive and $3.88 \pm 0.51 \mu\text{m}$ when fixed in agreement with previous measurements (Kornmann, 1955; Parke *et al.*, 1971; Peperzak *et al.*, 2000). Cells are covered with organic scales with microfibrils arranged radially and upstanding rims (Fig. 7F). These cells possess superficial vesicles (Fig. 5E) which release star-forming filaments (Fig. 7B-E). The function of filaments is unknown. It has been hypothesized that they could play a role in mating as these flagellates are haploid and could serve as gametes

(Vaulot *et al.*, 1994). Filaments could also act as anchors for attachment to structures (Chrétiennot-Dinet, 1999), or alternatively have a role in defense against grazers (Dutz & Koski, 2006). These cells are capable of rapid vegetative reproduction (Kornmann, 1955; Parke *et al.*, 1971; Rousseau *et al.*, 1994; Vaulot *et al.*, 1994).

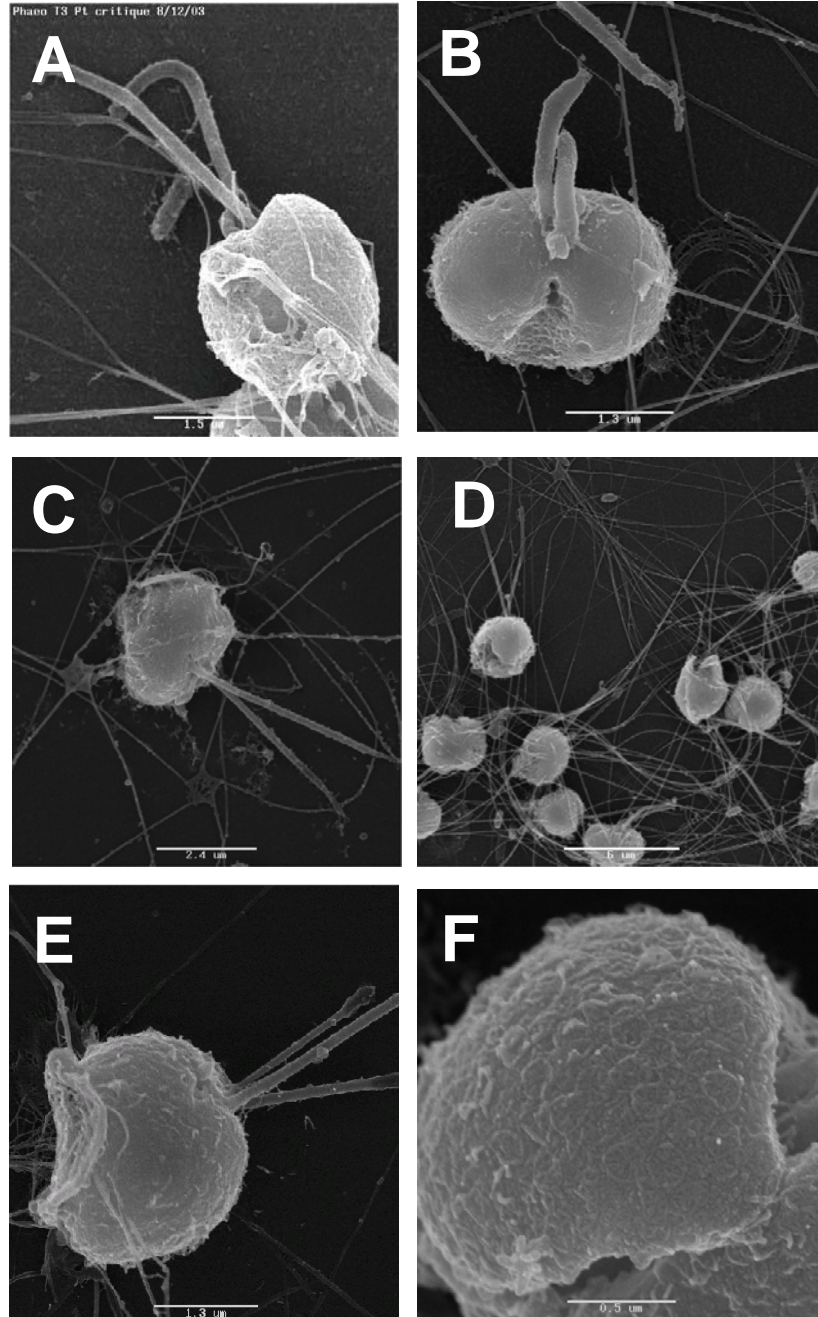


Figure 7: SEM micrographs of the haploid flagellates of *P. globosa* from strain BCZ99 and BCZ05 showing (A-E) 2 flagella, (A, B, E) haptonema with the distal swelling, (F) scale coverage and (A-E) filaments.

SEM analysis of samples collected at different periods of the year in the Channel and Southern Bight of the North Sea and BCZ show that haploid flagellates represent the life stage persisting in the water column between blooms of *Phaeocystis* colonies (Rousseau *et al.*, 2007). They are massively formed within colonies at the end of blooms and persist at cell densities varying from 80-220 10^3 cells L⁻¹. Colonial cells were recorded only during blooms while diploid flagellates were not observed in our field samples.

4.1.1.3 The haploid-diploid life cycle of *P. globosa*.

The occurrence of haploid and diploid morphologically different cell types and the ability of both morphotypes to divide mitotically support the existence of a haploid-diploid life cycle in *P. globosa* (Rousseau *et al.*, 2007). In such life cycle, haploid and diploid stages are related by sexual processes, *i.e.* meiosis and syngamy (Valero *et al.*, 1992; Houdan *et al.*, 2004). With such alternation of morphologically different haploid and diploid generations, *P. globosa* shares the features of most Haptophyceae (Houdan *et al.*, 2004). Based on available information from cultures and field studies, the *P. globosa* haploid-diploid life cycle has been reconstructed (Fig. 8; Rousseau *et al.*, 2007). The occurrence of haploid flagellates in the water column between blooms of diploid colonial cells provides evidence that *P. globosa* colony bloom initiation and termination involve sexual processes, with the length of the diploid phase being restricted to the colony blooms (Fig. 8). The formation of a diploid non-motile colonial cell from haploid flagellates implies that syngamy must occur at the time of colony bloom initiation. Conversely, meiosis is necessary to form haploid flagellates from diploid colonial cells. This may well occur during the massive production of haploid flagellates within colonies often reported at the end of the *P. globosa* bloom, before disappearance of the colonial stage (*e.g.* Rousseau *et al.*, 1994; Peperzak *et al.*, 2000). Besides sexual reproduction, the vegetative reproduction of the diploid stage occurs through two distinct pathways involving colonial cells and diploid flagellates (Fig. 8). One consists of mitotic division of colonial cells within the colony, *i.e.* colony growth. The second pathway involves the transition through short-lived diploid flagellates that are released from colonies and are able to reinitialize the colonial stage. Diploid flagellates therefore co-occur with colonial cells and propagate the colonial stage, a pathway commonly used to produce colony cultures in the laboratory. However, its significance in the natural environment is highly questionable and is probably reduced due to the short life span of diploid flagellates (Kornmann, 1955; Cariou *et al.*, 1994).

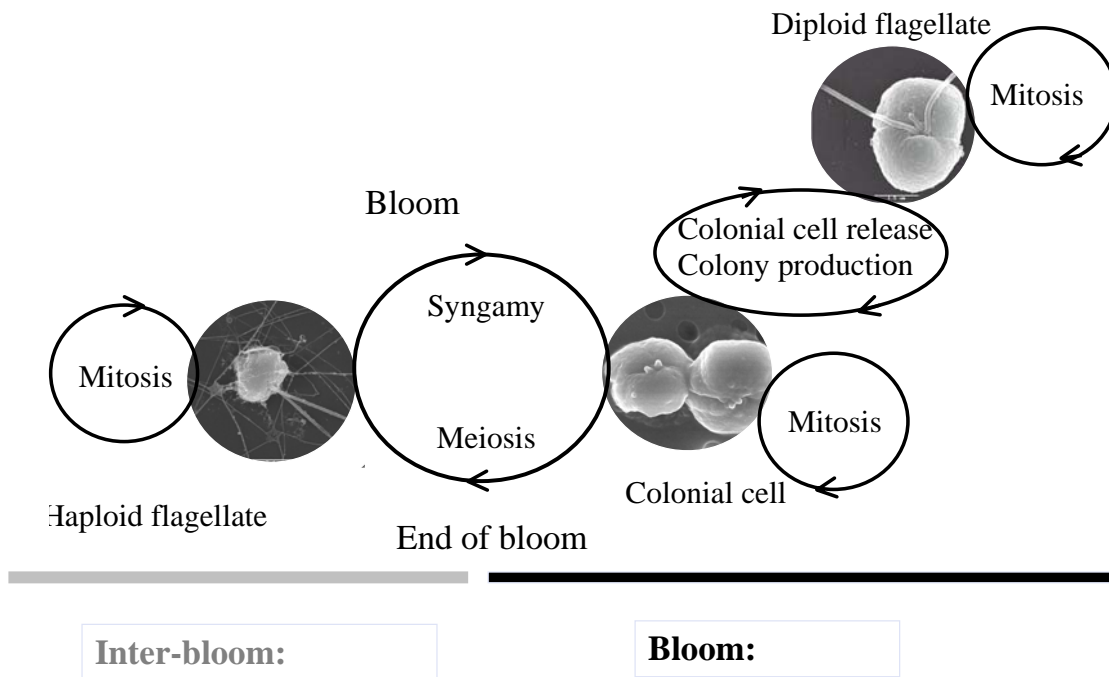


Figure 8: The haploid-diploid life cycle of *P. globosa*.
Redrawn from Rousseau *et al.*, 2007

4.1.1.4 Ecological relevance of the haploid-diploid life cycle of *P. globosa*.

Haploid-diploid life cycles are widespread among diverse sexual eukaryotic organisms such as red algae, most brown algae, many green algae, fungi, foraminiferans, mosses, and ferns. This suggests that such life cycles result from an adaptive evolution providing selective advantages to organisms (Valero *et al.*, 1992; Mable & Otto 1998). Based on theoretical and empirical considerations, haploid-diploid life cycles have been shown to combine advantages from sexual reproduction and those from being haploid and diploid (Kondrashov & Crow, 1991; Mable & Otto, 1998). At the ecological level, the diploid stage has been suggested to represent a *r*-selected strategy with high growth rates, use of inorganic nutrients, and resistance to turbulence, while the haploid stage would have a *K*-selected strategy, being better adapted to nutrient-limited conditions with low growth rates, motility and mixotrophy (Valero *et al.* 1992). The nutritional advantage of haploid over diploid cells under nutrient limited conditions is due to their smaller size (Lewis, 1985). Surface to volume ratios calculated for two cells of 4 μm and 8 μm in diameter, typical of haploid and colonial cells of *P. globosa* respectively, vary from 1.5 to 0.75 respectively. This suggests that haploid cells increase by a factor two their morphological potential to acquire nutrients at low concentrations. In addition, haploid cells may also halve the energetic cost of DNA replication during cell division (Lewis, 1985). Maintenance of a haploid-diploid heteromorphic life cycle is generally considered as an evolutionary

adaptation to an environment that is seasonally variable or contains two different niches (Stebbins & Hill, 1980 cited in Valero *et al.*, 1992). Many tentative hypotheses have been proposed to understand the dominance, alternation and succession of *P. globosa* life forms, *i.e.* nanoplanktonic cells and large gelatinous colonies (Lancelot & Rousseau, 1994; Lancelot *et al.*, 1998; Verity & Medlin, 2003). In general, these studies conclude to an advantageous status of the colonial stage over free-living cells due to the better resistance of colonies to losses. However, comparative studies of the autoecology and grazing sensitivity of *Phaeocystis* haploid and diploid cells are insufficient to demonstrate a possible ecological differentiation between stages and to provide support for ecological niche separation (Rousseau *et al.*, 2007). Understanding the ecological significance of blooming as diploid cells but persisting as haploid stage throughout the year should be appraised through eco-physiological characterization of pure cultures of haploid and diploid stages combined with cell morphology and ploidy determination.

4.1.2 Seasonal dynamics of phosphorus and microbial dominance

MIRO model results (Lancelot *et al.*, 2005) suggest that the spring growth of *Phaeocystis* is sustained by excess nitrates (*i.e.* left over after early spring diatom growth) and uses regenerated forms of P. Under such conditions, phytoplankton is competing with bacteria for P acquisition. To better understand the dynamics of P in the Southern Bight of the North Sea, field measurements of P forms (inorganic vs dissolved and particulate organic), DOP hydrolysis by natural communities and Chl *a*, phyto- and bacterio-plankton biomasses were performed during the spring phytoplankton bloom 2004. Data obtained were combined with previous 2000 and 2003 observations in order to reconstruct an average seasonal cycle (Fig. 9).

The seasonal dynamics of P is characterized by high concentrations of PO₄ during winter while DOP is the dominant P form available for phytoplankton and bacteria from spring to fall (Fig. 9A). Interestingly, APA is very elevated during spring, reaching its maximum at the end of April (Fig. 9B). From May to September, APA is low (<4 nmol MUF L⁻¹ h⁻¹) despite elevated DOP but low PO₄ concentrations (Fig. 9A-B) and non negligible phyto- and bacterio-plankton biomasses (Fig. 9C). This would suggest that bacterial remineralisation is at that time sufficient to sustain P requirements of planktonic communities. In springtime, high APA coincides with blooms of *Phaeocystis* colonies and the diatom *Guinardia delicatula* and high biomass of bacterioplankton (Fig. 9C) and low PO₄ concentrations (Fig. 9A).

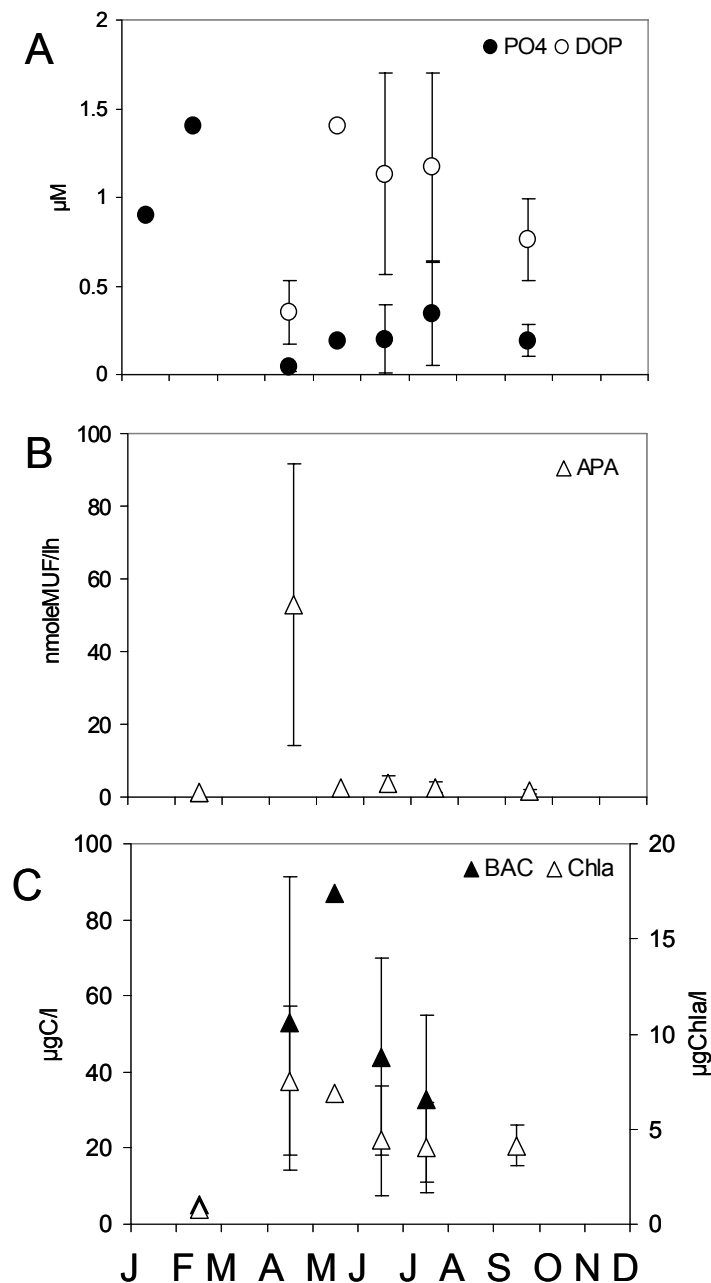


Figure 9: Seasonal cycle of
 (A) PO₄ and DOP concentrations;
 (B) APA;
 (C) bacteria and Chlorophyll a concentrations reconstructed on basis
 of the measurements performed in 2003 and 2004
 as well as data from the weekly sampling of St 330.

Cross-correlation analysis between total APA and APA associated to $> 2 \mu\text{m}$ on the one hand and on the other hand nutrients (PO₄, DOP), organic matter (POP, POC) and biological variables (Chl *a*, diatoms, *Phaeocystis* and bacteria biomasses) during spring suggests that phytoplankton and attached bacteria ($> 2 \mu\text{m}$) are the major contributors to DOP hydrolysis. Based on specific APA measured on axenic P-limited *Phaeocystis* ($0.22 \text{ nM MUF h}^{-1} \mu\text{gC}^{-1}$) and diatoms ($0.29 \text{ nM MUF h}^{-1} \mu\text{gC}^{-1}$)

cultures and respective carbon biomasses, the contribution of phytoplankton to the total spring APA can be estimated to 59-80%. Altogether, these results suggest that DOP hydrolysis is a main source of PO₄ during springtime. They also confirm the ability of *Phaeocystis* to grow on organic sources of P when PO₄ is depleted (van Boekel & Veldhuis, 1990) but also suggest that diatoms and attached bacteria play a major role in this hydrolysis.

4.1.3 Dynamics of gelatinous zooplankton: *Noctiluca* and *Oikopleura*

Several mass developments of gelatinous organisms (*Noctiluca scintillans*, *Oikopleura dioica*) have been recurrently recorded in BCZ between ~15 April and 30 June (Hecq, 1982; Rousseau *et al.*, 2000) but little is known about their trophic status. Such important questions as their diet, their opportunistic behaviour and voracity and their link with phytoplankton blooms are addressed in this section. Abundance, biomass and diet of *Noctiluca scintillans* and *Oikopleura dioica* have been determined during spatio-temporal surveys. Gelatinous-specific diet and feeding rate were investigated under shipboard and laboratory-controlled conditions based on food vacuole/gut content measurements.

4.1.3.1 *Noctiluca* biomass, diet and feeding activities

4.1.3.1.1 Spatio-temporal distribution of *Noctiluca* biomass

Seasonal distribution at St 330 shows that *Noctiluca* biomass culminates in June/July (Fig. 10). *Noctiluca* starts blooming at the decline of *Phaeocystis* colonies and culminates between two blooms of diatoms, mainly *Guinardia delicatula*, *G. striata*, *Cerataulina bergonii* and *Rhizosolenia shrubsolei* (Fig. 10). The magnitude reached by *Noctiluca* significantly varies from year to year, from 10 to 155 mgC m⁻³ in 1988 and 1994 respectively (not shown). The spatial distribution of *Noctiluca* indicates a clear inshore-offshore gradient of biomass both in spring (Fig. 11A) and in summer (Fig. 11C). No significant difference in *Noctiluca* biomass was found between spring and summer. *Noctiluca* cell diameter varies largely, from 100 to 1100 µm, with however a quite similar modal size in spring (593 µm) and summer (612 µm). Interestingly, a reverse trend in size distribution is observed with much smaller organisms near shore than offshore (Fig. 11B, D).

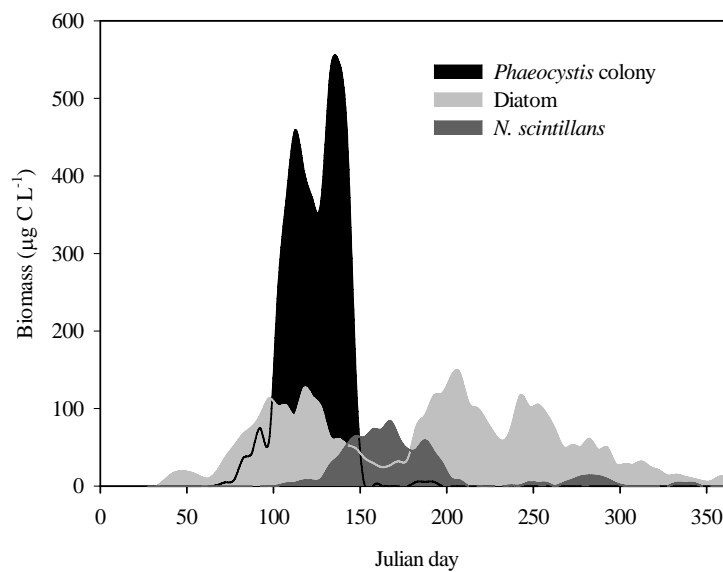


Figure 10: Seasonal variations of diatom, *Phaeocystis* colony, and *Noctiluca* biomass at St 330. Data are 5-days averaged, based on 1988, 1993, 1994, and 1998-2001 samples.

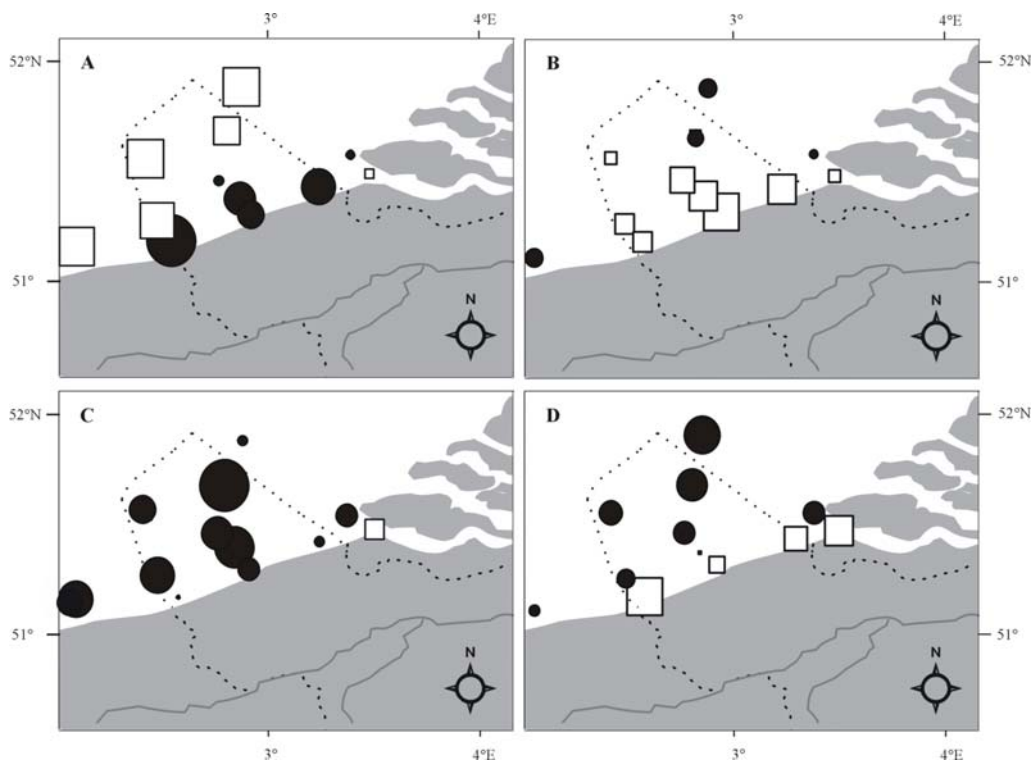


Figure 11: Spatial distribution of *Noctiluca* biomass ($\log \text{mgC m}^{-3}$) and size (μm) in the Southern Bight of the North Sea, in spring (A and B respectively) and in summer (C and D respectively).

Data represent maximum biomass and minimal cell size (standardized value) for each station sampled over the 5 years.

Circles and squares are corresponding to stations with a biomass (size) higher and lower than the mean, respectively.

Symbol size is proportional to the absolute value at each station.

4.1.3.1.2 Diet and feeding strategy of *Noctiluca*

Composition of the diet: The diet of *Noctiluca* consists in diatoms, *Phaeocystis* aggregates, copepod eggs and moult, faecal pellets, various protists (dinoflagellates, ciliates and suctorians) and yeast. The Costello (1990) analysis - based on a two-dimensional representation of prey-specific relative abundance (% A) and frequency of occurrence (% F) in the diet (Fig. 12) - suggests that *Noctiluca* has a generalist feeding strategy. Both in spring and in summer, diatoms are by far the most important food item in *Noctiluca* vacuoles ($A \sim 40-60\%$; $F \sim 70\%$; Fig. 12). In spring, preferred diatoms are the chain-forming *Cerataulina bergonii* and *Guinardia delicatula* ($F > 20\%$; $A > 10\%$; not shown) while species like *G. striata*, *Melosira marina*, *Thalassiosira* spp. and the single-celled *Odontella sinensis* are observed less frequently ($F < 10\%$) and found in lower abundance ($A < 10\%$) in the food vacuoles. In summer, the chain-forming *G. delicatula*, *G. striata* and *Rhizosolenia shrubsolei* are the dominant prey ($F = 20\%$; $A = 25\%$) and *G. flaccida* and *M. marina* are reported as minor (Fig. 12). In addition, eggs of copepod (*Temora longicornis*), and *Phaeocystis* aggregates are a significant part of the *Noctiluca* diet in spring ($A > 20\%$; $F > 30\%$; Fig. 12). At the same time, copepod moult and protists can be regarded as minor food items (Fig. 12). In summer, phytoplankton-derived aggregates ($F > 30\%$; $A > 20\%$) and copepod eggs ($F > 30\%$; $A > 15\%$) constitute significant prey (Fig. 12). Faecal pellets and protists are, as in spring, only minor components of the food vacuole (Fig. 12). Such a diet composed of a high variety of large prey and few small-sized organisms has been observed in other areas (Enomoto, 1956; Prasad, 1958; Kimor, 1979).

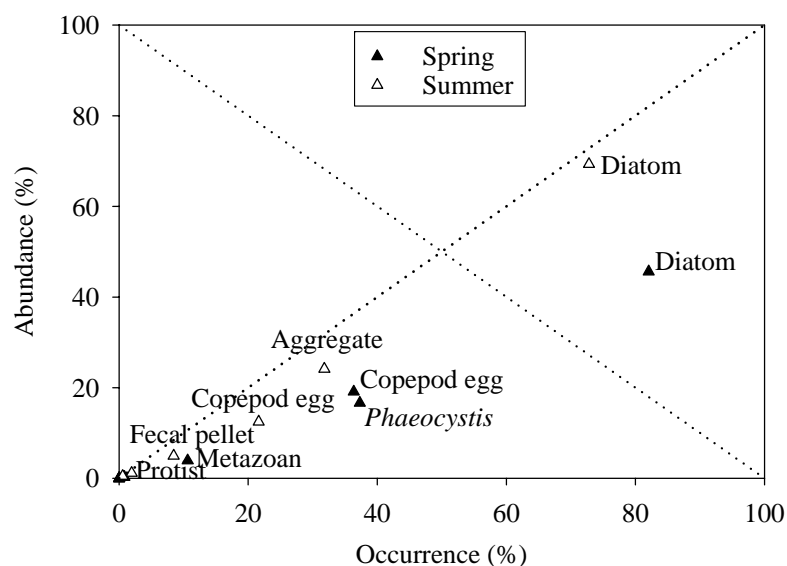


Figure 12: Diet and feeding strategy of *Noctiluca* in the Southern Bight of the North Sea, based on the Costello (1990) analysis.

Relationship between percentage of abundance and frequency of occurrence is based on the prey groups.

Carbon content of the diet: The carbon diatom biomass represents in average some $45\pm 57\%$ (mainly *C. bergonii* and *G. striata*) and $49\pm 54\%$ (mainly *G. striata* and *G. delicatula*) of the *Noctiluca* diet in spring and summer respectively (Fig. 13). Owing to a specific carbon content in average 4 times higher than diatoms, copepod eggs contribute to respectively $42\pm 28\%$ in spring and $33\pm 28\%$ in summer of the *Noctiluca* carbon diet (Fig. 13). *Phaeocystis* aggregates, while representing a large volume, represent only a minor contribution ($1\pm 1\%$) to the *Noctiluca* carbon diet (Fig. 13). Among other minor contributors to the *Noctiluca* carbon diet are the copepod moult ($6\pm 3\%$ in spring and $9\pm 3\%$ in summer), the faecal pellets and protists ($<5\%$), except in summer when faecal pellets have a higher contribution ($9\pm 15\%$; Fig. 13).

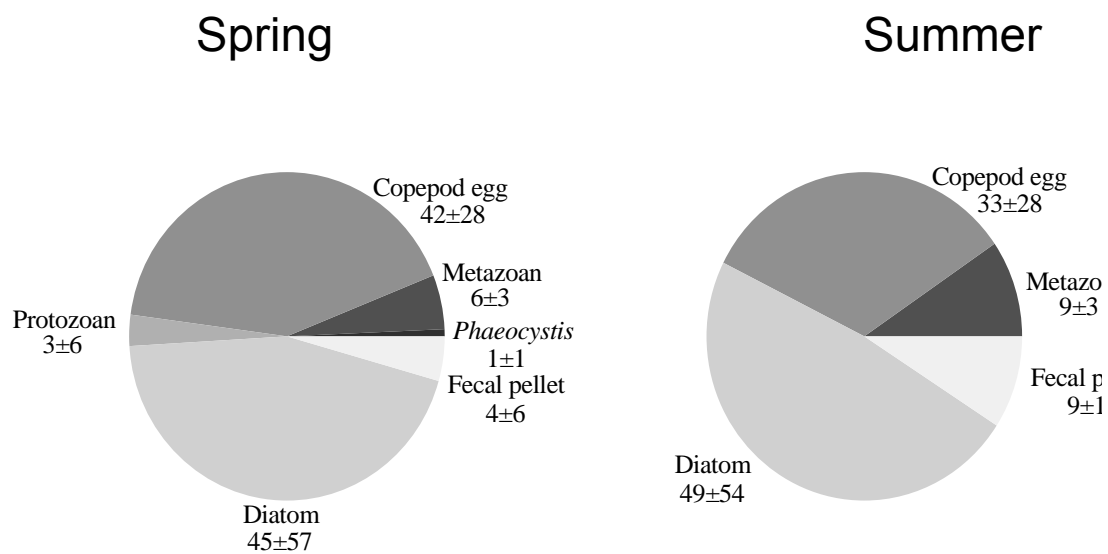


Figure 13: Relative proportion of the carbon biomass (% μgC) of the different prey to the *Noctiluca* diet in spring and in summer.

The predominance of diatoms in the diet of *Noctiluca* could well explain the highly significant relationship existing between diatoms and *Noctiluca* carbon biomass integrated over the whole period (Fig. 14).

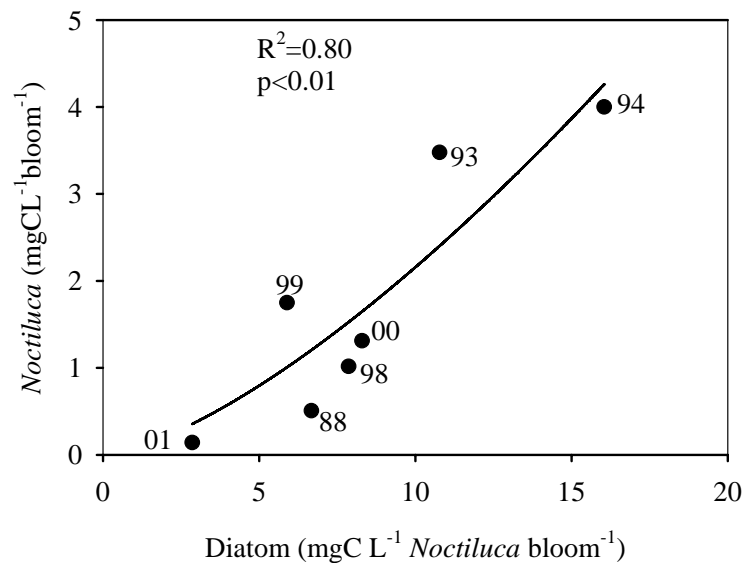


Figure 14: Relationship between *Noctiluca* ($\mu\text{gC bloom}^{-1}$) and diatom biomasses ($\mu\text{gC summer}^{-1}$) at St 330. The curve corresponds to a power model fit.

Size and biovolume of the diet: A highly significant positive relationship was found between the prey size and the *Noctiluca* cell diameter in both spring ($r^2=0.94$) and summer ($r^2=0.90$). This corresponds to a predator:prey size ratio of 5:1, *i.e.* close to the 4:1 ratio determined in laboratory conditions (Kiorboe & Titelman, 1998) and is typical for a raptorial feeder (Hansen *et al.*, 1994). Occurrence of prey in the diet of *Noctiluca scintillans* responds to an unimodal function of biovolume prey, both in spring and summer (Fig. 15A-B). Interestingly, in spring, the optimum biovolume is $3.5 \cdot 10^5 \mu\text{m}^3$, *i.e.* equivalent to a diameter of $87 \mu\text{m}$ and corresponds to the size of copepod eggs (Fig. 15A). By contrast, un-preyed *Phaeocystis* free-living cells and healthy colonies are respectively at the lower and upper limits of the size range (Fig. 15A) suggesting a trophic size mismatch. During the bloom, size of un-preyed *Phaeocystis* colonies is indeed 5 times larger than those observed in *Noctiluca* food vacuoles (not shown). Colonies of adequate size account for only 3% of the total *Phaeocystis* carbon biomass. By contrast, the aggregates found in *Noctiluca* vacuoles at the end of the bloom and which represent 22% of *Phaeocystis* carbon biomass, have a smaller size and can represent suitable prey. These observations suggest that trophic interaction between *Phaeocystis* colony and *Noctiluca* might be significant during the collapse of the bloom. In summer, the optimum biovolume is $6.9 \cdot 10^5 \mu\text{m}^3$ corresponding to the diatom *G. delicatula* (Fig. 15B).

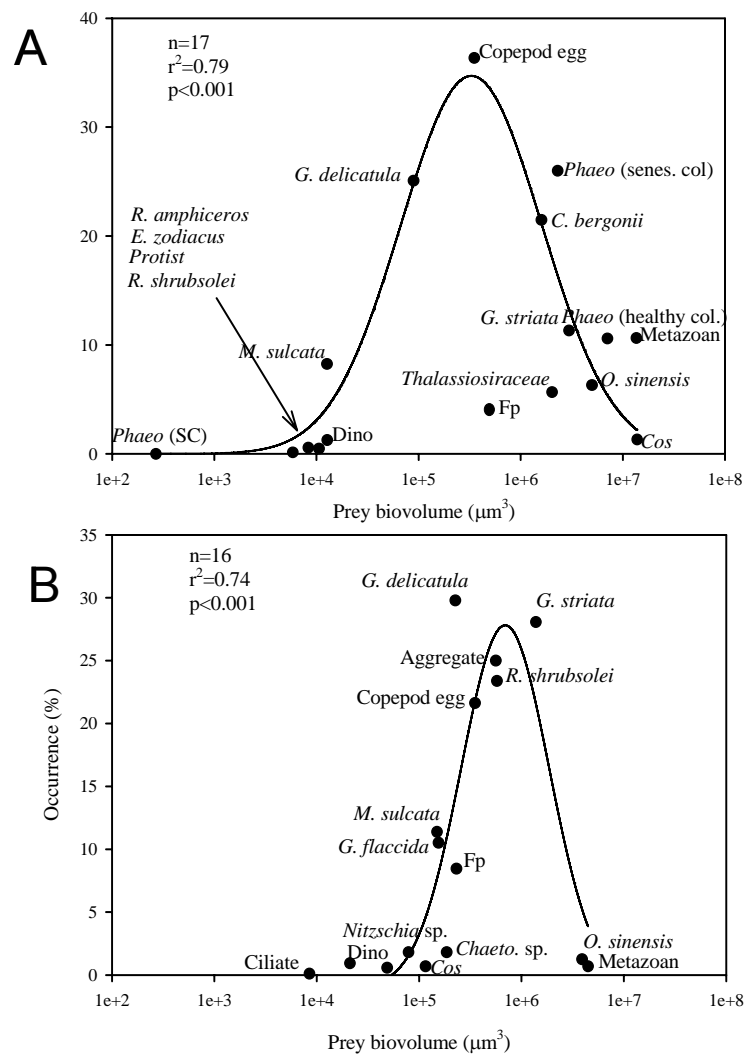


Figure 15: Gaussian relationships between biovolume of the various prey items and their occurrence (%) in the diet of *Noctiluca* in (A) spring and (B) summer. Biovolume was calculated from equivalent spherical diameter, and represents the average of all measurements of each prey detected in *Noctiluca*.

4.1.3.1.3 Daily ingestion rates

Total ingestion rates of *Noctiluca* vary between 0.02 to 0.50 µgC ind⁻¹ d⁻¹, with an average of 0.27±0.08 µgC ind⁻¹ d⁻¹ in spring and 0.14±0.06 µgC ind⁻¹ d⁻¹ in summer. This corresponds to a daily ingestion ranging from 2 to 289% of the body carbon, with a total average of 118±63 in spring and 59±19% d⁻¹ in summer. The maximum *Noctiluca* specific ingestion rates of diatoms, copepod eggs, metazoans, and faecal pellets are about 2.2, 0.93, 1.8 and 0.73 body C ingested d⁻¹, respectively. The lowest value is found for *Phaeocystis* colony ingestion, *i.e.* 0.11 body C ingested d⁻¹. Daily grazing pressure on *Phaeocystis* colonies and aggregates is low in average (0.06±0.05 and 2±2% d⁻¹, respectively) but it is much higher (60±98% d⁻¹) when considering small-sized *Phaeocystis*-derived aggregates (<300 µm). In spring, daily

grazing pressure on diatom is low, *i.e.* $3.03 \pm 3.62\% \text{ d}^{-1}$ but in summer, it reaches $15 \pm 9\% \text{ d}^{-1}$. By contrast to phytoplankton, the *Noctiluca* daily pressure on copepod eggs is very high, *i.e.* in average $52 \pm 39\% \text{ d}^{-1}$ in spring and $31 \pm 26\% \text{ d}^{-1}$ in summer.

4.1.3.1.4 Laboratory feeding and growth experiments

The functional feeding strategy of *Noctiluca* has been determined under laboratory-controlled experiments where ingestion rates were measured for increasing amount of food source. The latter included either cultured diatoms (*C. costatum*, *S. costatum*, *N. delicatissima*, *R. shrubsolei*), *T. longicornis* egg, *Phaeocystis* colonies less than $300 \mu\text{m}$ or a natural sample composed of *Phaeocystis* aggregates, copepod eggs, diatoms and ciliates. In these experiments, the ingestion rates of *Noctiluca* are comparable to field observations and vary from 0 to $0.17 \mu\text{gC ind}^{-1} \text{ d}^{-1}$, depending on food concentration (Fig.16). Interestingly and contrasting with copepods, no saturation level but a linear functional feeding response to food concentration, is observed up to a food availability of $4700 \mu\text{gC L}^{-1}$ (Fig. 16). When offered as unique food, *Phaeocystis* colonies were ingested at rates similar than that of diatoms (Fig. 16). The ability of the different food resource to sustain *Noctiluca* growth is estimated from the gross growth efficiency GGE calculated as the growth to ingestion rate ratio. GGE is the highest when *Noctiluca* fed on copepod eggs (57%) and on the natural sample with *Phaeocystis* aggregates (50%). It is the lowest for the two diatom species (<20%) and *Phaeocystis* colonies in late stationary phase and is 0 for *Phaeocystis* colonies in exponential growth phase. Interestingly, GGE decreases when the proportion of healthy *Phaeocystis* colonies over unhealthy increases in the food, but increases when the proportion of protists increases (not shown).

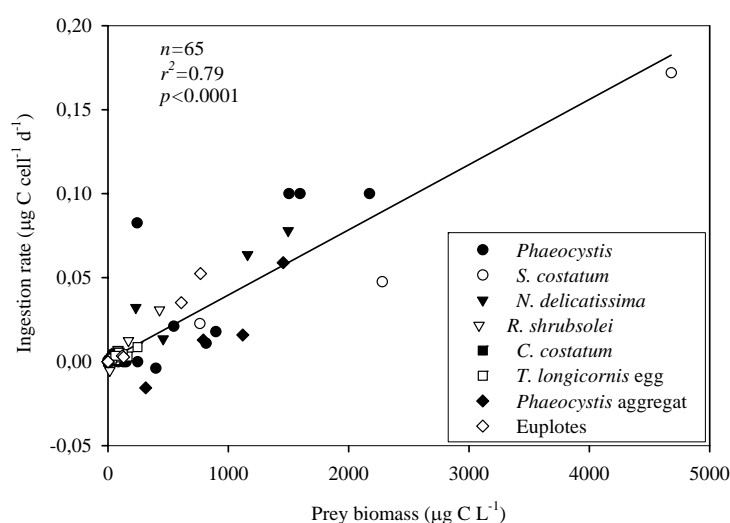


Figure 16: *Noctiluca* ingestion rates ($\mu\text{g C ind}^{-1} \text{ d}^{-1}$) in response to increasing concentrations of various cultured (*Phaeocystis* colonies, *S. costatum*, *N. delicatissima*, *C. costatum*, *R. shrubsolei*, of *T. longicornis* eggs) and natural (*Phaeocystis* aggregates, ciliates, copepod eggs, and diatoms sampled at the station S01 in April 2005) food items.

4.1.3.2 *Oikopleura* biomass, diet and feeding activities

4.1.3.2.1 Spatio-temporal distribution of *Oikopleura* abundance and biomass

Contrasting with *Noctiluca*, the spatial distribution of *Oikopleura* (Fig. 17) shows maximum and minimum abundance respectively offshore and nearshore, both in spring (Fig. 17A) and in summer (Fig. 17B). *Oikopleura* abundance does not differ between spring and summer (t test; $p > 0.05$) amounting to $9 \cdot 10^3 \text{ ind m}^{-3}$. *Oikopleura* average biomass is $2.82 \pm 1.49 \text{ mgC m}^{-3}$, i.e. only 3 % of the copepod biomass recorded during the same period. *Oikopleura* size, measured as the trunk length, ranges between 200 and 900 μm , with a modal size of 500 μm . A general inverse linear relationship is found between *Oikopleura* trunk length and seawater temperature ($r^2 = 0.53$, $p < 0.001$), suggesting that temperature is a significant direct or indirect factor controlling the development of *Oikopleura* population. By contrast, no significant relationship is found between spatial and temporal biomass of *Oikopleura* and any environmental parameter measured.

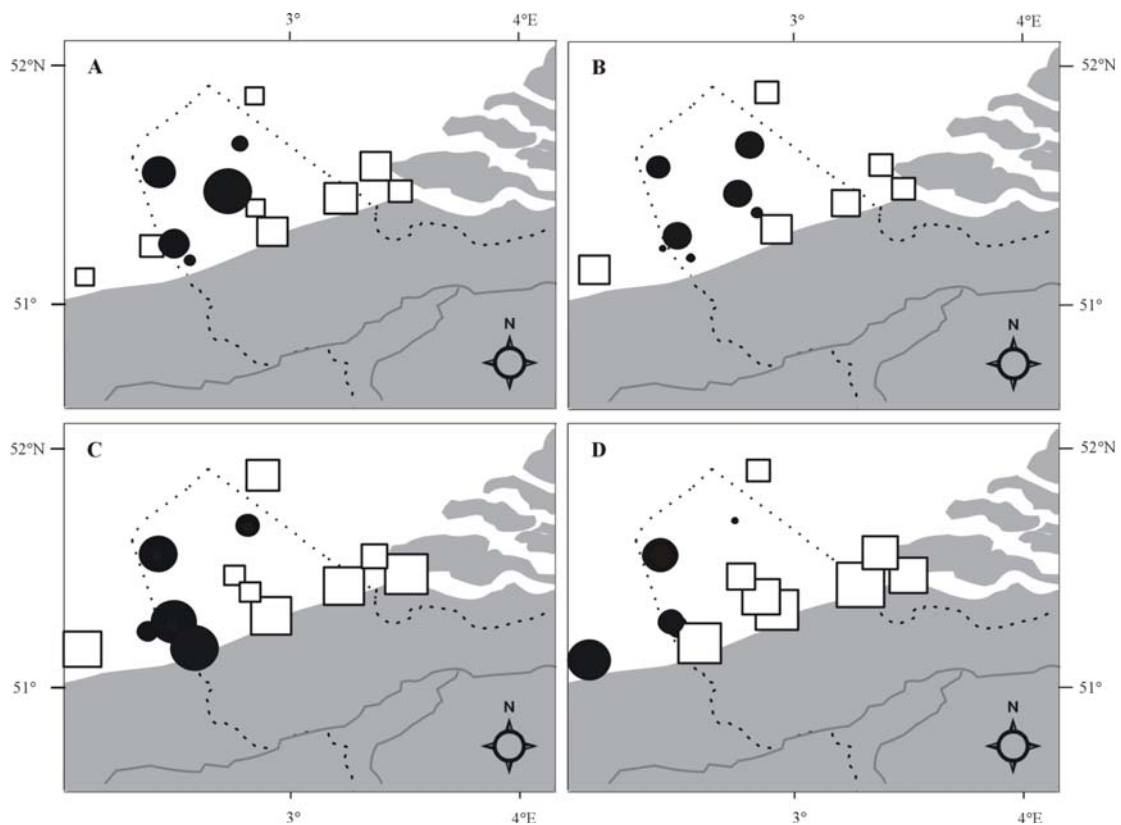


Figure 17: Spatial distribution of *Oikopleura* abundance and trunk length (μm) in the Southern Bight of the North Sea, in spring (A and B respectively) and in summer (C and D respectively).

Data represent maximum abundance and minimal trunk length (standardized value) for the 5 years at each sampling station.

Circles and squares: stations with abundance (trunk length) higher and lower than the mean, respectively.

Symbol size is proportional to the absolute value at each station.

4.1.3.2.2 Diet of *Oikopleura*

The diet of *Oikopleura* was qualitatively estimated based on light and environmental scanning electron microscopy analysis of the content of their houses and faecal pellets (Fig. 18). Houses contain numerous pieces of large diatom frustules, amorphous detritus and *Phaeocystis* colonies (Fig. 18A-B). Faecal pellets enclose fine-grained lithogenic particles, broken diatom frustules and coccoliths (Fig. 18C-D). *Phaeocystis* colonies and cells are not observed in the faecal pellets but the star-like chitinous filaments of *Phaeocystis* flagellates (Fig. 7) are visible at the end of the bloom. The contribution of lithogenic particles was decreased towards offshore, while the proportion of retrieved coccoliths increased. The average carbon content of faecal pellets which is estimated to $0.33 \pm 0.19 \text{ pgC } \mu\text{m}^{-3}$, does not vary seasonally (Kruskall-Wallis, $n=45$, $KW=5.97$, $p>0.05$).

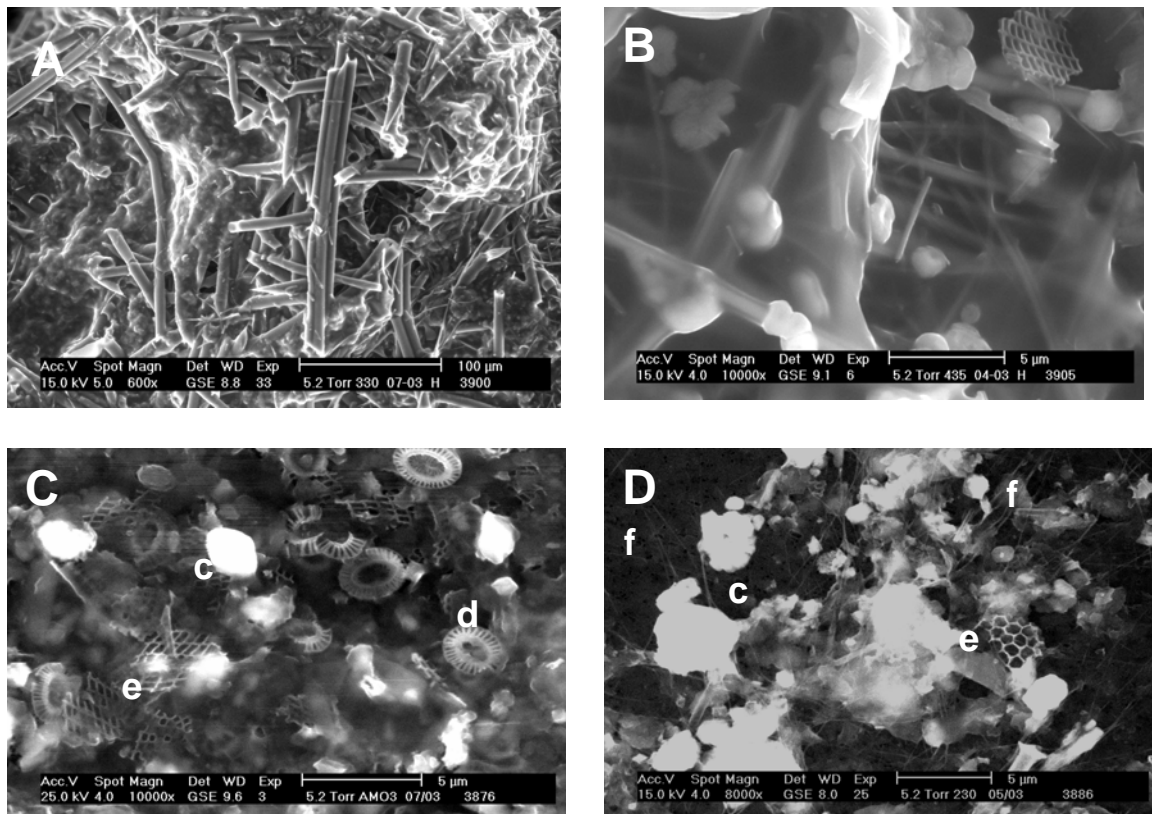


Figure 18: SEM micrographs of *Oikopleura* (A-B) house content showing (A) pieces of the large diatom *R. shrubsolei* and (B) *Phaeocystis* colonies; (C-D) faecal pellets: c) clay; d) coccolith; e) pieces of frustule; f) *Phaeocystis* filament.

4.1.3.2.3 Ingestion rate and feeding strategy of *Oikopleura*.

Ingestion rate of *Oikopleura* on total particles was estimated based on the gut food-volume content (GVC). Some 34 % of GVC variability is related to body size of *Oikopleura* suggesting that large organisms are eating more than smaller ones. GVC corrected for body size (ANCOVA test), is significantly related to the external concentration of DYP suggesting that small-sized detritus constitute a food source for *Oikopleura*.

The ingestion of small-sized prey by the microfilter-feeder *Oikopleura* was estimated based on field ingestion measurements of nano- and pico-phytoplankton cells carried out in spring and summer. The dependence of ingestion rate on food could be described by a functional feeding response of type IV (Gentleman *et al.*, 2003; Fig.19) characterized by a linear dependence at low food abundance up to a threshold above which ingestion sharply decreased. The initial slope of this relationship varies over season and is the highest during summer *i.e.* when DYP is minimal. The resulting inverse relationship between GVC and DYP ($n=7$, $r^2=0.71$, $p<0.005$), therefore suggests that the presence of small-sized detritus has a negative impact on the *Oikopleura* ingestion of nano- and pico-plankton.

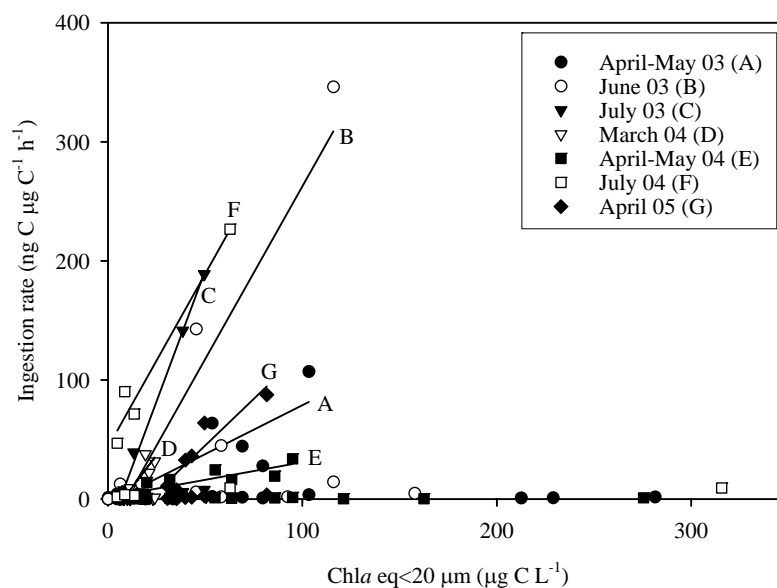


Figure 19: Functional response of *Oikopleura* specific ingestion rates ($\text{ngC } \mu\text{gC}^{-1} \text{h}^{-1}$) to autotrophic prey (nano- and pico-phytoplankton in $\text{Chl } a \text{ eq } <20 \mu\text{m}$) ($\mu\text{g C L}^{-1}$).

4.2 Long-term trend analysis of diatom and *Phaeocystis* blooms in BCZ

4.2.1 Diatom/*Phaeocystis* blooms at St 330 between 1988 and 2001

The phytoplankton data base collected at St 330 in central BCZ (Rousseau, 2000) shows presence of diatoms year-round while *Phaeocystis* colonies occurred as a spring event lasting between 4 and 13 weeks (Fig. 20). The diatom-*Phaeocystis*-diatom succession is observed every year, but the magnitude of the blooms shows important interannual fluctuations with most years clearly dominated by *Phaeocystis*, but a few by diatoms (Fig. 20). No direct link between *Phaeocystis* events and nutrient loads could be evidenced for the 14-year sampled period (Rousseau, 2000) suggesting that climate-driven hydrodynamics could also play a role.

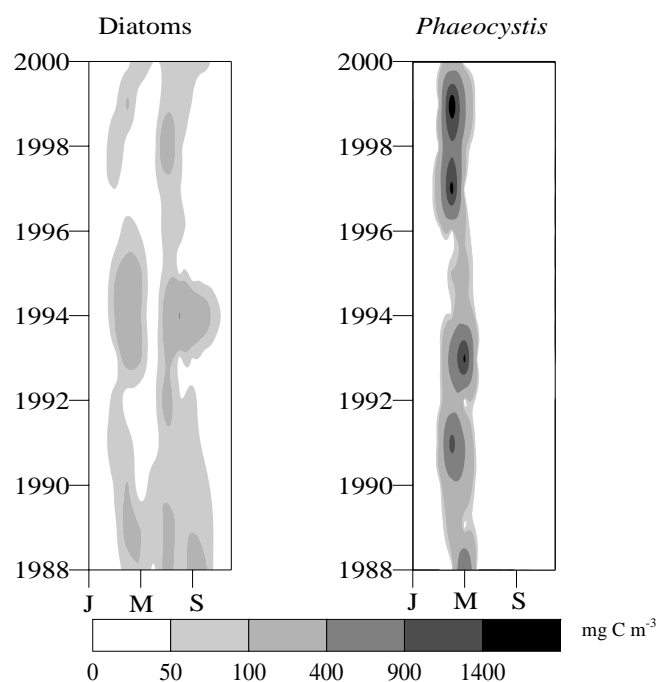


Figure 20: Seasonal pattern of diatom and *Phaeocystis* colony biomass (mg C m^{-3}) at St 330 from 1988 to 2000 (JMS: January, May, September).

4.2.2 Hydroclimatic modulation of diatom-*Phaeocystis* blooms in central BCZ

The effect of climate variability (NAO index) and human activities (Scheldt nutrient loads) on the magnitude of diatom and *Phaeocystis* blooms in the BCZ, was investigated by conducting a serial statistical analysis based on a comprehensive suite of nutrient loads, hydrometeorology, and phytoplankton data collected at St 330 between 1988 and 2001 (Breton *et al.*, 2006). This analysis concludes that the long-term diatom biomass and the spring dominance of *Phaeocystis* colonies over diatoms (Phaeo:dia) are determined by the combined effect of the North Atlantic Oscillation (NAO) and freshwater and continental nitrate carried by the Scheldt (Breton *et al.*, 2006). The strong correlation between diatoms and the NAO index

(Fig.21A) is largely explained by the modulating effect of the latter on the water budget at the monitoring station. The relationship between *Phaeocystis* spring blooms and winter NAO (NAO_w) is indirect, better expressed by springtime *Phaeocystis* dominance over diatoms (Phaeo:dia) due to the higher response of the latter to the NAO (Fig.21A). Interestingly enough the relationship is non-linear and non-monotonic with spring Phaeo:dia being negatively (or positively) linked to positive (or negative) NAO_w values (Fig.21B). Further, a nonlinear but monotonic relationship is found between *Phaeocystis* colony bloom magnitude and winter NO_3 enrichment at St 330 (Fig. 21C). Such a link was not found for winter PO_4 enrichment pointing the key role of NO_3 in determining the height of *Phaeocystis* colony blooms. This result is consistent with previous studies that demonstrate a positive link between *Phaeocystis* cell density and NO_3 excess after the early spring diatom bloom controlled by PO_4 and $Si(OH)_4$ (Lancelot *et al.*, 1998; Rousseau, 2000).

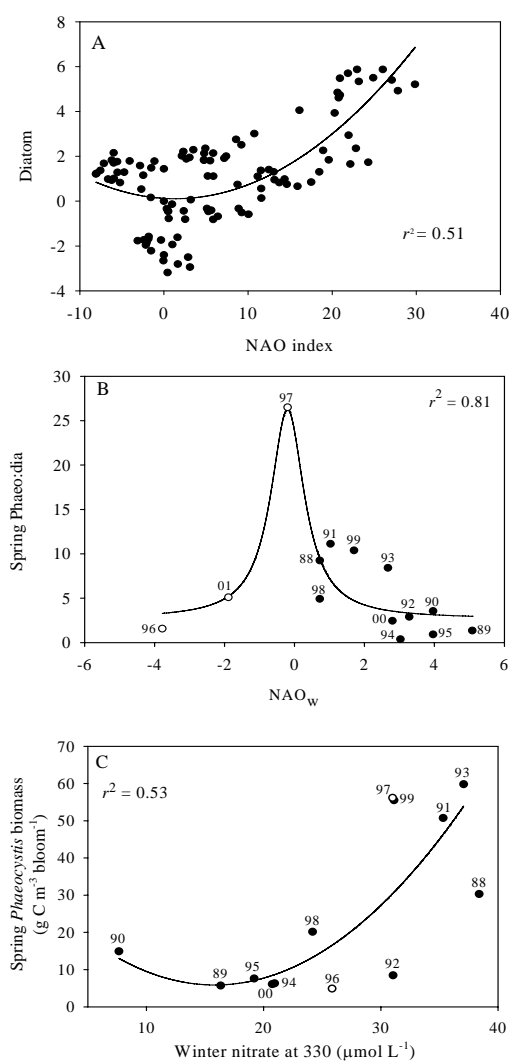


Figure 21: Relationships between (A) NAO and diatoms, and (B) NAO_w and the Phaeo:dia spring biomass ratio at St 330 and (C) winter NO_3 and spring *Phaeocystis* colony bloom ($g C m^{-3} bloom^{-1}$) at St 330. Solid lines represent (B) Lorentzian and (C) quadratic model fits.

The mechanisms behind relationships of Fig. 21 were deciphered by investigating the links between NAO index variations and the local meteorological (wind strength and direction, rainfall) and the hydrodynamical [Eastern Channel Water Inflows (ECWI) in BCZ, Scheldt runoff and freshwater influence at St 330] trends over the 14-year period (Breton *et al.* 2006). Results obtained suggest a complex cascade of natural events entangled with human activity in the watershed (Fig. 22) as follows:

- Climate variability first drives meteorological conditions, *i.e.* local wind dominance expressed as the ratio between N+E and SW winds, (N+E):SW, (low for high positive NAO and rainfall (high for high positive NAO) in the Scheldt watershed.
- Wind and rainfall, in turn, determine the hydrodynamical features and water budget in BCZ, thus at St 330. For instance a higher propagation of Atlantic waters and higher Scheldt water and nutrient discharge are predicted under SW wind dominance and high rainfall.
- Wind direction also influences the spreading of the Scheldt plume at St 330 with lower freshwater and NO₃ influence under SW wind dominance. This unexpected result is the consequence of two opposite phenomena. On the one hand, Scheldt runoff is positively related to the NAO index via rainfall on the Scheldt watershed. On the other hand, freshwater influence and winter NO₃ enrichment at St 330 depends on (N+E):SW, which is negatively correlated to rainfall.

Altogether, these results strongly suggest that the long-term trend of diatom biomass at St 330 is mostly related to a change in hydrodynamics, *i.e.*, the balance between ECWI in the BCZ and freshwater inputs from the Scheldt (Fig. 22). The nonlinear relationship between *Phaeocystis* and climate variability results from the opposite NAO modulation of Scheldt freshwater and NO₃ discharge on the one hand, and their spreading in the BCZ on the other hand. Indeed, high NAO values (>2) are associated with high rainfall and river runoff, which results in high Scheldt NO₃ inputs to the BCZ (Fig. 22A). However, because high NAO values are also related to the dominance of SW over N+E winds, they drive the spreading of the Scheldt plume into a north-eastward direction, which consequently reduces (or prevents) the spreading of Scheldt NO₃ to St 330 (Fig. 22A). Therefore, during high NAO years, NO₃ loads at St 330 are low and *Phaeocystis* blooms are expected to be less important (Fig. 22A). Low NAO years (<-2) also generate low *Phaeocystis* blooms, but that is due to NAO-driven low Scheldt runoff. Therefore, our results suggest that the conditions for intense *Phaeocystis* blooms at St 330 are those for which Scheldt runoff and plume spreading do not offset each other, *i.e.*, when these two parameters display average conditions, which coincides with $0.5 < (N+E):SW < 1.5$ (Fig. 22C).

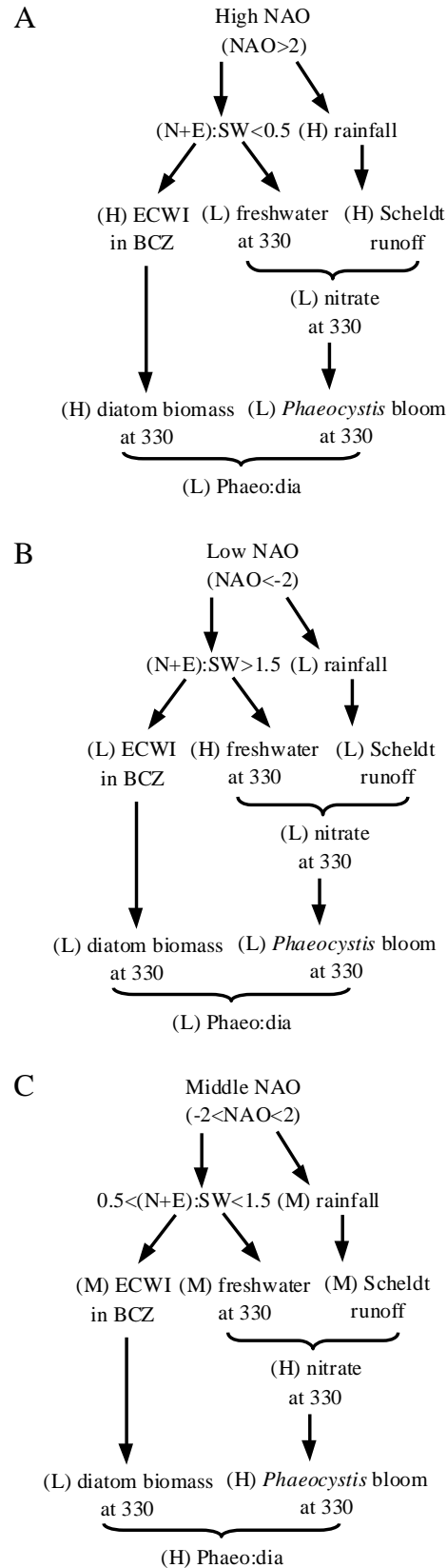


Figure 22: Mechanisms linking NAO, meteorological, hydrodynamical, physico-chemical characteristics and diatom and *Phaeocystis* spring blooms at St 330 under (A) High (H) NAO, (B) Low (L) NAO and (C) Middle (M) NAO. H, L and M refer to high, low and middle respectively

4.3 Mathematical modelling

4.3.1 Analyzing and testing the current 0D multi-box MIRO model

4.3.1.1 Sensitivity analysis of MIRO results to parameter choice

Two sensitivity analysis were used to access the sensitivity of the modeled variables to the chosen parameter set described in original MIRO (Lancelot *et al.*, 2005):

- the variational adjoint method (Lawson *et al.*, 1995, 1996; Spitz *et al.*, 1998, 2001) which analyses the influence of the full set of parameters on all the model state variables;
- the sensitivity factor derived from perturbation experiment of individual parameters.

4.3.1.1.1 Sensitivity to the full set of parameters

The sensitivity of the model parameter set on all the state variables was investigated based on an identical twin experiment. In this numerical experiment the observations are the model output sampled every hour and the first guess for the parameter values is taken as the reference values (Lancelot *et al.*, 2005) reduced by 30%. The number of iterations necessary to recover the parameter set was quite high (about 15000 iterations) but all the parameters were recovered. The cost function decreases of four orders of magnitude during the first 400 iterations and an additional eight orders of magnitude during the following 10000 iterations. Results obtained show that parameters related to microzooplankton, copepods and *Phaeocystis* colonies lysis are recovered during the first 400 iterations suggesting that these parameters will have a large impact on the model results and may require additional field or laboratory experiments to define them. Some of the parameters related to the microbial loop (including the temperature dependence) are also recovered in less than 1000 iterations, indicating that these processes are important too. Somewhat surprising is the late recovery (over 2000 iterations) of the parameters related to the light availability (etam) and the photosynthesis rate of diatom and *Phaeocystis*. We know from field observations at St 330 that these parameters have a large impact on the timing of diatom and *Phaeocystis* blooms in spring (Rousseau, 2000). This unexpected result might be a consequence of the choice of the parameter perturbation (decrease of 30% from the reference values). The sensitivity analysis presented in 4.3.1.1.2 shows clearly that a decrease of the light-related parameters by 30% has little impact of the blooms contrary to an increase of 30%. In addition, as shown in Lawson *et al.* (1995), the recovery of the parameters using the variational adjoint method might be slower depending of the mathematical formulation of the

phenomenon. This example of sensitivity of the model results to the parameter set call for caution when using the variational adjoint method as the results can depend upon the perturbation applied to the reference value of the parameter set.

4.3.1.1.2 Sensitivity of the maximum biomass of diatom and *Phaeocystis* to individual parameters

In this section we explore which parameters and which pathways have the highest impact on the timing and magnitude of diatom-*Phaeocystis*-diatom blooms. The maximum diatom biomass is mainly controlled by the parameters describing the copepod dynamics, the diatom dynamics and the light availability in the water column. The maximum *Phaeocystis* biomass is mainly controlled by parameters describing its growth, mortality and lysis followed by those characterizing the microbial dynamics and the microzooplankton dynamics. While several parameters influence the maximum of diatom and *Phaeocystis* biomass, only a few parameters influence its timing (Gypens, 2006). In order to illustrate further the sensitivity of the time evolution of the diatom and *Phaeocystis* biomass we perturbed a given parameter around its reference value by $\pm 30\%$ and kept the other parameters constant. Results obtained are shown in Figs. 23 and 24 for respectively the diatom and *Phaeocystis* biomass.

For diatoms it is shown that, even though the amplitude of the diatom spring and summer blooms vary considerably depending upon the choice of the parameter values, their blooms are always simulated (Fig. 23). The maximum rate of photosynthesis and the lysis rate are very important for the set-up of the diatom spring bloom and can affect greatly its magnitude (Fig. 23A-B). An increase of the maximum rate of photosynthesis or a decrease of the lysis rate has a larger effect on the magnitude of diatom summer bloom than on the spring bloom. In addition, an increase of the photosynthesis rate compared to its reference value has a larger effect than a decrease. This is even more pronounced for the summer bloom (Fig. 23A). Similarly, a decrease of the lysis rate has a larger effect than an increase of the lysis (Fig. 23B). As expected, the copepod grazing rate and growth efficiency do not affect the set-up of the spring diatom bloom (Fig. 23C-D). But they greatly influence the maximum of diatom biomass, especially during summer. A decrease of 30% of these two parameters compared to their reference values can lead to almost six times more diatom during summer (Fig. 23C-D).

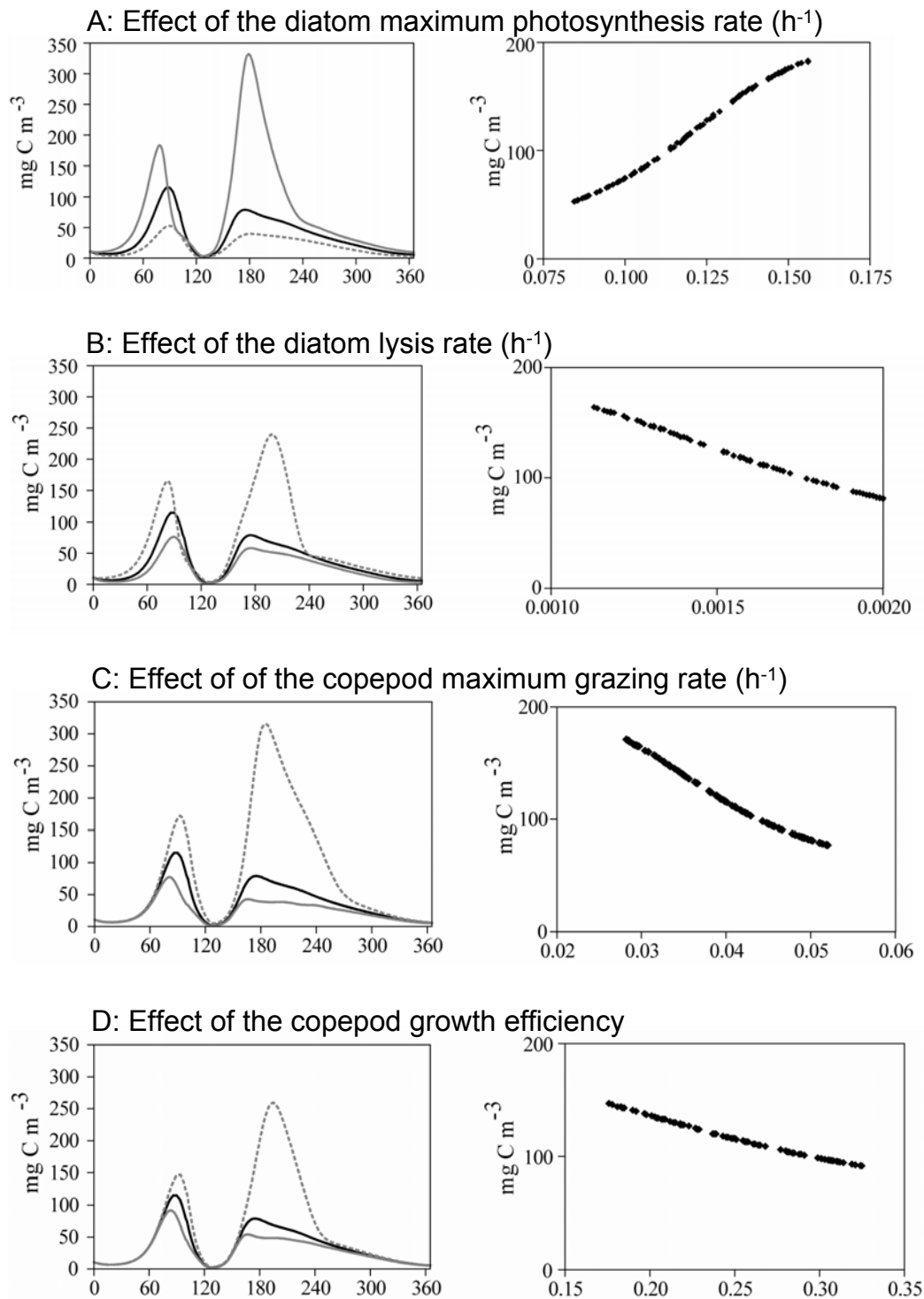


Figure 23: Time evolution of diatom biomass (left panels) and variation of the maximum of the spring bloom as a function of two of the diatom parameters (A-B) and copepod parameters (C-D) perturbed by $\pm 30\%$ around their reference values (right panel)

The dark black line on the left panel corresponds to the reference value, the grey line to an increase of 30% of the parameter reference value and the dotted grey line to a decrease of 30%.

Some of the parameters related to the *Phaeocystis* dynamics, such as the maximum rate of photosynthesis, light availability (not shown) and lysis rate of the *Phaeocystis* colonies, determine whether or not some significant biomass of *Phaeocystis* will persist during summer (Fig. 24A-B). An increase or a decrease of the *Phaeocystis* maximum photosynthesis rate compared to its reference value will lead to the persistence of significant biomass during the summer (Fig. 24A). Similarly, a decrease of the lysis rate of the colonies will lead to some biomass of *Phaeocystis* during summer (Fig. 24B). It appears also that the maximum attained during spring bloom can vary by limiting the resources for *Phaeocystis* [e.g. via decreasing bacteria growth or remineralization (Fig. 24D) or increasing loss through lysis (Fig.24C)]. It is worth noting that the impact on the timing of the bloom is primarily due to the choice of the maximum photosynthesis rate.

Altogether this sensitivity analysis suggests that the timing of the spring bloom of diatom and *Phaeocystis* seems to be determined by the light availability and their maximum photosynthetic rate. The determination of light availability is crucial for MIRO&CO-3D applications when the model domain covers regions of spatially and temporally varying turbidity. Determination of cloud coverage could also be crucial if interannual variability of the spring bloom is to be studied. In addition, the balance between gain and loss for the plankton community also plays an important role. The subsistence of the *Phaeocystis* bloom during summer seems to be related to the lysis rate of colonies. Unfortunately, this component of the ecosystem is still not completely understood and more laboratory or field experiments will be needed to determine the process of rupture of *Phaeocystis* colonies. The dynamics of the copepods has also been shown important for the magnitude of summer diatom bloom. Little information about their diet and growth rate, however, exists for the BCZ.

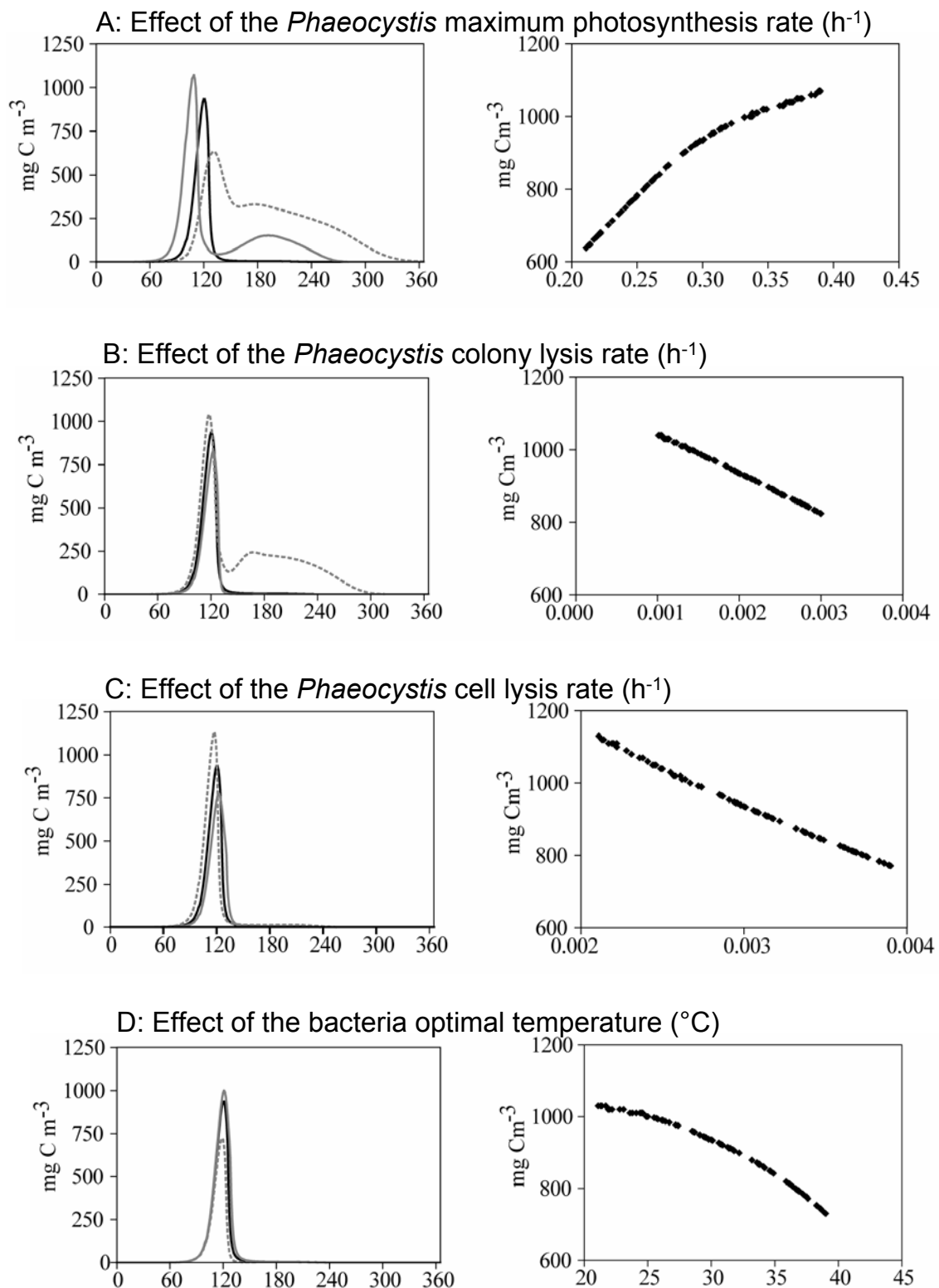


Figure 24: Effect of parameters related to *Phaeocystis* dynamics on bloom timing, duration and magnitude: *Phaeocystis* maximum rate of photosynthesis (A); *Phaeocystis* colony lysis rate (B); *Phaeocystis* cel lysis rate (C) and bacteria optimal temperature (D).

4.3.1.2 Assessment and causes of interannual variability of diatom and *Phaeocystis* blooms in BCZ in 1989-2003

4.3.1.2.1 Diatom-*Phaeocystis* blooms in 1989-2003

The current MIRO model (Lancelot *et al.*, 2005) was used to assess the response of diatom and *Phaeocystis* blooms to changing nutrient loads and meteorological conditions over the 1989-2003 period. For this application, MIRO is implemented in a simplified 3-box representation of the domain including BCZ up to the Baie de Seine. Forcing functions include the actual daily GSR, seawater temperature and Seine and Scheldt nutrient loads for the 1989-2003 period. Monthly residence time of water mass in FCZ and BCZ is calculated based on monthly budgets of water masses (Atlantic water and freshwater discharge of respectively Seine and Scheldt) calculated from 1993-2003 simulations of the 3D hydrodynamical model COHSNS-3D (Lacroix *et al.*, 2004). A correction factor based on COHSNS-3D simulations, was applied to Scheldt loads in order to take into account the modulating effect of wind on the plume extension in the simulated area.

Comparison between model results and observations at St 330 shows the model capacity to correctly reproduce the order of magnitude and the timing of the observed seasonal and interannual variations of nutrients and phytoplankton (Fig. 25). However, extreme winter nutrient and spring phytoplankton observations are less well described due to the simplified description of hydrodynamics and river forcing in 0D multi-box MIRO. It is therefore suggested that the monthly scale of the river inputs forcing and the related water mass residence time estimation might be too long for considering the short-term hydrological variations resulting from the wind-forced and tidally-dependant freshwater influence captured in the data set (Gypens *et al.*, 2007).

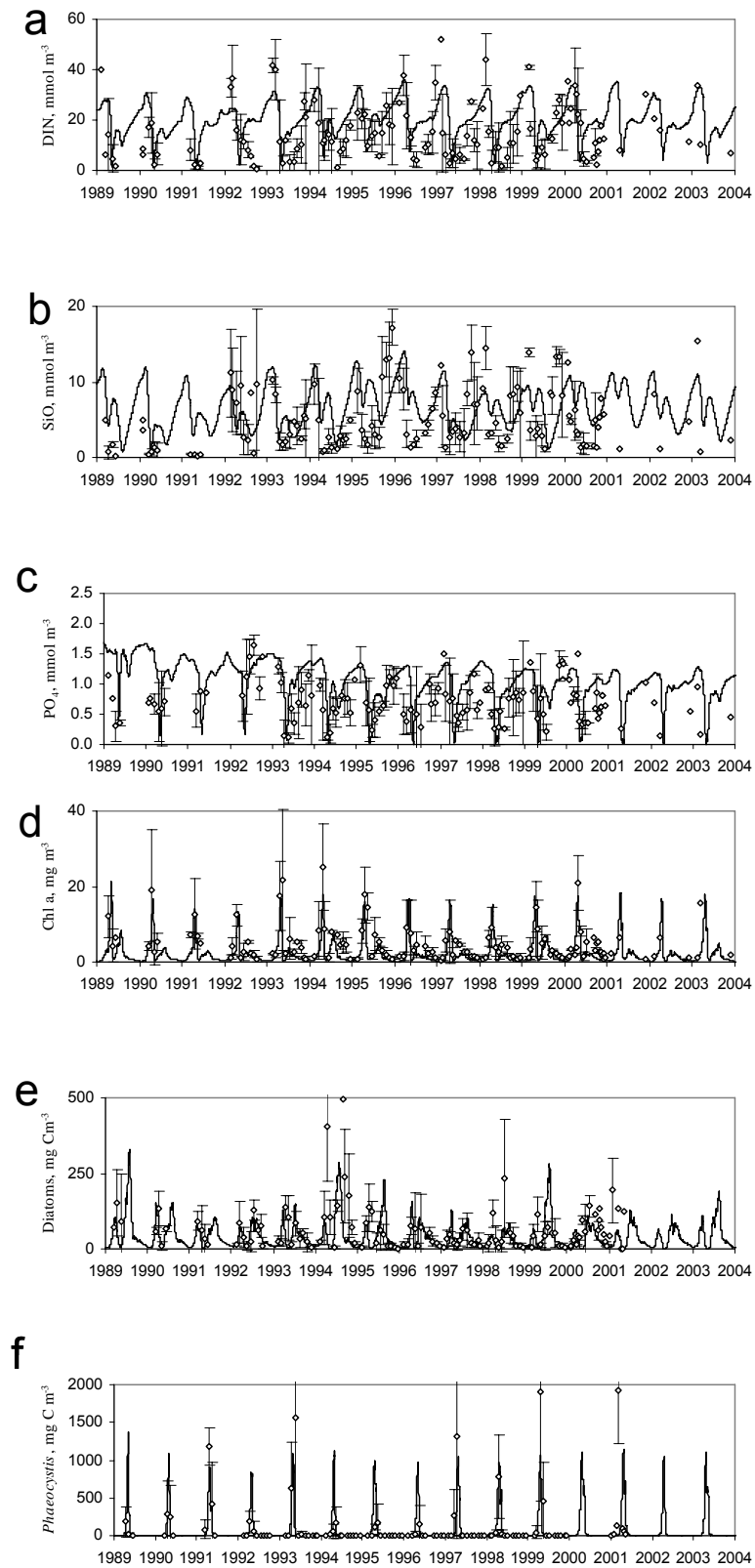


Figure 25: 0D multi-box MIRO simulations (solid line) and observations (\diamond) of DIN (a), Si(OH)_4 (b), PO_4 (c), Chl a (d), diatoms (e) and *Phaeocystis* (f) over the 1989-2003 period.

4.3.1.2.2 Causes of diatom/*Phaeocystis* interannual variability

The contribution of nutrient loads, light availability and temperature to the simulated 1989-2003 variability of spring diatoms, *Phaeocystis* and summer diatoms was investigated based on the comparison between 1989-2003 0D multi-box MIRO results and those obtained by running the model with a constant forcing of either light, temperature or nutrient loads averaged over the simulated period (Gypens *et al.*, 2007). Model results analysis points incident light and temperature as important triggers of the diatom development during the simulated period while these forcings had a little effect on *Phaeocystis* growth. This can be explained by the high sensitivity of diatoms to light (Lancelot & Mathot, 1987), while *Phaeocystis* colonies are adapted to a large range of ambient light (Schoemann *et al.*, 2005). On the opposite, the 1989-2003 changing nutrient loads were affecting both diatoms and *Phaeocystis* but in a different way. The N loads (and mainly NO₃ loads) were mainly modulating the *Phaeocystis* development while Si(OH)₄ and mainly the P loads were limiting the diatom blooms during the considered period.

4.3.2 Upgrading the current 0D multi-box MIRO model

4.3.2.1 The CO₂ module: MIRO-CO₂

4.3.2.1.1 Validation

The MIRO version upgraded with the CO₂ module (MIRO-CO₂; Gypens *et al.*, 2004) was tested in the 0D multi-box frame making use of 1996-1999 climatological forcings for hydro-meteorological conditions and river inputs. Model results were daily-averaged and successfully compared with available biological and chemical data available at St 330. As an example figure 26 compares the seasonal simulation of the surface CO₂ partial pressure of (pCO₂) surface water pCO₂ data (Gypens *et al.*, 2004). The modelled surface water pCO₂ are close to saturation in winter, under-saturated in early March-May at the time of diatom and *Phaeocystis* blooms when a minimum is reached (145 ppm, Fig. 26) and over-saturated in summer.

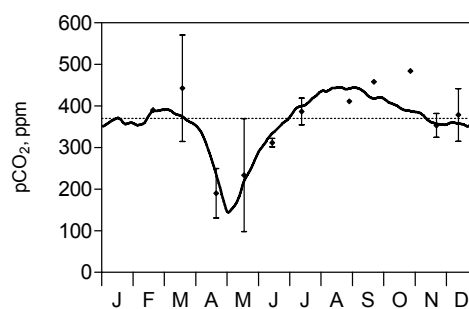


Figure 26: Model results (solid line) and observations (♦) of surface water pCO₂. The dotted line corresponds to the atmospheric equilibrium

4.3.2.1.2 Role of eutrophied BCZ as a sink/source of atmospheric CO₂.

Budget calculations based on model simulations of carbon flow daily rates indicate that under the meteorological and eutrophied conditions of 1996-1999, BCZ was acting as a low annual sink of atmospheric CO₂ ($-0.17 \text{ mol C m}^{-2} \text{ y}^{-1}$; Fig. 27). Interestingly, the same budget made on waters not influenced by river loads like the Western Channel (WCH) in our 0D multi-box frame, is close to zero (Fig. 27) suggesting that river loads are directly or indirectly responsible for the annual uptake of atmospheric CO₂ in BCZ.

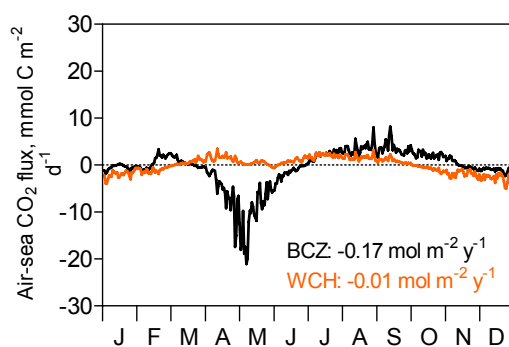


Figure 27: Seasonal evolution of MIRO-CO₂ simulations of daily air-sea CO₂ flux computed for WCH and BCZ boxes. The calculated annual CO₂ air-sea fluxes are indicated.

The relative contribution of biological, chemical and physical processes to the modelled seasonal variability of pCO₂ in BCZ was therefore explored by running model scenarios with separate closure of biological activities and/or river inputs of carbon (Fig. 28). The suppression of biological processes reversed the direction of the CO₂ flux in BCZ that became, on an annual scale, a significant source for atmospheric CO₂ ($+0.53 \text{ mol C m}^{-2} \text{ y}^{-1}$; Fig. 28b). This suggests that biology is responsible for the annual sink predicted in BCZ by taking up to $0.7 \text{ mol C m}^{-2} \text{ y}^{-1}$ of atmospheric CO₂. Overall biological activity had a stronger influence on the modelled seasonal cycle of pCO₂ than temperature ($-0.32 \text{ mol C m}^{-2} \text{ y}^{-1}$; Fig. 28d). Especially *Phaeocystis* colonies, which growth in spring was associated with an important sink of atmospheric CO₂ ($-0.48 \text{ mol C m}^{-2} \text{ y}^{-1}$) that counteracted the temperature-driven increase of pCO₂ at this period of the year. However, river inputs of organic and inorganic carbon are shown to increase the surface water pCO₂ and hence the emission of CO₂ to the atmosphere (Fig. 28c). River inputs of carbon thus represent a significant source of atmospheric CO₂ ($+0.87 \text{ mol C m}^{-2} \text{ y}^{-1}$) that is counteracted by nutrient-driven biological activity ($-0.7 \text{ mol C m}^{-2} \text{ y}^{-1}$) and temperature ($-0.32 \text{ mol C m}^{-2} \text{ y}^{-1}$) on an annual scale. Interestingly enough same calculations conducted in

WCH, show that temperature is the main factor controlling the seasonal pCO₂ cycle in these open ocean waters (details in Gypens *et al.*, 2004).

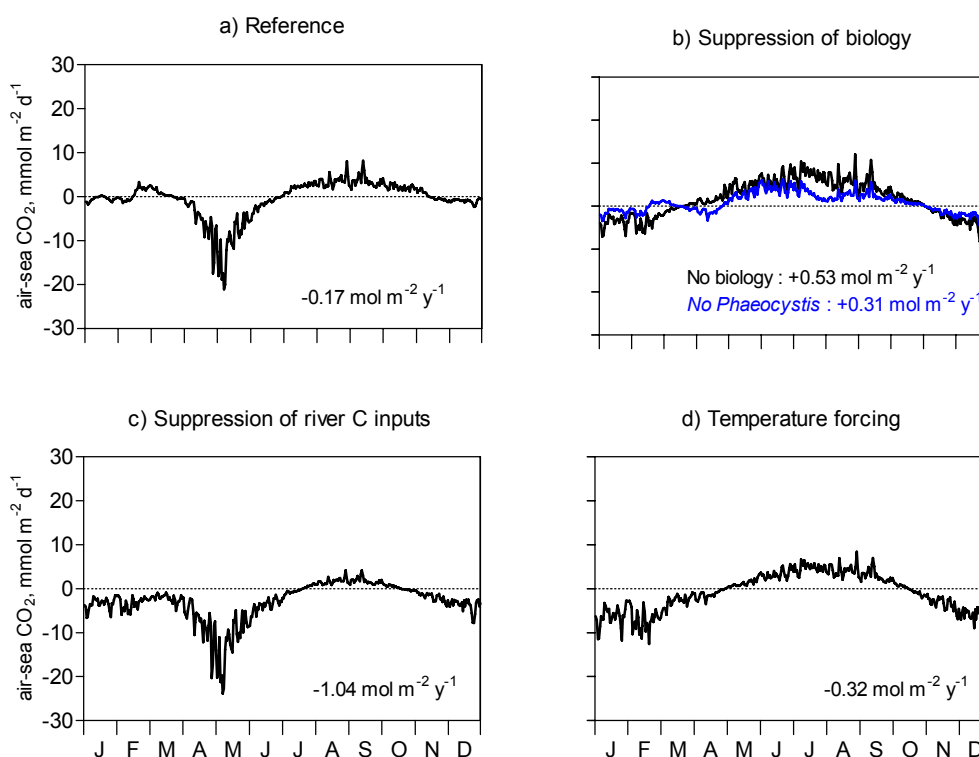


Figure 28: Relative contribution of biological, chemical and physical processes to the modelled seasonal variability of pCO₂ in BCZ:reference (a); suppression of biology (b); suppression of river C inputs (c); temperature forcing (d).

4.3.2.2 Upgrading and simplification of the diagenetic module

4.3.2.2.1 Verification and validation of the two-layer diagenetic model.

The new two-layer diagenetic model described in 3.3.1.1.1 was first verified by comparing depth profiles and mineralization characteristics along a eutrophication gradient with results obtained under the same conditions with a dynamic, vertically resolved model (Gypens *et al.*, submitted). The verified model was then applied to North Sea stations characterized by different sediments and the obtained results were compared with observed NO₃, NH₄, PO₄ and O₂ sediment profiles and sediment-water fluxes.

The verified two-layer diagenetic model for the North Sea ecosystem was then validated by applying it at three sediment systems representative of the North Sea (Lohse *et al.*, 1995): Cluster I representing silty sediments found in depositional areas; Cluster II consisting in fine sandy sediment subjected to frequent, temporary deposition of organic material and; Cluster III including areas characterized by

medium sand where erosion is dominant and organic matter deposition limited. As shown in Fig. 29, the three sedimentary environments nutrient profiles generated by the model are in fair agreement with data.

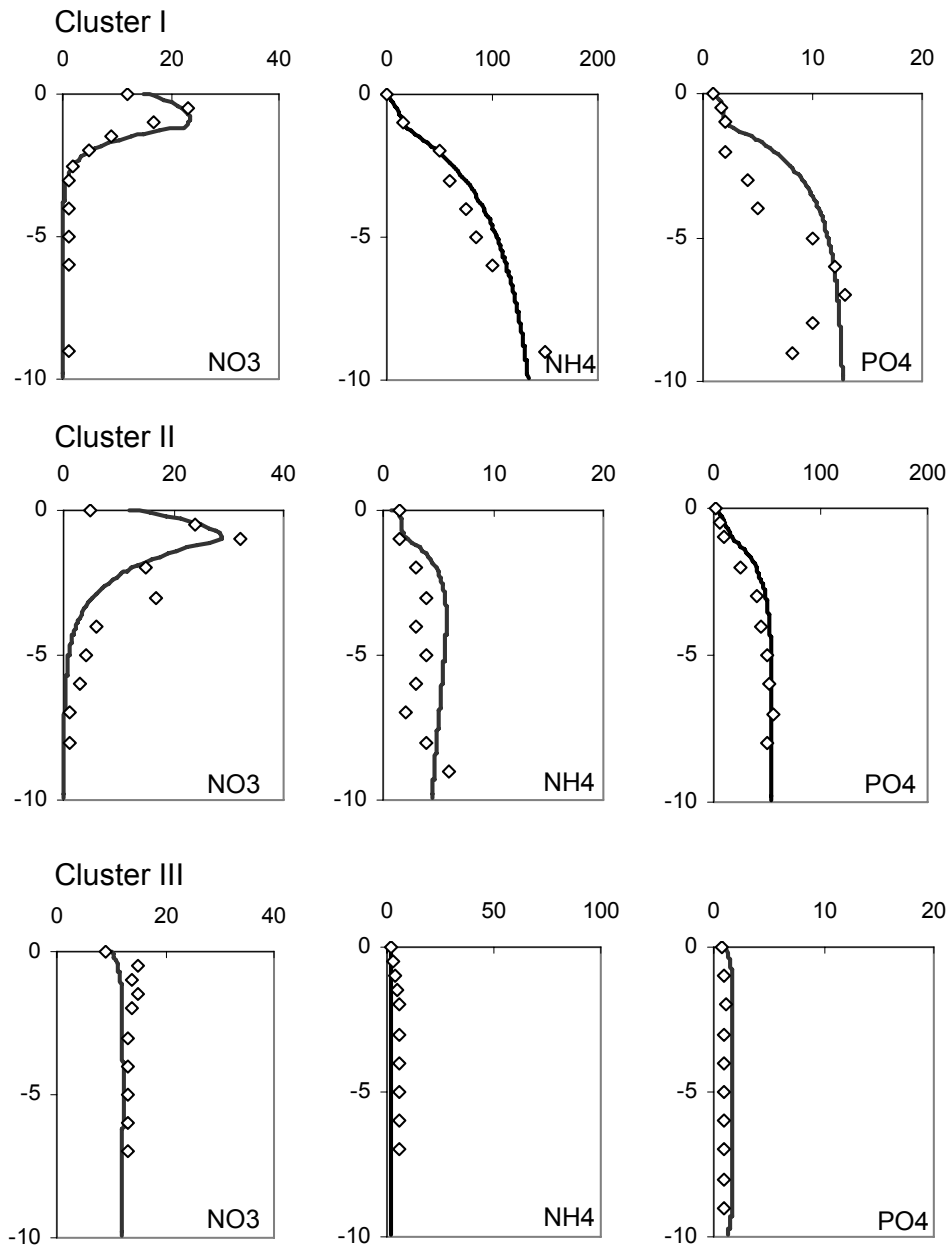


Figure 29: Simulated vertical profiles (black curve) of NO₃, NH₄ and PO₄ plotted in comparison with observations (◇).

4.3.2.2.2 From diagenetic modelling to simple parameterisations

Simulations obtained with the two-layer diagenetic model were then used to derive simplified mathematical relationships of benthic N and P fluxes at the sediment water

interface of the North Sea with the further objective of implementing them in the MIRO&CO-3D model (Lacroix *et al.*, 2007a). Nutrient fluxes at the sediment-water interface were then estimated based on the major reactions affecting their cycle:

NH_4 flux = N mineralization – Nitrification

NO_3 flux = Nitrification – Denitrification

PO_4 flux = P mineralization – Fe-bound P formation + P release – authigenic P formation.

The two-layer diagenetic model was then run 5000 times with random combinations of model parameter and constraints to determine how these fluxes varied due to changing the C mineralization flux and the sedimentary environment. The statistical procedure of Soetaert *et al.* (2000) was applied. Obtained relationships are detailed in Gypens *et al.* (submitted). First tests of their implementation in MIRO&CO-3D are described in Gypens (2006).

4.3.3 Testing the prediction capability of MIRO&CO-3D

4.3.3.1 1991-2003 seasonal trends of nutrients and phytoplankton

4.3.3.1.1 1991-2003 seasonal cycle of nutrients and phytoplankton at St 330.

Fig. 30 compares the mean seasonal evolution of MIRO&CO nutrient, Chl *a*, diatom and *Phaeocystis* simulations at St 330 for the 1993-2003 period with a seasonal cycle constructed from existing observations (Lancelot *et al.*, 2005). A reasonable agreement is shown between simulations and observations both in timing and in magnitude (Fig.30). Especially well described is the seasonal cycle of PO_4 . The spring decrease of DIN and SiO is correctly simulated but with a time delay of 3 weeks compared to the data (Fig. 30). This is due to the late onset of the simulated spring phytoplankton bloom in comparison with the field. This delay is probably explained by the crude parameterisation of light availability which is based on an average climatology of suspended matter (details in 3.3.2.2). The simulated seasonal cycle of diatoms shows two maxima, one in spring and one in summer that compare very well with the data (Fig. 30). The *Phaeocystis* bloom is simulated with a time-delay of about 10 days and the maxima reached is twice lower than observed (Fig. 30). This lower simulated *Phaeocystis* biomass explains the underestimation of simulated Chl *a* maxima compared to the field (Fig. 30). Preliminary analysis of model results seems to indicate that the low simulated *Phaeocystis* and Chl *a* could result from a combined effect of an overestimation of phytoplankton autolysis losses and PO_4 limitation.

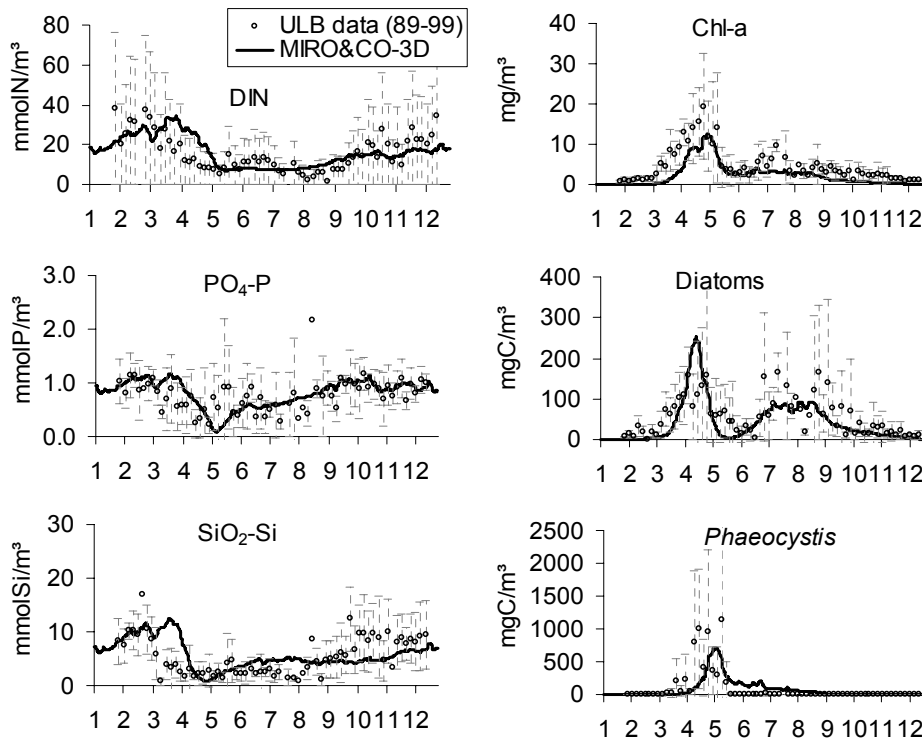


Figure 30: Seasonal evolution of MIRO&CO-3D results at St 330 (solid line) for the period 1991-2003 compared to existing data [5-day averaged (+/- standard deviation) at St 330 (dots)].

4.3.3.1.2 Seasonal average (1993-2003) of surface winter nutrients and spring Chl a in the MIRO&CO geographical domain.

Fig. 31 compares 1993-2003 simulation fields of winter (Dec-Jan-Feb average) surface nutrients and spring (Mar-Apr-May average) surface Chl a with corresponding data collected at different stations of the MIRO&CO simulated domain (data sources in Lacroix *et al.*, 2007a). In Fig.31, field data averaged over the same season are superimposed as coloured circles. Examination of Fig. 31 suggests that, globally for the considered seasons and sampling locations, the model tends to underestimate *in situ* concentrations. Indeed the model underestimates DIN, PO₄, SiO and Chl a for respectively 78, 51, 89 and 92 % of the observed stations but overestimates these state variables for 22, 49, 11 and 8% of the stations. A significant overestimation of Chl a and PO₄ (> 50 %) is found at respectively two stations close to the Scheldt estuary and one station very close to the northern boundary (Fig.31). Simulated DIN, PO₄ and SiO show moderate (25-50%) overestimation close to the Rhine/Meuse mouth and the Scheldt estuary (for PO₄ only). Significant underestimation (<-50%) is found mainly for Chl a (29 stations), then for SiO (6 stations) and for DIN (3 stations). PO₄ seems better simulated than the other nutrients. For respectively 45% (DIN), 72% (PO₄) and 40% (SiO) of the

stations, the model gives a fairly good estimation *i.e.* the relative difference between model results and field observations is within the range -25 , +25 %.

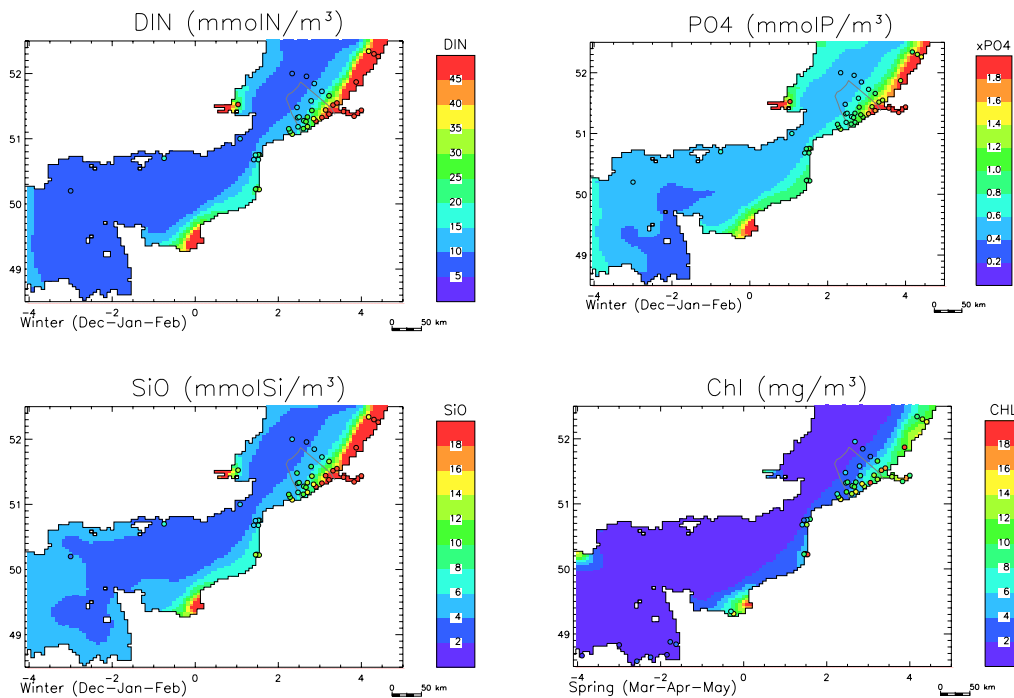


Figure 31: 1993-2003 averaged surface winter (spring) nutrient (Chl a) fields based on MIRO&CO-3D simulations.

Superimposed coloured circles correspond to the averaged observations over the same season. Colour scale is the same for model results and data.

4.3.3.2 Spatio-temporal trends: surface Chl a in 2003

Surface Chl a derived from MERIS have been used to test the model capability of describing the spatio-temporal evolution of global phytoplankton in the MIRO&CO-3D geographical domain. For this purpose the satellite-derived Chl a was averaged horizontally over the model grid cells. Fig. 32 shows the monthly MIRO&CO-3D and MERIS mean surface Chl a as well as their relative difference for the period March-July 2003. The MERIS monthly mean images (Fig. 32, left panel) show that the maximum Chl a in March is found in a coastal region between the Somme and the Scheldt rivers and to the north of the Rhine/Meuse and Thames river mouths. The highest Chl a are seen in April when nearly the entire Southern Bight of the North Sea exhibits elevated concentrations. From May to July, high Chl a is limited to coastal regions with the highest values close to the river mouths. During the summer months, a 50 km large patch of high Chl a is recorded in the western Channel (49.5°N, 4°W). This has been identified as a bloom of the toxic dinoflagellate *Karenia mikimotoi* (Fernand *et al.*, 2004; Lyons *et al.*, 2004; Vanhoutte-Brunier *et al.*, 2004). Compared to these images, the MIRO&CO Chl a fields (Fig. 32, middle panel) show

a clear coastal-offshore gradient with highest values in April and near the river mouths. However there is general tendency of the model to underestimate the surface Chl *a* with some exceptions amongst which the more striking are: north of the Scheldt mouth in March, the Bay of Seine in March and April, the Thames mouth in May and June, close to the western boundary in March, April and May and in a small area South of UK in March, April and June (Fig. 32). On the other hand, overestimated MIRO&CO Chl *a* compared to MERIS-derived surface concentration are localised in areas close to the river mouths and the western boundary.

The correlation between the spring average MIRO&CO and MERIS Chl *a* is shown in Fig. 33. This graph confirms the general tendency of the model to underestimate the satellited-derived surface Chl *a* during the spring bloom (90% of the domain) with only 10 % of the simulated Chl *a* being higher than that estimated from MERIS. For respectively 8.1, 22.5, 39.1 and 20.4% of the domain, the relative difference between MIRO&CO and MERIS Chl *a* is between -25 - 0%, -50 - -25%, -75 - -50% and < -75 %. The most severely underestimated Chl *a* are located in the region North and East of the Thames estuary.

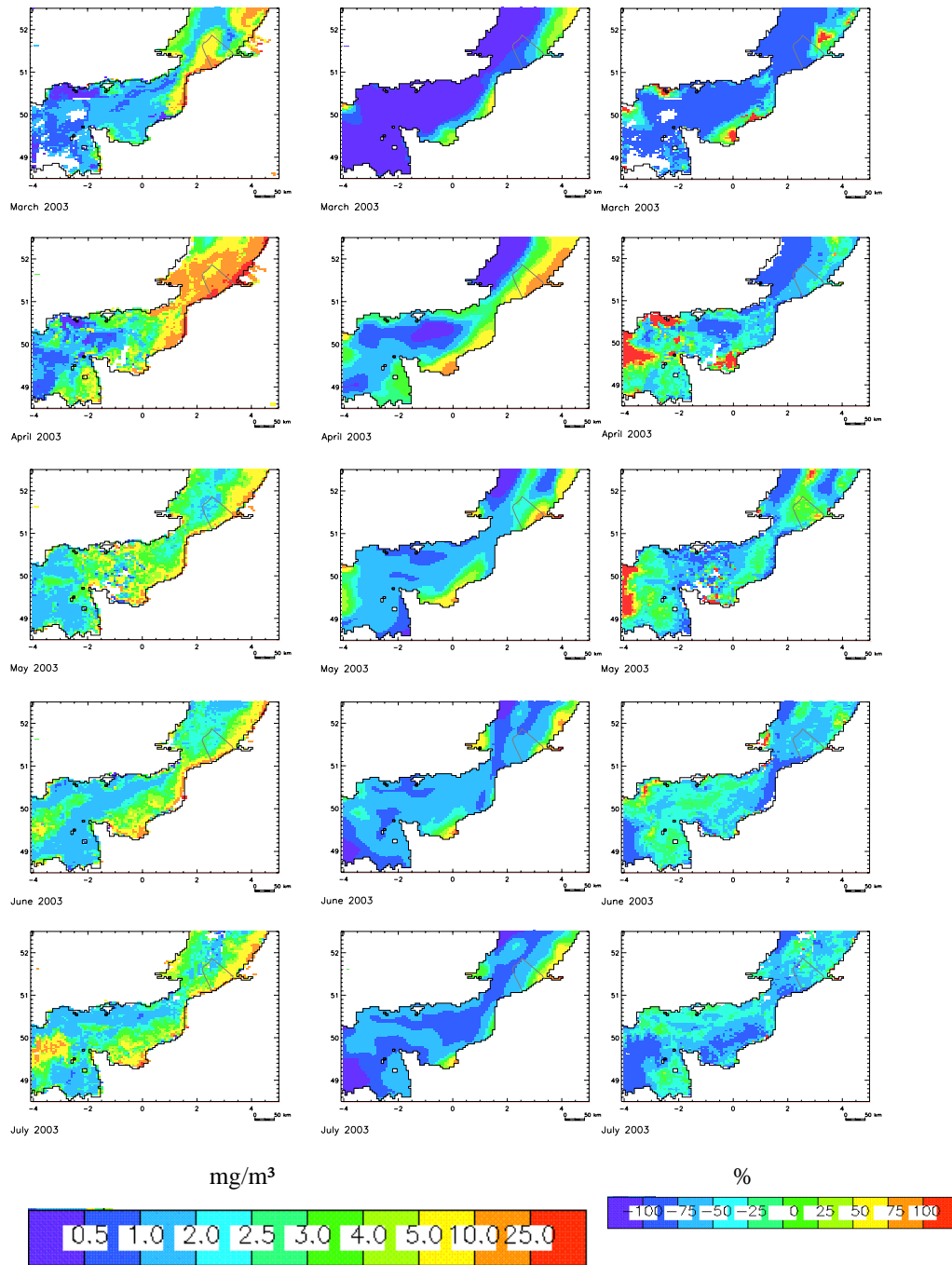


Figure 32: Left panel: monthly mean Chl *a* derived from MERIS satellite images adapted to the MIRO&CO-3D grid. 69 MERIS images were used for the period of March 2003 - July 2003. In average, 2.9 images were valid for a grid cell in these monthly images. Middle panel: monthly mean surface MIRO&CO-3D Chl *a*. Right panel: monthly mean relative difference $[(\text{Model-MERIS})/\text{MERIS} \times 100]$ between model and MERIS surface Chl *a*. Positive (negative) values indicate a model overestimation (underestimation).

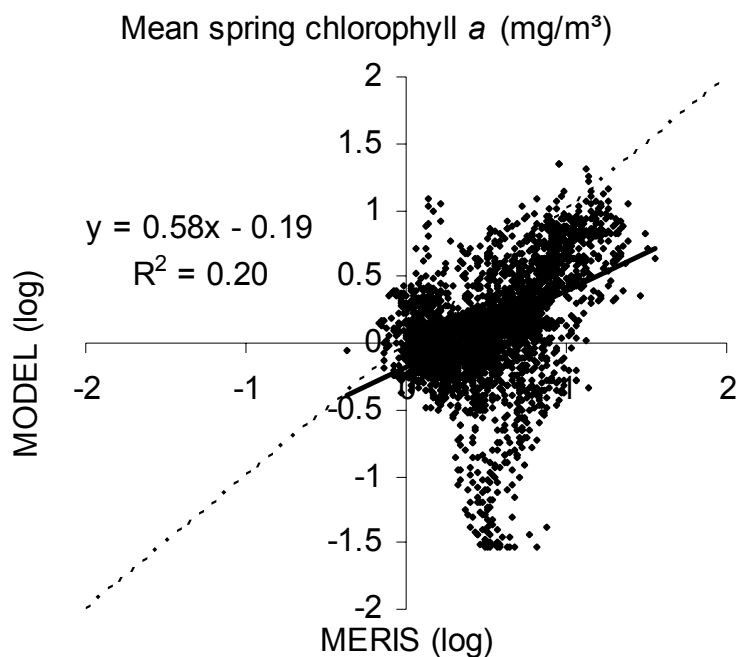


Figure 33: Log-log correlation between simulated and MERIS Chl a in spring 2003 for the MIRO&CO-3D domain. The solid line corresponds to the regression in the log-log space. The dashed line shows a simulated vs MERIS Chl a of 1:1

4.3.4 0D multi-box MIRO application: river nutrient reductions

Several model runs have been performed with changing nutrient loads to explore the response of diatoms and *Phaeocystis* colonies in BCZ to reduced nutrient conditions by reference to the 1989-2003 period. Chosen scenarios include 50% reduction of NO₃ and/or PO₄ Seine and/or Scheldt loads. The resulting effect on phytoplankton is estimated by comparison with the nominal run under 1989-2003 actual conditions. Table 1 shows the effect of changing nutrient loads by both Scheldt and Seine rivers on annual diatom and *Phaeocystis* biomass for selected dry and wet years corresponding to the first and second half of the simulated period. First of all, changing nutrient load has no effect on the diatom–*Phaeocystis*–diatom succession (not shown) but impacts on the magnitude of their blooms. The extent of the phytoplankton decrease depends on the target nutrient(s), N or P reduction acting differently on the diatom and *Phaeocystis* biomass. According to our model scenarios, a decrease of the annual diatom biomass is simulated after PO₄ reduction and this decrease is particularly enhanced during wet years (-8.4 g C m⁻³ in 1994 and -5.6 g C m⁻³ in 1999; Table 1). On the opposite, *Phaeocystis* biomass is generally little modified by a PO₄ reduction of both Scheldt and river loads (< 12%, *i.e.* ~3g C m⁻³, for selected years, Table 1). As expected from previous model result analysis, N

reduction has a significant negative effect on *Phaeocystis* which simulated biomass decreases by more than 38% for every year tested (Table 1). The highest reduction of *Phaeocystis* biomass is simulated during dry years (1990 and 1996; 9 g C m⁻³; Table 1). Annual diatom biomass is little affected by N reduction (< 5 g C m⁻³) and an increasing biomass is even simulated in 1996 (+1.6 gC m⁻³; Table 1). This suggests a strong competition between *Phaeocystis* and diatoms for low PO₄. The combined NO₃ and PO₄ reduction decreases both diatoms and *Phaeocystis* biomass. These drops are similar (35-40%; *i.e* 6-7 g C m⁻³ for diatoms and ~8.5 g C m⁻³ for *Phaeocystis*; Table 1) during wet years while *Phaeocystis* biomass is more affected during dry years than diatoms (Table 1).

Table 1: Effect of Scheldt and Seine nutrient reductions on annual diatom and *Phaeocystis* biomass in BCZ, expressed in %

Year	PO ₄ reduction		NO ₃ reduction		PO ₄ +NO ₃ reduction	
	Diatom	<i>Phaeocystis</i>	Diatom	<i>Phaeocystis</i>	Diatom	<i>Phaeocystis</i>
1990 (dry)	-20	-11	-9	-43	-20	-41
1994 (wet)	-40	-6	-22	-38	-37	-36
1996 (dry)	-24	-11	14	-43	-11	-31
1999 (wet)	-31	-2	-22	-34	-32	-34

In order to explore the respective contribution of Scheldt and Seine nutrient loads to BCZ enrichment and the subsequent phytoplankton blooms, two additional scenarios were performed in which Scheldt (Table 2) or Seine (Table 3) nutrient loads were modified separately. As a general trend these scenarios show that the reduction of nutrient loads by only one river (Seine or Scheldt) is not enough to decrease significantly the phytoplankton biomass. This is particularly evident when only Scheldt nutrient loads are reduced (Table 2). A 50% reduction of Scheldt N and P loads for the selected years leads to a maximum decrease of annual *Phaeocystis* biomass of 20% without affecting diatoms (Table 3). The effect of a Scheldt PO₄ reduction is less significant, decreasing the annual diatom biomass by a maximum 6% in 1994 (Table 2). Similarly, a NO₃ reduction of Seine loads leads to a maximum *Phaeocystis* decrease of 21-24% (Table 3). On the opposite, the reduction of Seine PO₄ loads (Table 4) has a larger decreasing effect on diatoms (> 70%; Table 3) than the same reduction applied to Scheldt loads. Due to the different effect of N, P and Si limitation on diatom and *Phaeocystis* growth, the only N reduction loads leads to a significant drop of *Phaeocystis* bloom without negatively affecting diatoms while P reduction negatively impacts on diatoms. As suggested by Skogen *et al.* (2004), a

decreasing P loads with respect to the present-day nutrient load won't have a positive effect on the ecosystem. Moreover, due to the importance of Atlantic nutrient loads, reduction of Scheldt nutrient loads only is not sufficient to significantly decrease nutrient concentrations in the BCZ and phytoplankton blooms.

Table 2: Effect of Scheldt nutrient reduction on annual diatom and *Phaeocystis* biomass in BCZ, expressed in %

Year	PO ₄ reduction		NO ₃ reduction		PO ₄ +NO ₃ reduction	
	Diatom	Phaeocystis	Diatom	Phaeocystis	Diatom	Phaeocystis
1990 (dry)	-5	0	-3	-20	-7	-21
1994 (wet)	-6	-3	-3	-3	-9	-4
1996 (dry)	-3	-6	0	-3	-4	-5
1999 (wet)	-5	-1	-2	0	-7	-5

Table 3: Effect of Seine nutrient reduction on annual diatom and *Phaeocystis* biomass in BCZ, expressed in %

Year	PO ₄ reduction		NO ₃ reduction		PO ₄ +NO ₃ reduction	
	Diatom	Phaeocystis	Diatom	Phaeocystis	Diatom	Phaeocystis
1990 (dry)	-15	-6	-5	-24	-15	-22
1994 (wet)	-36	-5	-15	-24	-32	-22
1996 (dry)	-20	-8	10	-21	-13	-2
1999 (wet)	-27	2	-16	-22	-28	-23

4.3.5 MIRO&CO-3D application: contribution of different rivers (Rhine/Meuse, Scheldt and Seine) to the nutrient pool

The origin of nutrients (DIN and PO₄) available for biological production in BCZ has been investigated by running MIRO&CO-3D sensitivity scenarios with decreasing nutrient inputs from inflowing Channel waters, Scheldt/Leie/Ijzer and Rhine/Meuse by respectively 1% (Lacroix *et al.*, 2007b). Such a small decrease has been chosen in order to ensure a *quasi* linear ecosystem response. The effect of this reduction is estimated by comparing the obtained average 1993-2003 field concentrations with those obtained with the standard run (STD). The N and P reduction scenarios involve

those by the Rhine (MSR), the Scheldt (MSE), the Seine (MSS), and the Channel (MSF). Results (PO_4 and DIN average fields) expressed in % variation (the ratio of the perturbed surface nutrient concentration minus the standard surface nutrient concentration divided by the standard surface nutrient concentration) are shown in Fig. 34. Negative value indicates a reduction of the surface nutrient of concern compared to the standard simulation. Clearly, the decrease of nutrient river loads has a direct impact on the surface nutrient (DIN and PO_4) concentrations, especially close to the respective estuary mouths (Fig. 34). The reduction of Channel nutrient inflow has a direct effect on the surface nutrients over the whole domain (Fig. 34). Comparing the three rivers suggests that the effect of the Seine river is the most important for the whole domain considered though the Rhine/Meuse will impact waters to the NE *i.e.* outside the model domain. The reduction of nutrient loads from the Seine leads to a significant decrease (-1.0 - -0.1 %) of the surface nutrient concentration reaching the totality of BCZ for DIN and the offshore area for PO_4 . The Rhine nutrient reduction leads to a significant decrease of surface nutrient from the coast to almost 60 km (30 km) offshore in the BCZ for DIN (PO_4). The Rhine river loads reduction affects the Scheldt estuary moderately (-0.1 - -0.01%) for PO_4 and significantly (-1.0 - -0.1%) for DIN. Overall, the decrease of PO_4 surface concentration seems more localized than that of DIN. On average nutrient reduction from all rivers would have a similar decrease of DIN in BCZ (-0.51%) than those obtained from the Channel nutrient reduction (-0.48%). The impact of nutrient reduction from all the rivers on PO_4 in BCZ (-0.23%) is almost 3 times lower than that resulting from the Channel nutrient reduction (-0.65%). The effect of nutrient reduction from all rivers is therefore higher for DIN than that for PO_4 expressing a stronger sensitivity of DIN to riverine nutrient reduction because rivers supply relatively more DIN than PO_4 as compared to the Atlantic inflow.

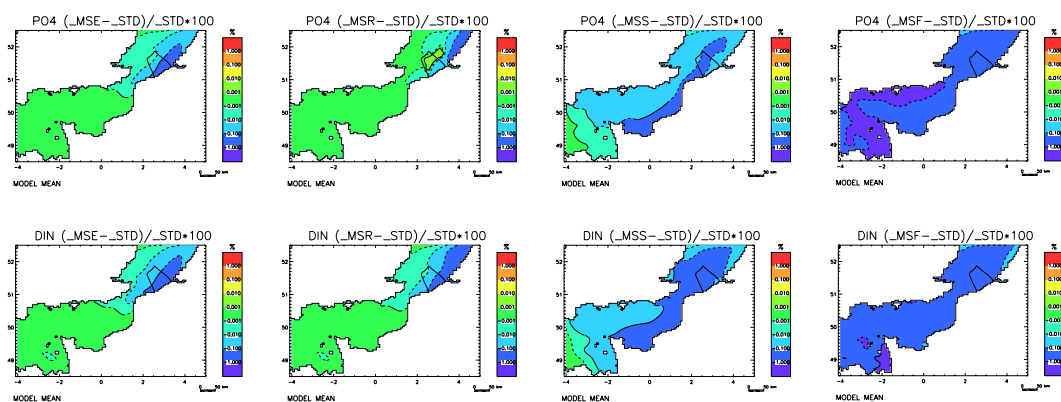


Figure 34: Average 1993-2003 surface nutrient relative difference (%) between perturbed (DIN and PO_4 reduction) and standard simulations.

Fig. 35 illustrates which river contributes the most to the surface nutrient relative difference. Clearly, the nutrient reduction from the Seine has the strongest impact on surface DIN and PO_4 in the whole MIRO&CO-3D domain, except the Belgian and Netherlands coastal zones (Fig. 35). Interestingly enough, the Scheldt has a larger effect than the Seine in the Belgian coastal waters where eutrophication is most severe. The region of highest influence by the Rhine/Meuse (NE area of the model domain) extends more southward (until the Scheldt mouth) for DIN than that for PO_4 (Fig. 35).

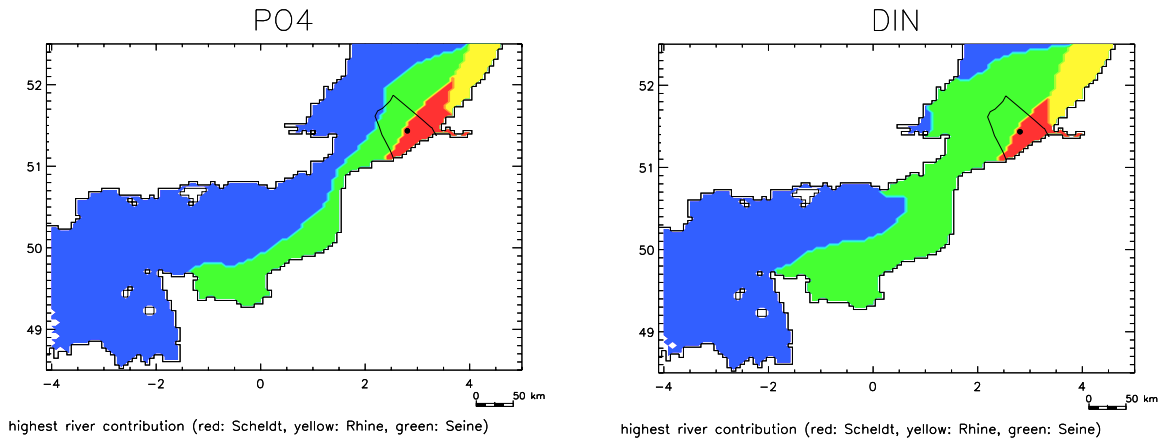


Figure 35: Highest river contribution to the surface nutrient in the MIRO&CO-3D domain. Red: Scheldt (+Leie, IJzer), yellow: Rhine/Meuse, green: Seine (+ Somme, Authie, Canche).

5 CONCLUSION AND RECOMMENDATIONS

5.1 Improved knowledge on the ecology of the *Phaeocystis*-dominated Southern Bight of the North Sea

5.1.1 *Phaeocystis* species identification and life cycle

For the first time in the region, molecular tools have identified as *P. globosa* the *Phaeocystis* species blooming in the Southern Bight of the North Sea (Rousseau *et al.*, submitted). As reported by Lange *et al.* (2002), the *P. globosa* clade regroups strains from cold-temperate and tropical waters. In agreement, our phylogenetic analysis suggests that the strains collected in BCZ and in the German Bight constitute a small subgroup and, due to their geographical position can therefore be considered as representative of the original *P. globosa* described by Scherffel (1900) in Helgoland waters (German Bight).

Experimental studies on the *Phaeocystis* life cycle have focused on the identification (Rousseau, 2002) and ecological role of *Phaeocystis* life forms (Lancelot *et al.*, 2002). One outstanding result is the identification of a haploid-diploid life cycle in which haploid flagellates persist in the water column between two blooms of diploid colonial cells, suggesting that colony bloom initiation and termination involve sexual processes (Rousseau *et al.*, 2007). Further research is however needed to substantiate this life cycle, by direct observation of short-lived syngamy and meiosis, the characterisation of the mating system and capability (isogamy vs anisogamy, homothallism vs heterothallism), and the knowledge of the factors inducing sexuality. Among them, the possible role of early spring diatoms in syngamy must be specifically addressed. These diatoms have indeed been suggested as triggers of colony formation.

5.1.2 Mechanisms controlling diatom-*Phaeocystis*-diatom successions

Monitoring data collected at St 330 since 1988 have shown that the diatom-*Phaeocystis*-diatom succession is a recurrent phenomenon. However the relative contribution of diatom and *Phaeocystis* to the spring bloom was varying between years and could not be directly linked to changing nutrient loads by the Scheldt (Rousseau, 2000). The statistical analysis of diatom and *Phaeocystis* data collected between 1992 and 2000 at St 330 in BCZ have showed that the relative contribution of these two phytoplankton groups to the spring community was in fact determined by both nutrient loads (mankind) and hydro-climatic conditions (under influence of the North Atlantic Oscillation NAO; Breton *et al.*, 2006). Years with elevated *Phaeocystis* blooms in central BCZ were identified as those characterized by a medium NAO index, *i.e.* when a maximum of NO₃ delivered by the Scheldt are spread over BCZ (Breton *et al.*, 2006). The further analysis of the effect of NAO fluctuations on the

North Atlantic phytoplankton community suggests however specific regional responses. These regional differences are not due to local meteorological conditions but rather on the way local wind and rainfall affect hydrodynamics and nutrient loads. Therefore, because of these geographical peculiarities, a deeper understanding of the causal mechanisms linking NAO and phytoplankton is required before concluding that there is a common rule that determines phytoplankton structure over large areas. Finally, our results point to the importance of the choice of monitoring stations for eutrophication in coastal areas such as the BCZ, where the geographical extent of river loads is highly variable, depending in a complex and opposite way on wind direction and rainfall, both driven by NAO.

5.1.3 Fate of *Phaeocystis* blooms

Our studies on the fate of *Phaeocystis* have explored the use of tracers (Antajan *et al.*, 2004; Hamm & Rousseau, 2003) and process-level studies (laboratory-controlled grazing experiments and egg production). Altogether results demonstrate that healthy *Phaeocystis* colonies are not grazed by either copepods (Gasparini *et al.*, 2000) or gelatinous organisms (Breton *et al.*, submitted) but mostly degraded in the water column (Becquevort *et al.*, 1998; Rousseau *et al.*, 2000).

5.2 Advances in ecological modeling: 0D multi-box MIRO

5.2.1 New developments

Most of the ecological advances have been integrated in the MIRO ecological model (Lancelot *et al.*, 2005) which parameterization is public (www.int-res.com/journals/suppl/appendix_lancelot.pdf). The MIRO has been validated in a multi-box frame and its results explored in terms of ecological trophic efficiency and nutrient budget (Lancelot *et al.*, 2005). Further published developments and applications included (i) the addition and test of a CO₂ module (Gypens *et al.*, 2004) pointing the role of riverine nutrient loads in stimulating the uptake of atmospheric CO₂ in BCZ, (ii) the upgrading of the sediment diagenetic module and its further simplified parameterization for integration in MIRO&CO-3D (Gypens *et al.*, submitted) and, (iii) the exploration of causes of diatom-*Phaeocystis* bloom variability in the Belgian waters over the last decade (Gypens *et al.*, 2007). The latter study concluded that while the diatom variability was depending on both meteorological conditions (light and temperature) and nutrient loads, *Phaeocystis* blooms were mainly controlled by nutrients, especially NO₃.

5.2.2 Sensitivity analysis

Results of the sensitivity analysis (variational adjoint method and sensitivity factor computation) identified processes associated to the microbial loop dynamics as main

controls of the time evolution of all the MIRO state variables in BCZ. More specific sensitivity tests were showing in addition that the timing of the spring bloom of both diatom and *Phaeocystis* was determined by the light availability and their maximum photosynthetic specific rate. This result sets severe constraints for three-dimensional studies when the model domain covers regions of spatially and temporally varying turbidity. In addition, the balance between gain and loss for the plankton community also plays an important role. The subsistence of the *Phaeocystis* bloom during the summer was indeed related to the colonies lysis rate. Unfortunately, this component of the ecosystem is still not completely understood and more laboratory or field experiments will be needed to determine the process of rupture of the *Phaeocystis* colonies. The dynamics of the copepods has also been shown important for the magnitude of summer diatom bloom. Little information about their diet and growth rate, however, exists for the BCZ.

5.2.3 Mitigation

Nutrient reduction scenarios confirmed the importance of nutrient limitation for the dynamics of diatom and *Phaeocystis* blooms and the need to consider all nutrient species when exploring the impact of nutrient reductions on diatom and *Phaeocystis* blooms. These scenarios also suggested that future management of nutrient emission reduction aiming at decreasing *Phaeocystis* blooms in BCZ without impacting on diatoms would target decrease of NO₃ loads from both the Seine and the Scheldt. However, the actual impact of a nutrient reduction will vary due to meteorological conditions (dry vs wet years).

5.3 Advances in ecological modeling: MIRO&CO-3D

The current MIRO&CO-3D resulting of the coupling between the MIRO ecological model and the COHSNS physical model has been validated based on a successful comparison of simulated salinity and *in situ* measurements (Lacroix *et al.*, 2004) and by comparing biogeochemical results [nutrient and phytoplankton (Chl *a*)] with field measurements (time series at fixed stations, surface seasonal mean, monthly mean MERIS-derived Chl *a*). Cost function analysis has concluded to a ‘very good’ simulation (Lacroix *et al.*, 2007a).

The first MIRO&CO-3D application explored the relative impact of the different rivers (Scheldt/Rhine/Seine) and Channel water on the nutrient availability in the Belgian waters by decreasing (1%) river nitrogen and phosphorus inputs for different origins separately (Lacroix *et al.*, 2007b). Results showed that Channel nutrient inflow had a direct effect on the surface nutrients over the whole domain. The comparison between the three rivers suggested that the effect of the Seine River is the most important for the whole domain considered except in BCZ areas where

eutrophication is severe due to Scheldt loads. The reduction of nutrient loads from the Seine in particular decreased the nutrient concentrations reaching the whole BCZ for DIN and offshore for PO_4 . The Rhine nutrient reduction decreased surface nutrient from the coast to almost 60 km (30 km) offshore in the BCZ for DIN (PO_4). Interestingly enough, the effect of nutrient reduction from all rivers was higher for DIN than that for PO_4 , expressing a stronger sensitivity of DIN to riverine nutrient reduction because rivers supply relatively more DIN than PO_4 as compared to the Atlantic inflow. These results conclude that an integrated management plan involving riparian countries of the eastern channel and Southern Bight of the North Sea is needed to decrease eutrophication in BCZ. As a step in this direction, further MIRO&CO-3D applications will estimate the transboundary flow of nutrients in BCZ.

6 ACKNOWLEDGMENTS

The authors are indebted to the captains and crew of the *R.V. Belgica*, students and colleagues from Belgian marine institutions for helping us with sampling at station 330. They thank E. Antajan for the spring 2001 diatom and *Phaeocystis* data and Philippe Grosjean for his helpful comments on statistical analysis. Funding for station 330 time-series was provided by several Belgian and EU-Environment Programmes since 1988. The present work is a contribution of the AMORE (Advanced MOdelling and Research on Eutrophication) and IZEUT (Identification of Zones affected by EUTrophication) projects of the Belgian Programme “Scientific Support Plan for a Sustainable Development Policy - Sustainable Management of the North Sea” funded by the Belgian Science Policy under contract MN/DD/20, EV/11/19 and MN/11/93. Achievements also contribute to the project N° CV04000018 of the Programme LITEAU (« Modélisation intégrée des transferts de nutriments depuis les bassins versants de la Seine, Somme et Escaut jusqu’en Manche-Mer du Nord ») by the French Ministry of Ecology and Sustainable Development (MEDD) as well as to Streams 3 and 6 of the Integrated Project THRESHOLDS (Thresholds of Environmental Sustainability) funded by the European Commission under contract 003933. Over the AMORE II period, N. Gypens had financial support from the ‘Fonds pour la Formation à la Recherche dans l’Industrie et dans l’Agriculture’. The authors also wish to thank the SCOR WG 120 “*Phaeocystis*, major link in the biochemical cycling of climate-relevant elements.”

7 REFERENCES

- Ammernan J.W. 1991. Role of ecto-phosphohydrolases in phosphorus regeneration in estuarine and coastal ecosystems. In: Chrost R.J. (Ed.). Microbial enzymes in aquatic environments. Springer-Verlag, New-York, pp. 165-186.
- Antajan E. 2004. Responses of calanoid copepods to changes in phytoplankton dominance in the diatoms - *Phaeocystis globosa* dominated Belgian coastal waters. Phd thesis, 142 pp. Vrije Universiteit Brussel, Belgium.
- Antajan E., Chrétiennot-Dinet M.-J., Leblanc C., Daro M.-H. and C. Lancelot. 2004. 19'-hexanoyloxyfucoxanthin may not be the appropriate pigment to trace occurrence and fate of *Phaeocystis*: the case of *P. globosa* in Belgian coastal waters. J. Sea Res. 52: 165-77.
- Baumann M.E.M., Lancelot C., Brandini F.P., Sakshaug E. and D.M. John. 1994. The taxonomic identity of the cosmopolitan prymnesiophyte *Phaeocystis*: a morphological and ecophysiological approach. In: Lancelot C & Wassmann P (Eds) Ecology of *Phaeocystis*-dominated ecosystems. J. Mar. Syst. 5: 5-22
- Beamish R. J., Noakes D. J., McFarlane G. A., Klyashtorin L., Ivanov V. V. and V. Kurashov. 1999. The regime concept and natural trends in the production of Pacific salmon. Can. J. Fish. Aquat. Sci. 56: 516-526.
- Becquevort, S., Rousseau V. and C. Lancelot. 1998. Major and comparable roles for free-living and attached bacteria in the degradation of *Phaeocystis*-derived organic matter in Belgian coastal waters of the North Sea. Aquatic Microbial Ecology, 14 : 39-48.
- Belgrano A., Lindahl O. and B. Hernroth. 1999. North Atlantic Oscillation primary productivity and toxic phytoplankton in the Gullmar Fjord, Sweden (1985-1996). Proc. R. Soc. Lond. 266: 425-430.
- Billen G. 1982. An idealized model of nitrogen recycling in marine sediments. American Journal of Science, vol. 282:512-541.
- Billen G., Dessery S., Lancelot C. and M. Meybeck. 1989. Seasonal and inter-annual variations of nitrogen diagenesis in the sediments of a recently impounded basin. Biogeochemistry 8: 73-100.
- Borges, A.V. and M. Frankignoulle. 1999. Daily and seasonal variations of the partial pressure of CO₂ in the surface seawater along Belgian and southern Dutch coastal areas, J. Mar. Syst., 19, 251-266.
- Borges, A.V. and M. Frankignoulle. 2002. Distribution and air-water exchange of carbon dioxide in the Scheldt plume off the Belgian coast, Biogeochemistry, 59, 41-67.
- Borges, A.V. and M. Frankignoulle. 2003 Distribution of surface carbon dioxide and air-sea exchange in the English Channel and adjacent areas, J. Geophys. Res., 108(C8), 3140.
- Breton E., Rousseau V., Parent J.-Y., Ozer J. and C. Lancelot. 2006. Hydroclimatic modulation of diatom/*PHAEOCYSTIS* blooms in the nutrient-enriched Belgian coastal waters (North Sea). Limnol. Oceanogr. 51(3): 1401-1409.
- Breton E., Rousseau, V., Parent J.-Y., Becquevort S., M.-H. Daro and C. Lancelot. Diet and feeding ecology of the dinoflagellate *Noctiluca scintillans* in the Southern Bight of the North Sea (in prep).
- Buiteveld H. 1995. A model for calculation of diffuse light attenuation (PAR) and Secchi depth. Neth. J. Aquatic Ecology, 29(1): 55-65.
- Cadée G. C. and J. Hegeman. 1991. Historical phytoplankton data of the Marsdiep. Hydrobiol. Bull. 24: 111-188.
- Cariou V., Casotti R., Birrien J.-L. and Vaultot D. 1994. The initiation of *Phaeocystis* colonies. J. Plankton Res. 16: 457-470

- Chrétiennot-Dinet M.-J. 1999. An enigma in marine nanoplankton. The role of star-like structures produced by *Phaeocystis*. In: Seckbach J (Ed) Enigmatic microorganisms and life in extreme environments (pp 205-213). Kluwer Academic Publishers, The Netherlands
- Costello M. J. 1990. Predator feeding strategy and prey importance: a new graphical analysis. J. Fish Biol., 36: 261-263.
- De Vries, H., Breton M., De Mulder T., Krestinitis Y., Ozer J., Proctor R., Ruddick K., Salomon J.C. and A. Voorrips. 1995. A comparison of 2D storm surge models applied to three shallow European seas. Environmental Software 10: 23-42.
- Dutz J. and M. Koski. 2006. Trophic significance of solitary cells of the prymnesiophyte *Phaeocystis globosa* depends on cell type. Limnol. Oceanogr. 51(3): 12030-1238.
- Edvardsen B., Eikrem W., Green J.C., Andersen R.A., Moon-van der Staay S.Y. and L.K. Medlin. 2000. Phylogenetic reconstructions of the Haptophyta inferred from 18S ribosomal DNA sequences and available morphological data. Phycologia. 39 (1): 19-35
- Edwards M., Reid P. and B. Planque. 2001. Long-term and regional variability of phytoplankton biomass in the Northeast Atlantic (1960-1995). ICES Journal of Marine Science 58: 39-49.
- Enomoto Y. 1956. On the occurrence and food of *Noctiluca scintillans* in the waters adjacent to the West Coast of Kyushu, with special reference to the possibility of damage caused to fish eggs by that plankton. Bull. Jap. Soc. Scien. Fisheries 22:82-88.
- Fasham M.J.R., Sarmiento J.L., Slater R.D., Ducklow H.W. and R. Williams. 1993. Ecosystem behaviour at Bermuda Station 'S' and Ocean Weather Station 'India': a general circulation model and observational analysis. Global Biogeochemical Cycles 7 (2): 379-415.
- Fernand L., McCloghrie P., Raine R., Lyons S., Chambers C., Cussack C. and J. Wooltorton. 2004. Circulation of the western English Channel: a combination of factors, Abstract of the presentation at the "Challenger conference for marine science", Liverpool, 13-17 September 2004, http://www.ifremer.fr/delec/projets/efflores_phyto/Phaeocystis/poster_liverpool.pdf.
- Frost B. W. 1972. Effects of size and concentration of food particles on the feeding behavior of the marine planktonic copepod *Calanus pacificus*. Limnol. Oceanogr. 17: 805-815.
- Gentleman W., Leising A., Frost B., Strom S. and J. Murray. 2003. Functional responses for zooplankton feeding on multiple resources: a review of assumptions and biological dynamics. Deep-Sea Res., II 50, 2847-2975.
- Gervasi E., Jeuniaux C. and P. Dauby. 1988. Chitin production by zooplankton crustacean of Calvi Bay (Corsica, France). In: Le Gal Y, Van Wormhoudt A (eds) Meeting of Carcinology, Concarneau (France), 6 Jun 1987.
- Gilbert J.-C., and C. Lemaréchal. 1989. Some numerical experiments with variable-storage quasi-Newton algorithms. Mathematical Programming. 45: 407-435.
- Grasshoff K., Ehrhardt M. and K. Kremling. 1983. Methods of seawater analysis. Verlag-Chemie Weinheim, New-York. 317 p.
- Gypens N., Lancelot C. and A.V. Borges. 2004. Carbon dynamics and CO₂ air-sea exchanges in the eutrophied coastal waters of the Southern Bight of the North Sea: a modelling study. Biogeosciences, 1: 147-157.
- Gypens N. 2006. Modélisation des efflorescences algales et des cycles du C, N, P et Si dans l'écosystème eutrophisé de la mer du Nord. PhD Thesis, Université Libre de Bruxelles, Belgium.
- Gypens N., Lacroix G. and C. Lancelot. 2007. Understanding the 1989-2003 variability of diatom-*Phaeocystis* blooms in the Belgian coastal waters : the MIRO model. Journal of Sea Research (in press).

- Gypens N., Lancelot C. and K. Soetaert (submitted). Can simple parameterisations for describing N and P diagenetic processes in the North Sea work ?
- Hamm, C. and V. Rousseau. 2003. The fate of *Phaeocystis*-derived fatty acids during a *Phaeocystis globosa* bloom in the Southern North Sea. *Journal of Sea Research*. 50 (4): 271-283.
- Hannon E., Boyd P.W., Silviso M. and C. Lancelot. 2001. Modelling the bloom evolution and carbon flows during SOIREE: Implications for future in situ iron-experiments in the Southern Ocean, *Deep-Sea Research II*, 48, 2745-27773.
- Hansen F.C.R., Reckermann M., Klein Breteler W.C.M. and R. Riegman. 1994. *Phaeocystis* blooming enhanced by copepod predation on protozoa: evidence from incubation experiments. *Mar. Ecol. Progr. Ser.* 102: 51-57
- Hecq J.-H. 1982. Distribution et dynamique des communautés zooplanctoniques en relation avec le cycle du carbone en Baie sud de la mer du Nord. PhD thesis. Université de Liège. 249 pp.
- Honjo S. and M.R. Roman. 1978. Marine copepod fecal pellets: production, preservation, and sedimentation. *J Mar Res* 36: 45–57.
- Houdan A., Billard C., Marie D., Not F., Saez A.G., Young J.R. and Probert J. 2004. Holococcolithophore-heterococcolithophore (Haptophyta) life cycles: flow cytometric analysis of relative ploidy levels. *Systematics and Biodiversity*. 4: 453-465
- Hurrell, J. W. 1995. Decadal trends in the North Atlantic Oscillation: regional temperatures and precipitation. *Science* 269: 676-679.
- Hurrell J. W. and R. R. Dickson. 2004. Climate variability over the North Atlantic, p. 15-31. In N.C. Stenseth, G. Ottersen, J. W. Hurrell and A. Belgrano [eds.], *Marine Ecosystems and Climate Variation - the North Atlantic*. Oxford University Press.
- Irigoien X., Harris R. H., Head R. N., and D. Harbour. 2000. North Atlantic Oscillation and spring bloom phytoplankton composition in the English Channel. *J. Plankton Res.* 22: 2367-2371.
- Ishida K., Green B.R. and T. Cavalier-Smith. 1999. Diversification of a chimaeric algal group, the Chloroarchaniophytes: phylogeny of nucleus and nucleomorph small-subunit rRNA genes. *Mol Biol Evol* 16: 321-331
- Jahnke J. and M. Baumann. 1987. Differentiation between *Phaeocystis pouchetii* (Har.) Lagerheim and *Phaeocystis globosa* Scherffel. Colony shapes and temperature tolerances. *Hydrobiol. Bull.* 21:141-147
- Kayser H. 1970. Experimental-ecological investigations on *Phaeocystis pouchetii* (Haptophyceae): cultivation and waste water test. *Helgoländer Wiss. Meeresunt.* 20: 195-212
- Kimor B. 1979. Predation by *Noctiluca miliaris* Souriray on *Acartia tonsa* Dana Eggs in the Inshore Waters of Southern California. *Limnology and Oceanography*, 24:568-572.
- Kiorboe T., Mohlenberg E. and K. Hamburger. 1985. Bioenergetics of the planktonic copepod *Acartia tonsa*: Relation between feeding, egg production and respiration, and composition of specific dynamic action. *Mar. Ecol. Prog. Ser.* 26: 85-97.
- Klein-Breteler W. C. M., Fransz H. G. and S.R. Gonzalez. 1982. Growth and development of four calanoid copepod species under experimental and natural conditions. *Neth. J. Sea Res.* 16: 195-207
- Kondrashov A.S. and J.F. Crow. 1991. Haploidy or diploidy: which is better? *Nature*. 351: 314-317
- Kornmann P. 1955. Beobachtungen an *Phaeocystis*-Kulturen. *Helgoländer Wiss. Meeresunt.* 5: 218-233

- Krom M. D. and Berner R. A. 1980. Adsorption of phosphate in anoxic marine sediments. *Limnol. Oceanogr.* 25(5):797-806.
- Lacroix G., Ruddick K., Ozer J. and C. Lancelot. 2004. Modelling the impact of the Scheldt and Rhine/Meuse plumes on the salinity distribution in Belgian waters (southern North Sea). *J. Sea Res.* 52: 149-163.
- Lacroix G., Ruddick K., Park Y., Gypens N. and C. Lancelot. 2007a. Validation of the 3D biogeochemical model MIRO&CO with field nutrient and phytoplankton data and MERIS-derived surface chlorophyll a images. *J. Mar. Syst.* 64(1-4): 66-68.
- Lacroix G., Ruddick K., Gypens N. and C. Lancelot. 2007b. Modelling the relative impact of Rivers (Scheldt/Rhine/Seine) and Channel water on the nutrient availability and diatoms/*Phaeocystis* concentrations in Belgian waters (Southern North Sea), in press.
- Lancelot C. and S. Mathot. 1987. Dynamics of a *Phaeocystis*-dominated spring bloom in Belgian coastal waters. I. Phytoplanktonic activities and related parameters. *Marine Ecology Progress Series*, 37: 239-248.
- Lancelot C., Billen G., Sournia A., Weisse T., Colijn F., Veldhuis M.J.W., Davies A. and P. Wassmann. 1987. *Phaeocystis* blooms and nutrient enrichment in the continental coastal zones of the North Sea. *Ambio* 16 : 38-46.
- Lancelot C. and V. Rousseau. 1994. Ecology of *Phaeocystis*: the key role of colony forms. In: *The Haptophyte Algae*, Vol. 51 (Eds, Green JC, Leadbeater BSC), pp. 229-245. Clarenton Press, Oxford.
- Lancelot C., Billen G. and V. Rousseau. 1994. Modelling *Phaeocystis* blooms, their causes and consequences. Final Rep, EU Programme Science and Technology for Environmental Protection STEP. 133 pp
- Lancelot C. 1995. The mucilage phenomenon in the continental coastal waters of the North Sea. *The Science of the Total Environment.* 165: 83-102.
- Lancelot C., Keller M., Rousseau V., Smith W. O. Jr. and S. Mathot. 1998. Autoecology of the Marine Haptophyte *Phaeocystis* sp., p. 209-224. In D. A. Anderson, A. M. Cembella and G. Hallegraeff [eds.], *NATO Advanced Workshop on the physiological ecology of Harmful Algal Blooms*. NATO-ASI Series, Series G: Ecological Science 41.
- Lancelot C. and V. Rousseau. 2002. Life cycle in Haptophyta. In: Garcés E, Zingone A, Montresor M., Reguera B and Dale B (Eds) *Proceedings of the LIFEHAB workshop: Life histories of microalgal species causing harmful blooms*. Calvia, Majorca, Spain, October 2001. *Research in Enclosed Seas Series.* 12: 88-90
- Lancelot C., Rousseau V., Schoemann V. and S. Becquevort. 2002. On the ecological role of the different life forms of *Phaeocystis*. In: Garcés E, Zingone A, Montresor M., Reguera B and Dale B (Eds). *Proceedings of the workshop LIFEHAB: Life histories of microalgal species causing harmful blooms*. Calvia, Majorca, Spain, octobre 2001. *Research in Enclosed Seas series.* 12: 71-75
- Lancelot C, Rousseau V., Becquevort S., Parent J.-Y., Déliat G., Leblanc C., Daro M.-H., Gasparini S., Antajan E., Meyer A., Ruddick K., Ozer J. and Y. Spitz. 2004. Study and modelling of eutrophication-related changes in coastal planktonic food-webs: a contribution of the AMORE (Advanced MOdeling and Research on Eutrophication) consortium. Final report 70pp. OSTC publication.
- Lancelot C., Spitz Y., Gypens N., Ruddick K., Becquevort S., Rousseau V., Lacroix G. and G. Billen. 2005. Modelling diatom and *Phaeocystis* blooms and nutrient cycles in the Southern Bight of the North Sea: the MIRO model. *Mar. Ecol. Progr. Series* 289, 63-78.

- Lange M., Chen Y.-Q. and L.K. Medlin. 2002. Molecular genetic delineation of *Phaeocystis* species (Prymnesiophyceae) using coding and non-coding regions of nuclear and plastid genomes. *Eur. J. Phycol.* 37: 77-92
- Lawson, L.M., Spitz, Y.H., Hofmann, E.E., Long, R.B., 1995. A data assimilation technique applied to a predator-prey model. *Bulletin of Mathematical Biology* 57: 593-617
- Lawson L. M., Hofmann E. E. and Y. H. Spitz. 1996. Time series sampling and data assimilation in a simple marine ecosystem model. *Deep-Sea Res. II*, 43, 625-651.
- Lewis W.M. 1985. Nutrient scarcity as an evolutionary cause of haploidy. *Am. Nat.* 125: 692-701
- Lohse L., Malschaert J.F.P., Slomp C., Helder W. and van Raaphorst. 1995. Sediment-water fluxes of inorganic nitrogen compounds along the transport route of organic matter in the North Sea. *Ophelia* 41:173-197.
- López-Urrutia A. and J.L. Acuña. 1999 Gut throughput dynamics in the appendicularian *Oikopleura dioica*. *Mar.Ecol.Prog.Ser.* 191: 195-205
- Lopez-Urrutia A., Acuna J.L., Irigoien X., and R.P. Harris. 2003. In situ feeding physiology and grazing impact of the appendicularian community in temperate waters: seasonal dynamics in coastal and oceanic environments. *Marine Ecology Progress Series* 252,125-141
- Lorenzen G.J. 1967. Determination of chlorophyll and phaeopigments: spectrophotometric equations. *Limnol. Oceanogr.* 12: 343-346.
- Luyten P.J., Jones J.E., Proctor R., Tabor A., Tett P. and K. Wild-Allen. 1999. COHERENS documentation: A coupled hydrodynamical-ecological model for regional and shelf seas: user documentation, MUMM, Brussels.
- Lyons S., Chambers C., Raine R. and L. Fernand. 2004. *Karenia mikimotoi* populations in the western English Channel, Abstract of the presentation at the "Challenger conference for marine science", Liverpool, 13-17 September 2004,
- Mable B.K. and S.P. Otto. 1998. The evolution of life cycles with haploid and diploid phases. *BioEssays.* 20: 453-462.
- Mackas D. and R. Bohrer. 1976. Fluorescence analysis of zooplankton gut contents and an investigation of diel feeding patterns. *J. Exp. Mar. Biol. Ecol.* 25: 77-85.
- Makridakis S., Wheelwright S. and V. McGee. 1983. *Forecasting: Methods and Applications*, 2nd ed. Wiley.
- Medlin L.K., Lange M. and M.E.M. Baumann. 1994. Genetic differentiation among three colony-forming species of *Phaeocystis*: further evidence for the phylogeny of the Prymnesiophyta. *Phycologia* 33: 199-212
- Menden-Deuer S. and E. J. Lessard. 2000. Carbon to volume relationships for dinoflagellates, diatoms, and other protist plankton. *Limnol. Oceanogr.* 45: 569-579.
- Metropolis, N. and S. Ulam. 1949. The Monte Carlo method, *Journal of the American Statistical Association*, 44 (247), 335-341.
- Millero F.J., Zhang J.-Z., Fiol S., Sotolongo S., Roy R.N., Lee K. and S. Mane. 1993. The use of buffers to measure pH in seawater. *Marine Chemistry*, 44, 143-152.
- Moon-van der Staay S.Y., van der Staay G.W.M., Guillou L., Claustre H., Medlin L.K. and D. Vaultot. 2000. Abundance and diversity of prymnesiophytes in the picoplankton community from the equatorial Pacific Ocean inferred from 18S rDNA sequences. *Limnol Oceanogr* 45: 98-109
- Moon-van der Staay S.Y., Watcher R.D. and D. Vaultot. 2001. Oceanic 18S rDNA sequences from picoplankton reveal unsuspected eukaryotic diversity. *Nature* 409: 607-610

- Nechad B., De Cauwer V., Park Y. and K. Ruddick. 2003. Suspended Particulate Matter (SPM) mapping from MERIS imagery. Calibration of a regional algorithm for the Belgian coastal waters, MERIS user workshop, 10-13th November 2003. European Space Agency, Frascati.
- Nightingale P.D., Malin G., Law C.S., Watson A.J., Liss P.S., Liddicoat M.I., Boutin J. and R.C. Upstill-Goddard. 2000. In-situ evaluation of air-sea gas exchange parametrizations using novel conservative and volatile tracers, *Global Biogeochem. Cycles*. 14: 373-387.
- Owens N. J. P., Cook D., Colebrook M., Hunt H. and P. C. Reid. 1989. Long-term trends in the occurrence of *Phaeocystis* sp. in the North-East Atlantic. *J. Mar. Biol. Ass. U.K.* 69: 813-821.
- Paffenhöfer G.-A. 1976. On the biology of appendicularia of the southeastern North Sea. The 10th Europ.Symp.Mar.Biol., Ostend, Belgium, September 1975, Vol. 2: 437-455
- Park Y., De Cauwer V., Nechad B. and K. Ruddick. 2003. Validation of MERIS water products for Belgian coastal waters: 2002-2003, MERIS and AATSR Calibration and Geophysical Validation workshop, 20-24th October 2003. European Space Agency, Frascati.
- Parke M., Green J.C. and I. Manton. 1971. Observations on the fine structure of zooids of the genus *Phaeocystis* (Haptophyceae). *J. Mar. Biol. Assoc. UK*. 51: 927-941
- Peperzak L., Colijn F., Vrieling E.G., Gieskes W.W.C. and J.C.H Peeters. 2000. Observations of flagellates in colonies of *Phaeocystis globosa* (Prymnesiophyceae): a hypothesis for their position in the life cycle. *J. Plankton Res.* 22: 2181-2203
- Porter K.G. and Y.S. Feig. 1980. Use of DAPI for identifying and counting aquatic microflora. *Limnol. Oceanogr.* 25: 943-948.
- Posada D. and K.A. Crandall. 1998. Modeltest: testing the model of DNA substitution. *Bioinformatics* 14: 817-81
- Prasad RR. 1958. Swarming of *Noctiluca* in the Palk Bay and its effect on the Chaesai fishery, with a note on the possible use of *Noctiluca* as an indicator species. *Proc. Indian Acad Sci.* 38:82-88.
- Putt M. and D.K. Stoecker. 1989. An experimentally determined carbon:volume ratio for marine 'oligotrichous' ciliates for estuarine and coastal waters. *Limnol. Oceanogr.* 34: 1097-1103.
- Rousseau V, Mathot S and C. Lancelot. 1990. Calculating carbon biomass of *Phaeocystis* sp. from microscopic observations. *Mar. Biol.* 107: 305-314
- Rousseau V, Vaultot D, Casotti R, Cariou V, Lenz J, Gunkel J and M. Baumann. 1994. The life cycle of *Phaeocystis* (Prymnesiophyceae): evidence and hypotheses. In: Lancelot C and Wassmann P (Eds) *Ecology of Phaeocystis-dominated ecosystems*. *J. Mar. Syst.* 5: 23-40
- Rousseau V. 2000. Dynamics of *Phaeocystis* and diatom blooms in the eutrophicated coastal waters of the Southern Bight of the North Sea. Ph.D. thesis. Université Libre de Bruxelles. 205 pp.
- Rousseau V., Becquevort S., Parent J.Y., Gasparini S., Daro M.-H., Tackx M. and C. Lancelot. 2000. Trophic efficiency of the planktonic food web in a coastal ecosystem dominated by *Phaeocystis* colonies. *Journal of Sea Research.* 43 : 357-372.
- Rousseau V. 2002. The life cycle of HAB forming haptophytes. Proceedings of the EC workshop LIFEHAB: Life histories of microalgal species causing harmful blooms. Calvia, Majorca, Spain, octobre 2001. Research in Enclosed Seas series. 12 : 22-26.
- Rousseau V., Breton E., de Wachter B., Beji B., Deconinck M., Huijgh J. , Bolsens T., Leroy D., Jans S. and C. Lancelot. 2004. Identification of Belgian maritime zones affected by eutrophication (IZEUT). Towards the establishment of ecological criteria for the implementation of the OSPAR Common Procedure to combat eutrophication. Belgian Science Policy Publications. 77 pp. [D/2004/1191/28].

- Rousseau V., Chrétiennot-Dinet M.-J., Jacobsen A., Verity P. and S. Whipple. 2007. The life cycle of Rousseau et al. Morphological characteristics of cell types of *Phaeocystis globosa* (Prymnesiophyceae)
- Rousseau V., Lantoine F., Rodriguez F., Chrétiennot-Dinet M.-J. and C. Lancelot. (submitted). Morphological characteristics of cell types of *Phaeocystis globosa* (Prymnesiophyceae).
- Ruddick K.G. 1995. Modelling of coastal processes influenced by the freshwater discharge of the Rhine. PhD Thesis, Université de Liège, 247 pp.
- Schoemann V., Becquevort S., Stefels J., Rousseau V. and C. Lancelot. 2004. *Phaeocystis* blooms in the global ocean and their controlling mechanisms: a review. J. Sea Research 53(1-2): 43-66.
- Scherffel A. 1900. *Phaeocystis globosa* nov. spec. nebst einigen Betrachtungen über die Phylogenie niederer, insbesondere brauner Organismen. Wissenschaftliche Meeresuntersuchungen Abteilung Helgoland N F Bd 4: 1-29
- Simon M. and F. Azam. 1989. Protein content and protein synthesis rates of planktonic marine bacteria. Mar. Ecol. Prog. Ser. 51: 201-213.
- Skogen M.D., Sjøiland H. and E. Svendsen. 2004. Effects of changing nutrient loads to the North Sea. J. Mar. Syst. 46: 23-38.
- Slomp C., Epping E.H.G., Helder W. and W. van Raaphorst. 1996. A key role for iron-bound phosphorus in authigenic apatite formation in North Atlantic continental platform sediment. J. Mar. Res. 54:1179-1205.
- Slomp C.P., Malschaert J.F.P. and W. van Raaphorst. 1998. The role of sorption in sediment-water exchange of phosphate in North Sea continental margin sediments. Limnol.Oceanog. 43: 832-846.
- Soetaert K., Herman P. M. J. and J. Middelburg. 1996. A model of early diagenetic processes from the shelf to abyssal depths. Geochim. Cosmochim. Acta, 60(6):1019-1040.
- Soetaert K., Middelburg, J.J., Herman P.M.J. and K. Buis. 2000. On the coupling of benthic and pelagic biogeochemical models. Earth Reviews. 51: 173-201
- Soetaert K., DeClippele V. and Herman P. 2002. Femme, a flexible environment for mathematically modelling the environment. Ecological Modelling 151: 177-193.
- Spitz Y. H., Moisan J.R., Abbott M. R. and J. G. Richman. 1998. Data assimilation and a pelagic ecosystem model: parameterization using time series observations. J. Marine Systems. 16: 51-68.
- Spitz Y.H., Moisan J.R. and M.R. Abbott. 2001. Configuring an ecosystem model using data from the Bermuda-Atlantic Time Series (BATS). Deep Sea Research II, 48: 1733-1768.
- Stenseth N. C., Mysterud A., Ottersen G., Hurrell J. W., Chan K. S. and M. Lima. 2002. Ecological effects of climate fluctuations. Science 297: 1292-1296.
- Swofford D.L.2002. PAUP. Phylogenetic Analysis Using Parsimony and Other Methods, 4.0 edn, Sinauer, Sunderland, MA
- Tamura K and M. Nei. 1993. Estimation of the number of nucleotide substitutions in the control region of mitochondrial DNA in humans and chimpanzees. Molecular Biology and Evolution 10: 512-526
- Uye S. 1982. Length-weight relationships of important zooplankton from the Inland Sea of Japan. J. Oceanogr.Soc. Japan, 38, 149–158.
- Valero M., Richerd S., Perrot V. and C. Destombe. 1992. Evolution of alternation of haploid and diploid phases in life cycles. Trends in Ecology and Evolution. 7(1): 25-29
- van Boekel W.H.M. and M.J.W. Veldhuis. 1990. Regulation of alkaline phosphatase synthesis in *Phaeocystis* sp. Mar. Ecol. Progr. Ser. 61 : 281-289

- Van Cappellen P. and R.A. Berner. 1988. A mathematical model for the early diagenesis of phosphorus and fluorine in marine sediments. Apatite precipitation. *American Journal Science*, 288:289-333.
- Vanhoutte-Brunier A., Lyons S., Fernand L., Cugier P., Dumas F., Menesguen A. and F. Gohin. 2004. Modelling harmful algal events in the western English Channel applied to the *Karenia mikimotoi* bloom that occurred in summer 2003, Abstract of the presentation at the "Challenger conference for marine science", Liverpool, 13-17 September 2004,
- Vaulot D., Birrien J.-L., Marie D., Casotti R., Veldhuis M.J., Kraay G.W. and M.-J. Chrétiennot-Dinet. 1994. Morphology, ploidy, pigment composition and genome size of cultured strains of *Phaeocystis* (Prymnesiophyceae). *J. Phycol.* 30: 1022-1035
- Verity P.G. and L.K. Medlin. 2003. Observations on colony formation by the cosmopolitan phytoplankton genus *Phaeocystis*. *J. Mar. Syst.* 423: 153-164
- Watson S.W., T.J. Novitsky, H.L. Quinby and F.W. Valois. 1977. Determination of bacterial number and biomass in the marine environment. *Appl. Environ. Microbiol.* 33: 940-946.
- Weiss R.F. 1974. Carbon dioxide in the water and seawater: the solubility of a non-ideal gas, *Marine Chemistry*. 2: 203-205.
- Zingone A., Chrétiennot-Dinet M.-J., Lange M. and L. Medlin. 1999. Morphological and genetic characterization of *Phaeocystis cordata* and *P. jahnii* (Pymnesiophyceae), two new species from the Mediterranean Sea. *J Phycol* 35: 1322-1337